Cranfield University

Alexander David Nind

A Technoeconomic Risk Assessment of Conventional Aero-Gas Turbines: Technological Limits and Future Directions

School of Aerospace, Transport and Manufacturing

PhD Thesis

July 2016

Supervisors: Dr Vishal Sethi

Dr Devaiah Nalianda Karumbaiah

Abstract

Increasing environmental awareness, uncertain economic climates and fluctuating fuel prices have led to airlines investigating the means to lower aircraft fuel burn, emissions and noise, while maintaining the highest possible safety standards. This is done in order to reduce operating costs as well as a desire to offer customers more environmentally responsible transport options.

The jet engine has been a fundamental part of passenger aircraft travel and has evolved to become more efficient and quiet. With an aim to improve the overall efficiency of the gas turbine, the industry has consistently sought to improve thermal and propulsive efficiency. Higher thermal efficiencies have been achieved through increased overall pressure ratios and the turbine entry temperatures, while higher propulsive efficiencies has been achieved through increase in bypass ratios. Conventional technology is however reaching the limits of any further improvements.

This study seeks to investigate these design limits for the conventional aero gas turbine and focusses on the propulsion system of short to medium range jet aircraft, specifically catering to low cost airline operations in Europe.

A techno-economic risk analysis approach was followed through the utilisation of a flexible multi-disciplinary framework. This allows a multitude of critical parameters and factors to be investigated and their effects established. Some of the key parameters investigated include the effect of design optimisation on SFC, mission fuel burn, engine sizes and weights.

By first quantifying the current design parameters and associated constraints for the selected conventional propulsion system, an optimisation study is carried out to identify the possible design limits to which the conventional technology may be pushed. It is therefore possible to then quantify the maximum benefit available to this mature technology and also to further identify which future technologies may offer the most benefits for a particular airline market strategy.

The key contribution to knowledge from this study is to therefore provide a techno-economic risk assessment of an optimised conventional high bypass ratio turbofan and establish the design limits that may be needed to achieve further benefits from conventional designs. The study is undertaken from an operator/airline perspective and further quantifies the point at which the investment opportunity of a novel technology justifies the risks associated with it.

This study has shown that there is still potential for fuel burn improvement from the evolution of the conventional turbofan. This improvement could be up to 15-20% when compared to technology of the year 2000. This is shown to be achieved through improvement material and design of the high pressure compressor spool, aimed at essentially reducing weight and diameters.

The study also includes a qualitative discussion on novel, disruptive technologies, and the risks associated with their introduction as future propulsion systems.

Acknowledgments

Firstly I would like to express my thanks to easyJet, as well as the Engineering and Physical Sciences Research Council (EPSRC) for providing the funding for this PhD.

At Cranfield University I would firstly like to thank Professor Pericles Pilidis for offering the opportunity of studying for a PhD, and particular thanks to my two supervisors: Dr Vishal Sethi and Dr Devaiah Nalianda for their help, understanding and patience. Thanks also goes to Fran Radcliffe and Teresa Townsend, part of the University's support network, for their help in getting me through a difficult last few months.

There are many friends, office mates and colleagues who I have shared many experiences over the years, offering insights and assistance, including Wanis Mohammed, Peter Zhang, Lefteris Giakoumakis, Hasani Azamar Aguirre, Emmanuel Osigwe, Alejandro Block, Joshua Sebastiampillai, Diana Guiomar San Benito Pastor and Tala El Samad

My final acknowledgement is to my wife, Andrea, for her unconditional support and understanding. I can now repay you by looking after the kids and giving you a break!

Contents

Abstract i
Acknowledgments iii
Contents v
List of Figures vii
List of Tables ix
Nomenclature x
Acronyms and Abbreviations x
Letters and Symbols xi
1.0 Introduction 1
1.1 Objectives 2
1.2 Contribution to Knowledge 2
1.3 Thesis Structure 4
2.0 Literature Review 5
2.1 Aero-Engine Trends 5
2.2 Improving Fuel Consumption 9
2.3 Recent Engine Research 11
2.4 The Gap 16
2.5 TERA Overview 18
2.5.1 History of TERA 18
2.5.2 What is TERA? 20
2.6 Other Multi-Disciplinary Optimisation Tools 24
2.7 Environmental Policy and Targets Context 25
2.7.1 Global Policies 26
2.7.2 European Environmental Goals and Legislation 26
2.8 Alternative Aircraft Engine Technologies 29
2.8.1 Pulse Detonation Engines (PDE) 29
2.8.2 Wave Rotor 34
2.8.3 Intercooled, Recuperated and Intercooled & Recuperated Cores 39
2.8.4 Open Rotors/High Speed Propellers 44
2.8.5 Turboprops/Conventional Propellers 48
3.0 TERA Methodology and Models 52
3.1 General TERA Methodology 52
3.2 Engine Performance Module 53
3.3 Aircraft Performance Module 57
3.4 Engine Sizing Module - TETHYS 63
3.4.1 Fan 66
3.4.2 Compressors 68
3.4.3 Turbines 72
3.4.5 Nacelle 74
3.4.6 Ducts 80
3.4.7 Combustor 81
3.4.8 Verification 82
3.4.9 Model Limitations and Potential Improvements 84
3.5 Weight Estimation Module 84
3.5.1 Sargerser et al's Weight Estimation Method with Jackson's Updates 87

3.5.2 Model Structure 91
3.5.3 Model Verification 92
4.0 Baseline model setup and discussion 93
4.1 TURBOMATCH Model of CFM56-5B/4 Type Engine (CUEJ56) 93
4.2 Aircraft Model 100
4.3 Model Limitations 103
5.0 Airbus A320 NEO Engines (Pratt and Whitney GTF & CFM Leap) 104
5.1 New Engine Context 104
5.1.1 A320 NEO 104
5.1.2 CFM LEAP Very High Bypass Ratio Conventional Turbofan ("LEAP") 105
5.1.3 Pratt and Whitney PurePower Geared Turbofan ("PPGTF") 105
5.2 Engine Performance Modelling 105
5.2.1 Gearbox Modelling in TURBOMATCH 109
5.3 New Engine Characteristics 110
5.4 Aircraft Mission Performance 111
6.0 Optimisation 116
6.1 Engines for Optimisation 116
6.1.1 Engine Initial Parameters and Assumptions 116
6.1.2 Parametric Study 119
The Effect of High Pressure Compressor Ratio 119
The Effect of Fan Pressure Ratio 123
The Effect of Booster Pressure Ratio 124
The Effect of Bypass Ratio 126
6.1.3 Optimisation Setup 127
6.1.4 Optimisation Results 129
6.1.5 Fuel Burn Savings 133
6.1.6 Limits to Achieving Gains 135
6.1.7 Economic Analysis 141
6.1.8 Discussion 148
7.0 Conclusions 156
7.1 Recommendations for Future Work 160
8.0 References 161
Appendix 1 - HERMES Input File 173
Appendix 2 – Tethys Input File – CUEJ56 178
Appendix 3 – Technology Readiness Level 182

List of Figures

Figure 2.1: Aircraft Noise and Bypass Ratio Trends (Birch, 2000) 6
Figure 2.2: Turbine Entry Temperature Evolution (Kyprianidis, 2011) 6
Figure 2.3: THermal Efficiency Variation with Overall Pressure Ratio and Turbine Entry Temperature (Birch, 2000) 7
Figure 2.4: ICAO Nox Emission Charactistic Regulations (Dickson, 2014) 8
Figure 2.5: SFC Variation with OPR and TET (Birch, 2000) 10
Figure 2.6: Propulsive Fuselage Concept (Seitze and Gologan, 2015) 15
Figure 2.7: Philosophy of TERA (Ogaji et al, 2007, p.4) 20
Figure 2.8: Flow Costs in an Operating Costs Model (Nalianda 2012, p.68) 23
Figure 2.9: Pulse Detonation Cycle (Musielak, N.D.) 30
Figure 2.10: Pulse Detonation Engine for Aerospace Applications Diagram 30
Figure 2.11: T-S Diagram Comparison of Brayton Cycle (1-2-3'-4') Against Humphrey Cycle (1-2-3-4) (Akbari and Nalim, 2006, P.2) 31
Figure 2.12: Wave Rotor Drum showing cyclindrical channels (Akbari et al, 2006) 35
Figure 2.13: Wave rotor located within a gas turbine (Noppel, 2011) 36
Figure 2.14: T-S Diagram for Gas Turbine Topped Wave Rotor Cycle (Brayton Cycle shown Dashed) (Welch et al, 1995) 37
Figure 2.15: Fuel burn Comparison of TurbOProp and TurboFan Equipped Aircraft (Walsh and Bil, 2015, P.6) 50
Figure 3.16: TERA Framework 53
Figure 3.17: Brick Data Flow (Apostolidis et al, 2013 p.4) 56
Figure 3.18: Typical Flight Mission Profile with Stepped Cruise (Laskaridis et al, 2005, p4) 59
Figure 3.19: *Tethys* Structure 65
Figure 3.20: Turbine Velocity Triangles and Nomenclature (Ramsden et al. 2013) 73
Figure 3.21: CFM56 Engine on Airbus A320 Aircraft (Collins 2006) 75
Figure 3.22: nacelle Design Component Split (Sun, 2012) 76
Figure 3.23: Nacelle Intake Dimensions and Numbering(ENdara Mayorga 2015, p.43) 77
Figure 3.24: Nacelle Afterbody Dimensions and Nomenclature (ENdara Mayorga 2015, p.48) 79
Figure 3.25: CUEJ56 vs. CFM56-5B Layout (Endara Mayorga 2015, p.100) 83
Figure 3.26: CUEJ56 Layout using Tethys Program 83
Figure 3.27: Nacelle Dimensions used for Weight Estimation (Jackson 2009, p. 107) . 90
Figure 3.28: Weight Model Structure 91
Figure 4.29: Schematic of CUEJ56 93
Figure 4.30: Variation of Net Thrust with Altitude and Mach N^{o} for CUEJ56 Engine Model 97
Figure 4.31: Variation of SFC with Altitude and Mach N^{o} for CUEJ56 Engine Model 97
Figure 4.32: Variation of Net Thrust with Ambient Temperature and Turbine Entry Temperature for CUEJ56 Engine Model 99
Figure 4.33: Variation of SFC with Ambient Temperature and Turbine Entry Temperature for CUEJ56 Engine Model 100

Figure 4.34: Payload Range Diagram Comparing Cranbus EJ320 and Airbus A320.. 103
Figure 5.35: CUEJ-LEAP Fan Pressure Ratio Optimisation..... 108
Figure 5.36: CUEJ-PPGT Fan Pressure Ratio Optimisation..... 109
Figure 5.37: Gearbox Losses Across Flight Range (Anderson et al, 1984, p.20)..... 110
Figure 5.38: Payload-Range Diagram Comparison for the Baseline and Additional Engines 113
Figure 5.39: CRANBUS EJ320 Cruise Mach Number Variation..... 115
Figure 6.40: HPC Pressure Ratio vs Block Fuel Burn 120
Figure 6.41:HPC Pressure Ratio vs Hub-Tip Ratio..... 121
Figure 6.42: HPC Outlet Hub Radius vd Hub-Tip Ratio 122
Figure 6.43: Fan pressure Ratio vs Block Fuel Burn 123
Figure 6.44: Booster Pressure Ratio vs Block Fuel Burn..... 125
Figure 6.45: Booster Pressure Ratio vs HPC Hub Radius..... 125
Figure 6.46: Bypass Ratio vs Block Fuel Burn 127
Figure 6.47: Block Fuel Burn Comparison, Short Range Mission..... 130
Figure 6.48: Block Fuel Burn Comparison, Long Range Mission..... 131
Figure 6.49: Payload Range Diagram Comparison..... 134
Figure 6.50: CUEJ-DD1-SR Short Range Schematic 139
Figure 6.51: CUEJ-DD1-LR Long Range Schematic 139
Figure 6.52: CUEJ-GT1-SR Short Range Schematic..... 140
Figure 6.53: CUEJ-GT1-LR Long Range Schematic..... 140
Figure 6.54: Economic Sensitivity Analysis Model Structure 141
Figure 6.55: Sensitivity analysis for Short Range CEUJ-DD1 and CUEJ-GT1 models at a fuel price of $69 per barrel In Comparison to Baseline..... 143
Figure 6.56: Sensitivity analysis for Short Range CEUJ-DD1 and CUEJ-GT1 models at a fuel price of $140 per barrel In Comparison to Baseline..... 145
Figure 6.57: Sensitivity analysis for Long Range CEUJ-DD1 and CUEJ-GT1 models at a fuel price of $69 per barrel In Comparison to Baseline..... 146
Figure 6.58: Sensitivity analysis for Long Range CEUJ-DD1 and CUEJ-GT1 models at a fuel price of $140 per barrel In Comparison to Baseline..... 146
Figure 6.59: Sensitivity analysis for Short Range CEUJ-DD1 and CUEJ-GT1 models at a fuel price of $69 per barrel In Comparison to A320 NEO Engines 147
Figure 6.60: Sensitivity analysis for Short Range CEUJ-DD1 and CUEJ-GT1 models at a fuel price of $140 per barrel In Comparison to A320 NEO Engines 147
Figure 6.61: Sensitivity analysis for Long Range CEUJ-DD1 and CUEJ-GT1 models at a fuel price of $69 per barrel In Comparison to A320 NEO Engines 147
Figure 6.62: Sensitivity analysis for Long Range CEUJ-DD1 and CUEJ-GT1 models at a fuel price of $140 per barrel In Comparison to A320 NEO Engines 148
Figure 7.63: Summary of Different Technologies – Fuel Burn vs Technology Readiness Level Compared to Approximately Yr 2000 Baseline..... 157

List of Tables

Table 3.1: Weight Estimations Summary and Error (Lolis et al, 2014) 85

Table 3.2: Weight model component breakdown comparison 92

Table 4.3: Parameters and Assumptions Used for CUEJ56 94

Table 4.4: Comparison of CUEJ56 with CFM56-5B/4 Data from Janes (2011 p. 177-188) 96

Table 5.5: A320 NEO Engines Available Data 106

Table 5.6: Engine Parameters and Assumptions Comparison 107

Table 5.7: Engine Performance Comparison 111

Table 5.8: CUEJ-LEAP and CUEJ-PPGT Weights and Dimensions 112

Table 5.9: Engine Mission Performance Comparison 114

Table 6.10: Parameters and Assumptions for Engines for Optimisation 117

Table 6.11: Parameters altered for the study 119

Table 6.12: Upper and Lower Boundaries for the Optimisation Variables 128

Table 6.13: Constraints applied in the Optimisation 128

Table 6.14: Main Aircraft Mission Parameters 129

Table 6.15: Optimised Engines Physical Breakdown 131

Table 6.16: Optimised Engines Performance 131

Nomenclature

Acronyms and Abbreviations

ACARE	Advisory Council for Aeronautics Research in Europe	-
ANOPP	Aircraft Noise Prediction Program	-
BPR	ByPass Ratio	-
CAA	Civil Aviation Authority	-
CAEP	Committee on Aviation Environmental Protection	-
CC	Combustion Chamber	-
CH_4	Methane	-
CLEAN	Component vaLidator for Environmentally friendly Aero-engine	-
CLEEN	Continuous Low Energy, Emissions and Noise	-
CR	Contra Rotating	-
CRTF	Contra Rotating Turbofan	-
CO_2	Carbon Dioxide	-
DDTF	Direct Drive Turbofan	-
DOC	Direct Operating Costs	£
DREAM	valiDation of Radical Engine Architecture systeMs	-
EC	European Commission	-
EDS	Environmental Design Space	-
EGT	Exhaust Gas Temperature	K
EIS	Entry Into Service	-
ERA	Environmentally Responsible Aviation	-
EU	European Union	-
FAA	Federal Aviation Authority	-
FLOPS	FLight Optimisation System	-
GTF	Geared Turbofan	-
GWP	Global Warming Potential	-
HPC	High Pressure Compressor	-
HPT	High Pressure Turbine	-
ICAO	International Civil Aviation Organisation	-
ICRTF	InterCooled and Recuperated TurboFan	-
IPCC	International Panel on Climate Change	-
IRA	Intercooled Recuperative Aero Engine	-
ISA	International Standard Atmosphere	-
JTI	Joint Technology Initiative	-
LDI	Lean Direct Injection	-
LPC	Low Pressure Compressor (Booster)	-
LPT	Low Pressure Turbine	-
MTOW	Maximum Take Off Weight	kg
NASA	National Aeronautics and Space Administration	-
NEO	New Engine Option	-
NEWAC	NEW Aero-engine Core concepts	-
N_2O	Nitrous Oxide	-
NOx	Nitrogen Oxides	-
NPC	Net Present Cost	-
NPSS	Numerical Propulsion System Simulation	-

OEW	Operating Empty Weight	kg
OEM	Original Equipment Manufacturer	-
OPR	Overall Pressure Ratio	-
PDE	Pulse Detonation Engine	-
PDRE	Pulse Detonation Rocket Engine	-
PROOSIS	Project Object Oriented SImulation Software	-
RPM	Revolutions Per Minute	-
RQL	Rich Burn/Quick Quench/Lean Burn	-
SF_6	Sulphur Hexafluoride	-
SFC	Specific Fuel Consumption	mg/Ns
TERA	Technoeconomic and Environmental Risk Analysis	-
TET	Turbine Entry Temperature	K
TRL	Technology Readiness Level	-
UDF	Unducted Fan	-
UK	United Kingdom	-
UN	United Nations	-
USA	United States of America	-
VITAL	enVIronmenTaLly friendly aero-engine	-
VTOL	Vertical Take-Off and Landing	-
WATE	Weight Analysis of Turbine Engines	-
WeiCo	Weight, Dimensions and Costs	-

Letters and Symbols

A	Area	m^2
AR	Aspect Ratio	-
dB	Decibel	-
C_D	Drag Coefficient	-
C_{D0}	Zero Lift Drag Coefficient	-
C_f	Skin Friction Coefficient	-
C_L	Lift Coefficient	-
Cp	Specific Heat at Constant Pressure	j/kgK
CR	Contraction Ratio	-
D	Diameter	m
E	Aerodynamic Efficiency	-
ft	Foot/Feet	-
g	Acceleration due to Gravity	m/s^2
h	Height	m or ft
H	Enthalpy	j/kg
J	Joule	-
K	Kelvin	-
K	Lift Dependent Factor	-
K_B	Blading Factor	-
kg	Kilogram	-
km	Kilometre	-
kN	KiloNewton	-
L	Stage Loading	-
L	Length	m
lbs	Pounds (force)	-

M	Mach Number	-
m	Metre	-
m	Mass	kg
mg	Milligram	-
MW	Mega Watt	-
N	Newton	-
N	Relative Rotational Speed	-
N	Number of Stages	-
nm	Nautical Mile	-
p	Static Pressure	Pa
P	Total Pressure	Pa
Pa	Pascal	N/m^2
Q_c	Drag Interference Factor	-
Q	Flow Function	-
R	Specific Gas Constant	K/kgK
R	Radius	m
s	Second	-
Swet	Wetted Area	m^2
t	Time	s
t	Static Temperature	K
T	Total Temperature	K
U	Blade Speed	m/s
v	Velocity	m/s
w	Mass Flow Rate	kg/s
W	Watt	J/s
W	Aircraft Weight	kg
η	Efficiency	-
B_c	Semi Boat-tail Angle	RAD
B_f	Boat-tail Angle	RAD
π	Pi	-
γ	Ratio of Specific Heats	-
ρ	Gas Density	kg/m^2
φ	Component Form Factor	-
Ω	Work Done Factor	-
£	Pounds Sterling	-
$	Dollars (US)	-

1.0 Introduction

The airline industry is very competitive. Airlines are under pressure to offer quick, reliable services at reasonable ticket prices. With an uncertain economic climate and an uncertain price of jet fuel fluctuating from a high of around $140 per barrel between 2011 and 2013 and reaching a low of less than $50 now, there is a real interest within the airline industry to reduce mission fuel burn considerably.

The overall aim of the project is to undertake a Techno-economic Environmental Risk Analysis (TERA) analysis from an aircraft operator's perspective to enable them to better understand the factors involved in the engine development process, to be able to help bridge the gap between aircraft/engine manufacturer and operator. This may then assist in any discussions between operators and original equipment manufacturers (OEMs), to enable them to have more of an influence in the direction of development to better suit the business model of the operator.

This project aims to do this by investigating the limit (in terms of turbine entry temperature (TET), overall pressure ratio (OPR), bypass ratio (BPR)) of the current gas turbine for use as aircraft propulsion in a conventional format (i.e. providing thrust for the aircraft) for a short to medium range jet aircraft. By investigating the limit of a conventional gas turbine, it is possible to not only see the maximum benefit available to this mature technology, but also to determine which future technologies may offer the most benefits for a particular airline market strategy. By focusing on finding the limit of 'conventional' technology, the aim is to find the point at which fuel burn/ direct operating costs (DOC) becomes attractive for novel technologies in comparison to the best conventional, albeit advanced, gas turbine. In other words, what fuel burn and ultimately DOC benefit must come from new technology in order to beat the best of conventional gas turbofans.

1.1 Objectives

Using an established airline operator as a case study, this project aims to quantify the fuel burn and DOC benefits that can be achieved by taking conventional gas turbine technology to its limit, based on key constraints such as suitable timeframe and airframe size. A qualitative study on novel, disruptive technologies, and the risks associated with these technologies was used to identify a potential pathway that is suitable for a short to medium range aircraft operator.

The overall aim of the project was to undertake a TERA analysis from the point of view of an aircraft operator to assess new aircraft and engine configurations and to understand the risks and costs associated with these new technologies. The project primarily focussed on different powerplant technologies. The following goals were identified:

- Establish a baseline centred on the current easyJet fleet aircraft using a 'Business as Usual' approach;
- To integrate engine performance, aircraft performance, engine sizing and weight models into a TERA framework;
- Undertake a sensitivity/parametric analysis to understand which factors are the most important to the solution;
- Design space optimisation to find a suitable engine configuration to meet the aspirations of a short to medium range aircraft operator;
- DOC analysis to determine at what point novel technologies could become attractive compared to advanced conventional gas turbine engines under a range of different fuel price scenarios.

1.2 Contribution to Knowledge

Having performed a review of the relevant literature, it is clear that although design assessments have been performed on novel engine cycles previously, these have usually been carried out on behalf of either international political organisations or OEMs to try

and meet international environmental aims. Within these studies, the end user of the equipment, generally an airline, is often not the focal point, participant, or aware of the research. A significant quantity of research work is funded by supra-national bodies such as the EU to assist in meeting environmental targets set by those same bodies (such as the ACARE Flight Path 2050 goals), and as such the business case for aircraft operators may not be considered.

This study aims to help fill the gap by investigating the limit (in terms of TET, OPR, BPR) of the current gas turbine for use as aircraft propulsion in a conventional format (i.e. providing thrust for the aircraft) for a short to medium range jet aircraft. By investigating the limit of a conventional turbofan, it is possible to not only see the maximum benefit available to this mature technology, but also to determine which future technologies may offer the most benefits for a particular airline market strategy. By focusing on finding the limit of 'conventional' technology, the aim is to find the point at which fuel burn/DOC becomes attractive for novel technologies in comparison to the best conventional, albeit advanced, gas turbine. In other words, what fuel burn and ultimately DOC benefit must come from a new technology in order to beat the best of a conventional turbofan for a particular aircraft type. To the best of the author's knowledge, this type of study has not been carried out in this way before.

It is for this reason that this study has come about and the contribution to knowledge can be summarised as follows: to undertake a techno-economic risk assessment of a conventional high bypass ratio turbofan in order to find a potential optimised engine for a particular aircraft type; and thus to investigate some of the limiting design parameters, such as physical core size and bypass ratio, which may hinder the further development of conventional turbofan engines in their ability to deliver additional fuel burn benefits. The study is undertaken from an operator/airline perspective and further quantifies the point at which the investment opportunity of a novel technology (e.g. open rotors, intercooled recuperated cores, wave rotors and pulse detonation engines) justifies the risks associated with it, in terms of fuel pricing and sensitivity to acquisition and maintenance costs.

1.3 Thesis Structure

The thesis is arranged in to the following chapter structure:

Chapter two provides an overview of the relevant literature, to help identify the gap in knowledge and provide an overview of some novel engine technologies that may be suitable for a short to medium-range passenger jet aircraft .

Chapter three provides the overall methodology followed during the project and describes the individual models used.

Chapter four provides a description and analysis of the baseline aircraft and engine configuration, while chapter five introduces two new engines: high bypass ratio geared and direct drive turbofans based on the new engines for the Airbus A320 NEO.

Chapter six provides details and the results of the optimisation study into a very mature turbofan able to fit onto an Airbus A320 type aircraft in conventional configuration, while chapter seven provides a discussion into which potential future technologies may offer improvements over this engine. Chapter 8 summarises and provides conclusions to the work.

2.0 Literature Review

This chapter begins by providing an overview of aero gas turbine engine trends and description of the methods by which aero gas turbine fuel efficiency can be improved. This is followed by a review of recent research into improving the efficiency of aero engines and the gap in literature that this work aims to fill. A description of what TERA is and a description of the environmental policy context that applies to current and future technology is then provided. The chapter finishes by providing qualitative descriptions of some technologies that may assist in providing a step change in aero-engine efficiency including potential benefits, challenges and technological maturity.

2.1 Aero-Engine Trends

The jet engine has evolved rapidly since the early engines developed before and during the Second World War. While the original engines were designed for fighter aircraft applications, where fuel economy, noise and reliability were deemed unimportant compared to the primary goal of maximum thrust and minimum weight (Saravanamuttoo, 2002), it is difficult to imagine contemporary air travel without the use of gas turbine propulsion. Indeed, turbojets were originally thought a poor choice for civil aircraft propulsion, due to weight limitation issues (ibid.). However, since then, the jet engine and its derivatives have become the primary choice for civil passenger aircraft propulsion.

Improvements in the gas turbine in terms of fuel burn, reliability, noise and emissions for aircraft propulsion have come as a result of several different factors. Increases in engine bypass ratio have helped to alleviate noise (Fig. 2.1), as well as improve fuel burn due to better propulsive efficiency.

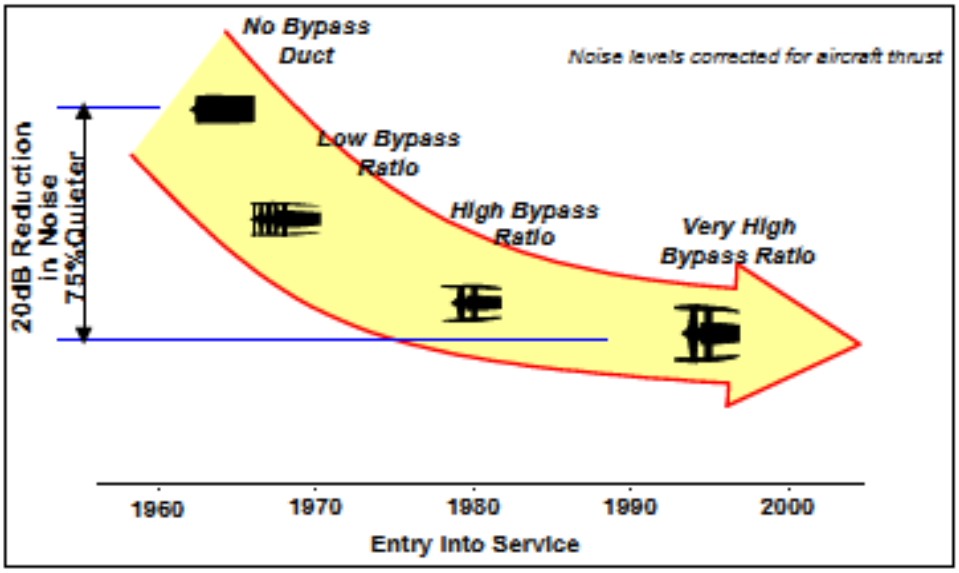

FIGURE 2.1: AIRCRAFT NOISE AND BYPASS RATIO TRENDS (BIRCH, 2000)

Improvements in material technology and turbine cooling systems have allowed for higher TETs, improving thermal efficiency (Figures 2.2 and 2.3). Improvements in our understanding of aerodynamics, including compressibility and boundary layer effects, have enabled compressors to achieve higher pressure ratios with fewer stages (Saravanamuttoo, 2002), helping reduce weight and manufacturing costs, while also helping to improve thermal efficiency and consequently fuel burn.

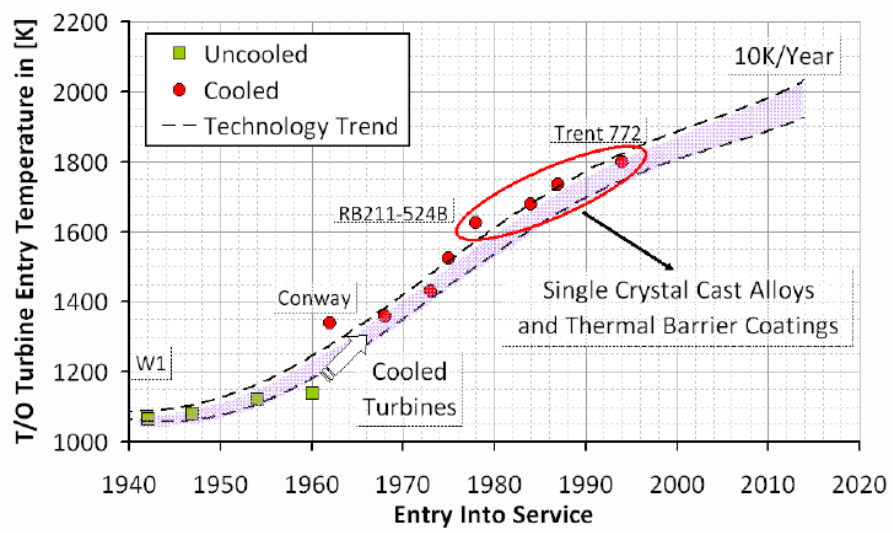

FIGURE 2.2: TURBINE ENTRY TEMPERATURE EVOLUTION (KYPRIANIDIS, 2011)

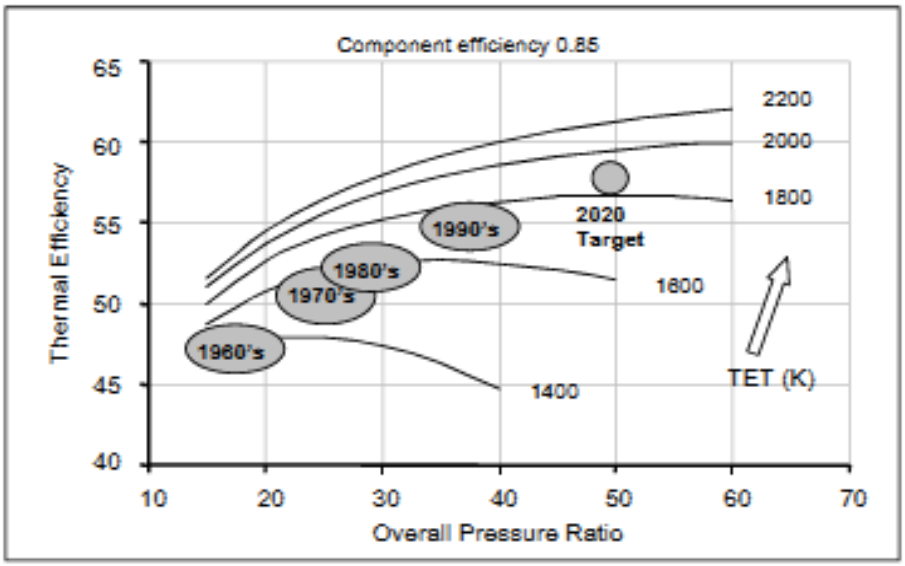

FIGURE 2.3: THERMAL EFFICIENCY VARIATION WITH OVERALL PRESSURE RATIO AND TURBINE ENTRY TEMPERATURE (BIRCH, 2000)

Engine reliability has improved mainly due to the maturity of engine control systems and increased testing of the engines during development (Birch, 2000), which has resulted in an in-flight engine shut down rate improvement of a factor of 10 since the 1970s.

In terms of emissions, however, while improvements in CO_2 reduction are commensurate with a reduction in fuel burn, increasing both TET and OPR tends to increase nitrous oxide (NOx) production within the combustion chamber (Lefebvre, 2010). There exists a potential conflict between the goals of fuel burn reduction and NOx emission reduction, which is recognised by the International Civil Aviation Organisation (ICAO), which provide worldwide NOx regulation limits around airports through the Committee on Aviation Environmental Protection (CAEP) limits. The ICAO regulations allow higher NOx production levels for higher OPR engines (Figure 2.4), which highlight the difficulties in achieving lower fuel burn and NOx emissions.

There are several different methods for achieving lower NOx emissions within the combustor, which include:

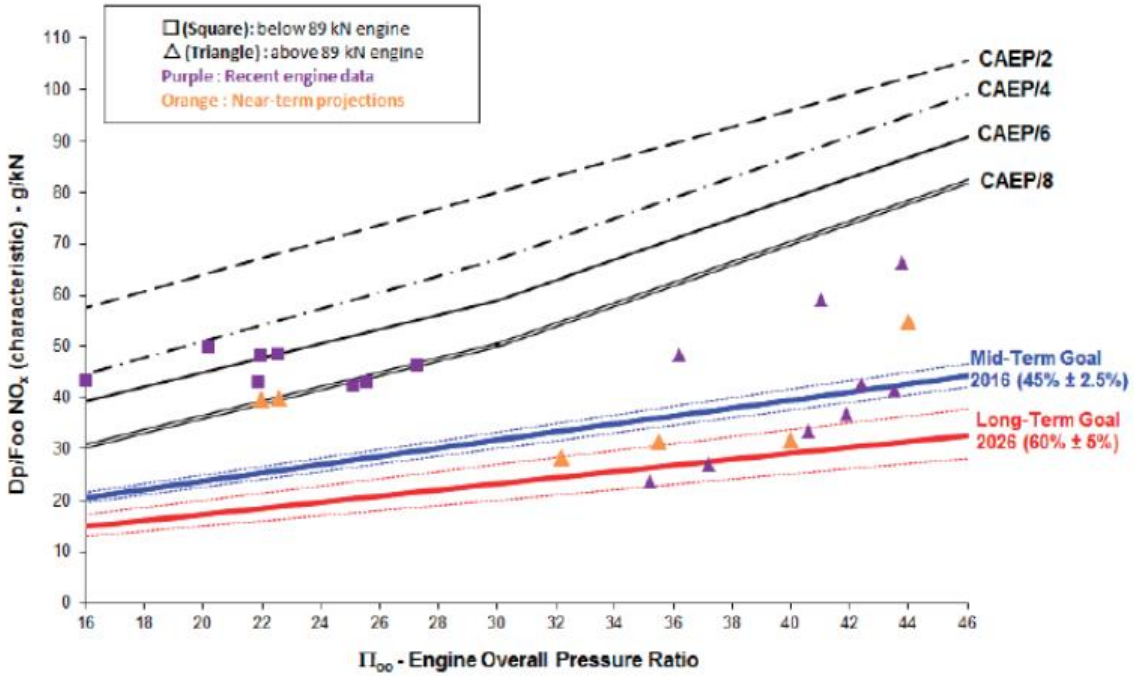

FIGURE 2.4: ICAO NOX EMISSION CHARACTISTIC REGULATIONS (DICKSON, 2014)

Lean-Premixed-Prevapourised combustion, in which the fuel and air are mixed prior to entering the combustion chamber, to provide a uniform mixture that aims to achieve a low temperature burn (Lefebvre, 2010; Tacina, 1990). This method first tried during the 1970's, however it is susceptible to auto ignition and flashback and has narrow stability limits (ibid.);

Rich Burn/Quick Quench/Lean Burn (RQL) where fuel is burnt rich within the primary combustion zone, quickly transitioning to lean combustion with a large quantity of secondary air being introduced further downstream, 'quenching' the flame. This method aims to avoid stoichiometric combustion as much as possible, reducing peak combustion temperature (ibid.). This approach also suffers from flame stabilisation issues and is more suited to stationary gas turbines than aero-engines, where there is a requirement for safety and reliability (el_Hossaini, 2014);

Lean Direct Injection (LDI) aims to operate with a lean-burn zone and also avoid stoichiometric flame temperatures. All of the air that is to be used for combustion, excluding that for liner cooling, enters the combustion chamber. Fuel is injected directly

into the stream of air. The key to avoiding hot spots is to have rapid fuel and air mixing, to achieve uniformity in the fuel-air mixture. This is done by using a swirler to create a vortical air flow and combined with a spray atomiser for the fuel (Tacina et al, 2014).

2.2 Improving Fuel Consumption

Given the advances and evolution of the gas turbine to near maturity, how can fuel consumption be further lowered? A good starting point is to look at specific fuel consumption (SFC). SFC is the fuel flow divided by the net thrust of the engine, but can also be related to cycle efficiency parameters (Birch, 2000):

$$SFC = V_0 / \eta_{th} \eta_{prop} F_{HV} \qquad \textit{equation 2.1}$$

Where V_0 is the flight speed, η_{th} is the thermal efficiency, η_{prop} is the propulsive efficiency and F_{HV} is the fuel calorific value. Given that flight speed has been remained fairly steady for subsonic jet aircraft at about Mach 0.8 for the last 50 years and that kerosene or equivalents are likely to remain as a fuel for the near future, further improvements in SFC will come from improving propulsive and thermal efficiencies.

The thermal efficiency of an engine is how efficiently the engine can convert the incoming energy from fuel in to useful work. It is a function of the OPR, TET and individual component efficiency (ibid.). Figure 3 shows how thermal efficiency is related to OPR and TET. The chart shows that improvements in efficiency come about from a combined increase on both TET and OPR (ibid.). This has been achieved through improved technology in terms of new materials able to withstand higher temperatures and better turbine cooling. To increase TET and OPR further, these technology improvements must continue to be made, otherwise the benefits from the cycle improvement will be negated by the need for increased cooling flows. This is demonstrated in Figure 2.5, which shows that SFC improvements can still be made with constant component efficiency, but with improvements in cooling technology such that the cooling flow requirement stays the same. If cooling technology remains constant, such that an increased turbine cooling flow is required, the gains from further cycle improvements is limited (Horlock et al, 2001,; Wilcock et al, 2005). Birch (2000)

considers that gains in SFC from improvements in thermal efficiency of a conventional cycle will be about 3%, provided that materials and cooling technology also improve.

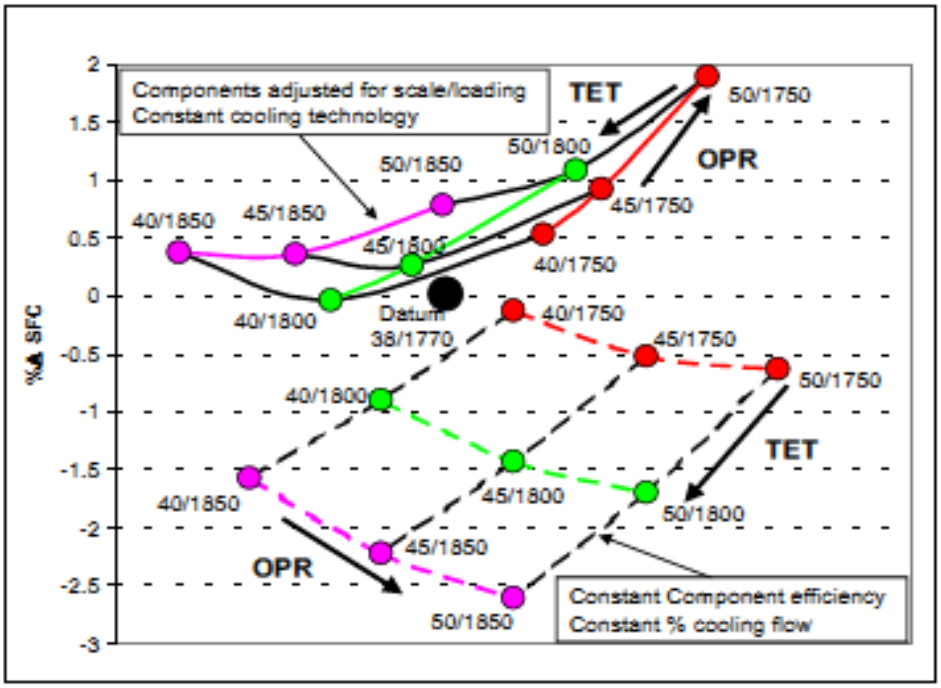

FIGURE 2.5: SFC VARIATION WITH OPR AND TET (BIRCH, 2000)

Propulsive efficiency is defined as being the *"useful propulsive power produced by the engine divided by the rate of kinetic energy addition to the air*" (Walsh and Fletcher 2004, p.294) with the formula:

$$\eta_{prop} = 100 * \frac{2}{1 + V_9 / V_o} \qquad \textit{equation 2.2}$$

Where stations 0 and 9 are free stream and propelling nozzle respectively (ibid. p. 312). As the formula shows, propulsive efficiency increases as the overall jet velocity reduces towards the free stream velocity. The propulsive efficiency of aero-engines has improved by increasing the bypass ratio (BPR), with larger diameter fans, increasing the overall mass flow through the engine, and hence reducing the specific thrust. Reducing specific thrust further by increasing bypass ratio and mass flow through the engine

should reduce fuel burn further through increased propulsive efficiency, however, this would result in larger engines, which would have the effect of increased weight and drag, offsetting the potential gains (Birch, 2000).

2.3 Recent Engine Research

Improving fuel efficiency will therefore come about from an increase in thermal and/or propulsive efficiencies. Several research projects have been undertaken to investigate improving these efficiencies.

The enVIronmenTALly friendly aero engines (VITAL) project ran between 2005 and 2007 (EU, 2006) and sought to investigate new direct drive, geared and contra-rotating turbofans to see if they could achieve the goals set out in the *European Aeronautics: A Vision for Europe 2020 (EC, 2001)* document, which is now administered by the Advisory Council for Aeronautical Research in Europe (ACARE). The project was carried out by a group of different companies, manufacturers, universities and organisations across Europe including Cranfield University, Rolls-Royce, MTU and Snecma. Overall, this project aimed to improve the propulsive and noise efficiency of gas turbine engines by concentrating on the low pressure sections of the engine. The project focussed on lightweight technologies for the fans, compressors and turbines including new polymer composite materials with improvements in manufacturing processes, as well as improved aerodynamic design of the turbomachinery.

Three different configurations were investigated: a direct drive turbofan (DDTF), a geared turbofan (GTF) and a counter-rotating turbofan (CRTF). The DDTF used low weight technologies for the fan to find a new optimum trade-off between the rotational speed of the fan and turbine. The GTF allows for the booster and low pressure turbine to rotate at higher speeds than the fan, potentially allowing for fewer turbine stages and saving weight and length on the engine. The CRTF has two counter rotating fans, which allows for lower rotational speeds. Korsia and Guy (2007) and Korsia (2009) provide a good description of the VITAL project.

As part of the VITAL project, a multi-disciplinary design space tool, TERA2020 (discussed later in this chapter), was developed by a number of Universities across Europe, including Cranfield University in the UK, Chalmers University in Sweden, the National Technical University of Athens, Aristotle University of Thessaloniki, ISAE/SUPAERO and the University of Stuttgart (Kyprianidis, 2010). TERA2020 was used to investigate the various benefits (fuel burn, lower DOC, lower noise, lower CO_2 and NOx emissions) that the VITAL engines might potentially give.

Colmenares Quintero (2009) used a version of the TERA2020 framework to investigate the engines created under the VITAL project and their feasibility for use on short range civil aircraft (the Airbus A320 was used as the baseline aircraft). Colmenares Quintero used a TERA framework consisting of engine and aircraft performance modules, NOx emission, weight and noise emission estimation modules and a financial module to assess both the proposed VITAL engines, but also versions of these engines optimised for low fuel burn, noise, emissions and DOC by varying the bypass ratio and fan pressure ratios. Colmenares Quintero then used a simpler version of TERA consisting of engine, aircraft, economic and emissions module to investigate intercooled and intercooled-recuperated, and constant volume combustion engines.

Although Colmenares Quintero investigated future engine designs suitable for a short-range civil aircraft, a number of considerations were not included in the work. Colmenares Quintero took into account the overall size of the engine to account for weight and drag for the aircraft performance, no consideration could be seen in the work that thought was given to being able to fit or install the engine on the aircraft. In addition, only the fan pressure ratio and bypass ratio were altered for the optimised cycles, leaving the overall pressure ratio and turbine entry temperatures the same, mainly because he was looking at potential engines with a 2020 EIS. As such, the work offered a snapshot of potential engines powering a short range civil aircraft in a 2020 timeframe, without considering the ultimate benefit that conventional engines could achieve.

Kyprianidis (2010) also investigated the VITAL engines using the TERA2020 tool, however instead of investigating any potential benefits these engines might offer, he instead looked at what the impact might be in terms of noise and CO_2 emissions should individual technological advancements within the VITAL project fail to be delivered.

Further research into improving thermal efficiency was investigated in the validation of Radical Engine Architecture systeMs (DREAM) project, also funded by the EU. It consists of a consortium of the major European aero-engine manufacturers, led by Rolls-Royce (DREAM, 2012a). The project looks solely at the engine, nacelle and pylon of a typical civil passenger aircraft in isolation and is looking at two new open rotor concepts (geared and direct drive), alternative fuels and innovative systems. (DREAM, 2012). Bellocq et al (2014, 2015) provide a good overview of the modelling and configurations in the DREAM project.

Bellocq et al (2014, 2015 & 2016) undertook preliminary multidisciplinary optimisation studies using a modified version of the TERA2020 framework to investigate the effects of controlling the propellers of a counter-rotating geared open rotor engine as part of the DREAM project. A 2020 EIS was used as the technology date for the engines. The engines were not compared to a baseline turbofan, but showed how control of the propellers could affect fuel burn, noise and emissions of the engine.

The open rotor concept has seen a resurgence in interest in recent years in both the DREAM project and also the Clean Sky Initiative. The Clean Sky project is a major EU 'Joint Technology Initiative' (JTI, Clean Sky, 2012) with leaders from the European aerospace manufacturing industry (Clean Sky, 2012a) and other partners from across the EU. Clean Sky seeks to *"demonstrate and validate the technology breakthroughs that are necessary to make major steps towards the environmental goals sets by ACARE ...to be reached in 2020"* (Clean Sky, 2012b). The project is set to run from 2008 until 2017 and will investigate not only new airframe and engine technologies, but also different ways of using existing aircraft to reduce their impact on the environment. An example of this work is given by Pervier et al (2011), where an optimisation was performed to optimise aircraft mission trajectories and shows the trade-offs between

mission time and fuel burn, and mission NOx generation for typical passenger jet aircraft over different ranges. As part of the Clean Sky project, Snecma is planning to test a counter-rotating double open-rotor engine in 2019 (Gubisch 2014), which claims to have a noise level comparable lower than currently available CFM-56 engine with a fuel burn up to 30% lower.

The interest in open rotor engine research has followed on from several research projects carried out in the 1980's such as the General Electric Unducted Fan and the Pratt & Whitney, Allison, and Hamilton Standard 578-DX (Kyprianidis, 2011), which both reached demonstrator stage. These programs garnered interest following the 1973 oil price shock, which saw the price of crude oil quadruple (Macalister, 2011) which saw demand for more fuel efficient engines rise. Open rotor configurations allow for high bypass ratios, with advanced propellers to allow higher flight speeds to be achieved over normal propeller designs (Barnard & Philpott, 2004). Open rotor engines can benefit from reduced nacelle drag and weight benefits compared to turbofans, but noise is a particular issue (Kyprianidis, 2011).

Further research on improving the propulsive efficiency of aircraft and engine configurations can be found in NASA's N3-X program, which combines a blended wing body with distributed propulsion. In this configuration, the power generator is separated from the thrust producing unit. This could potentially allow for far higher bypass ratios than are currently achievable, as a single gas turbine could power several distributed fans around the fuselage. This configuration also allows for different power sources to be used, potentially nuclear, although it also relies on several immature technologies, such as superconducting wires, and is therefore a significant period of time away from being fully realised. Kim et al (2014) provide a good introduction to the NASA N3-X project.

Seitze and Gologan (2015) of Bauhaus Luftfahrt have investigated a 'propulsive fuselage' aircraft, where a large engine is embedded in the rear of the fuselage (Figure 2.6). This concept aims to improve the synergy between the propulsion system and airframe to provide an overall benefit in propulsive efficiency. The concept uses

boundary layer ingestion from the rear engine, which effectively helps to suck the boundary layer from the fuselage, helping to reduce airframe drag, improving the overall efficiency of the engine/aircraft.

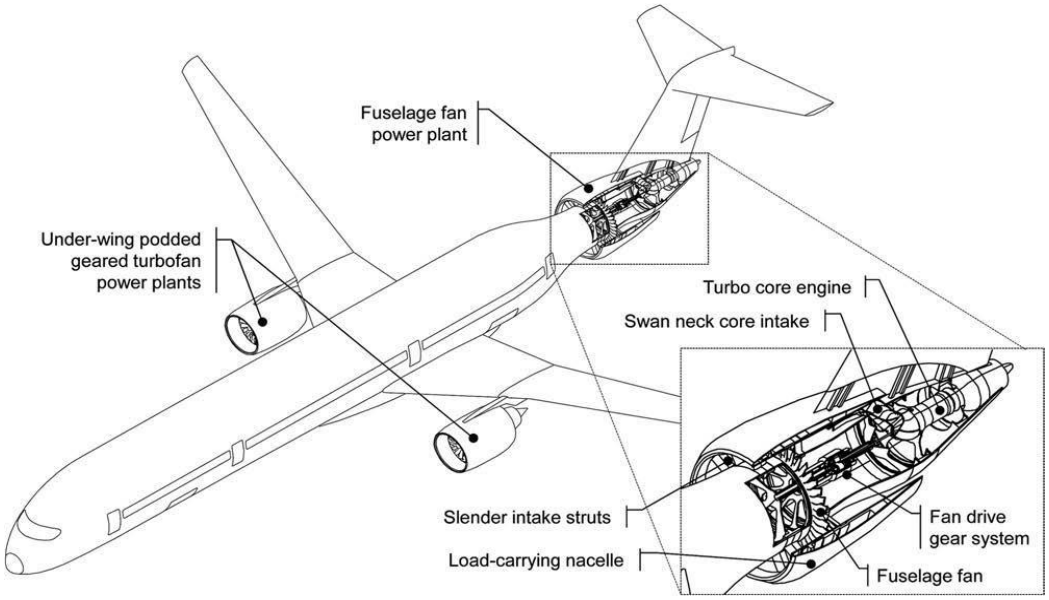

FIGURE 2.6: PROPULSIVE FUSELAGE CONCEPT (SEITZE AND GOLOGAN, 2015)

In terms of increasing thermal efficiency, the NEW Aero engine Core concepts (NEWAC) project was a complementary project to VITAL and sought to focus on engine core technologies to meet the ACARE Vision 2020 goals (EU, 2012). The project ran between May 2006 and April 2010, and investigated, amongst other technologies (a good overview can be found in Rolt & Kyprianidis, 2010 and Wilfert el al, 2007), four different types: intercooled core, intercooled recuperated core, active core and flow controlled core engines (NEWAC, 2016). The project was led by MTU and partners included the major European aero-engine and airframe manufacturers along with some European research institutions.

Kyprianidis (2010) used the TERA2020 tool consisting of engine and aircraft performance modules, engine weight and dimension estimation modules, noise, emissions and DOC estimation modules to perform a multidisciplinary optimisation on the intercooled, recuperated and intercooled recuperated engines that form part of the NEWAC project. Using an Airbus A330-200 long range aircraft flying a mission of

5,500km, Kyprianidis compared these engines to a 2020 EIS turbofan engine, and then performed an optimisation study to find a potential optimal turbofan engine for a 2020 EIS which includes heat exchange technology. Similar to Colmenares Quintero, although Kyprianidis investigated potential future engine designs, these were limited to a 2020 EIS date and were therefore constrained by technology predictions for that time.

A comparison of several different unconventional core architectures, introduced into a turbofan as part of a hybrid cycle, was carried out by Noppel (2011). A one dimensional engine simulation code was created to investigate a baseline turbofan, as well as wave rotor, pulse detonation and internal combustion engine hybrid turbofan cycles. An estimation of weight and aircraft block fuel burn was carried out. Noppel concluded that improvements in block fuel burn could be gained from both the pulse detonation and internal combustion combined cycles, with the wave rotor hybrid cycle offering little benefit. This study, however, failed to take into account any sizing considerations of the aircraft or engines - indeed no specific aircraft was considered, just an estimation of performance for a generic aircraft using the Breguet range equation. The study was therefore an investigation as to whether there was any potential in these cycles, rather than investigating the feasibility of them.

2.4 The Gap

Although much research has been carried out on new engine and airframe concepts in recent years in order to meet increasingly stringent environmental goals, one important stakeholder is not normally the focal point of the research - the airlines who operate the aircraft and engines. This is not perhaps too surprising, there is a market for airframe and engines, and all participants are competing within the same technology, so other constraints, particularly environmental concerns, become more important. However, there is demand from airlines, as evidenced by easyJet's 'ecoJet' proposal (easyJet, 2007), to push things on a little more than they appear to be (literally appearance - lots of research is carried out to improve engine efficiency, although the latest passenger aircraft to be released, the Boeing 787 Dreamliner, looks visually similar to a Boeing 707 released in the 1950's - a tube fuselage with engines mounted under the wings), to

have more radical designs entering the market. The author has not found a recent example of an airline being involved in an engine research project. Watts (1978) provided an airlines prediction of air travel and technology up to the year 2000, and was correct in his view that the environment would become increasingly important.

Another gap that is apparent from reading the literature is that no work has been found that investigates how much further a conventional gas turbine could go in terms of fuel efficiency when applied to a specific case. When reading the literature from the recent European Union funded projects investigating new engine technologies, the newer, disruptive technologies are usually compared with conventional turbofans for a particular entry into service date. This is not perhaps surprising. There is an underlying assumption that conventional technology will continue to evolve as it has done over the years, but to meet more challenging environmental goals, a step change in technology to meet these goals is investigated. Accordingly, new technologies are compared to conventional gas turbines for a specific EIS date. This is a sensible approach because it enables two engines of similar technology level to be compared.

However, a different approach could be taken. From the point of view of an aircraft operator who has to make purchasing decisions based on what is available in the market at a particular time, it may be beneficial to instead look at what could potentially be the best possible conventional engine for a particular aircraft configuration and market strategy. By finding this potential end point, new technologies can be compared against this and aircraft operators could make more informed choices when it comes to purchasing, or having input into the direction that manufacturers take for developing the new technology.

This study therefore aims to help fill the gap by investigating the limit (in terms of TET, OPR, BPR) of the current gas turbine for use as aircraft propulsion in a conventional format (i.e. providing thrust for the aircraft) for a short to medium range jet aircraft. By investigating the limit of a conventional gas turbine, it is possible to not only see the maximum benefit available to this mature technology, but also to determine which future technologies may offer the most benefits for a particular airline market strategy.

By focusing on finding the limit of ‘conventional’ technology, the aim is to find the point at which fuel burn/DOC becomes attractive for novel technologies in comparison to the best conventional, albeit advanced, gas turbine. In other words, what fuel burn and ultimately DOC benefit must come from new technology in order to beat the best of conventional gas turbines.

2.5 TERA Overview

The focus of jet engine design has evolved over the years as our understanding of the science and technology has improved. The traditional approach to jet engine design in the 1960's was to focus on specific thrust and specific fuel consumption (SFC) for an uninstalled engine (Hudson, 1999 cited in Whellens, 2002 p.10). This has moved on to now consider a whole raft of issues including direct operating costs (DOC - fuel costs, purchase costs, maintenance costs), environmental considerations (including CO_2 emissions, NOx emissions and noise) as well as the performance of the engine (ibid.). In order to design future generations of engines, a more 'front-loaded' approach is required to design the engines effectively, taking into account all of the constraints, and reduce overall design costs accordingly. This is where a Technoeconomic and Environmental Risk Analysis (TERA) framework comes in.

2.5.1 History of TERA

A brief history of TERA is given in Kyprianidis et al (2008), which is expanded upon here. TERA models have been developed at Cranfield University since the mid 1990's. One of the first to use this kind of approach was Vincente (1994), who studied the "*effect of bypass ratio on long range subsonic engines"* (ibid.). In the research, she provided a comparison between two existing aero-engines - Rolls Royce Trent and General Electric GE90 turbofans - and an 'imaginary' very high-bypass ratio engine. The engines themselves were modelled in TURBOMATCH, Cranfield University's in-house gas turbine performance code, while engine weight and drag were also modelled, to try and assess the 'installed' thrust and SFC's of the engines.

Following on from this, and showing the versatility of the TERA approach, Gayraud (1996) applied a technical and economic assessment to support the decision making process for industrial gas turbines in an electricity generating plant. He used TURBOMATCH to model a General Electric MS9001 FA engine and combined it with an economics model, taking into account pay-back time, cash flow and discounted cash flow. The ultimate result was to develop a 'Decision Support System' to aid in the selection of industrial gas turbines for independent private companies in the privatised electricity generation market.

Further work on TERA continued with Whellens et al (2003), who combined an engine performance model, engine weight model, aircraft mission model with a genetic-algorithm based optimiser, to study the benefits of an intercooled recuperated turbofan (ICRTF) over existing turbofan engines for a long-distance passenger aircraft. The objective of the optimisation was to reduce mission fuel burn by optimising various cycle parameters of the engine (such as bypass ratio, fan pressure ratio, overall pressure ratio and turbine entry temperature). The study found that the ICRTF engine could offer lower mission fuel burn (up to 6% lower), but only for smaller aircraft with lower thrust, with the example of long range business jets being given. The work also found, however, that for these smaller aircraft, take-off NOx was considerably higher than the optimum conventional turbo-fan by up to 1.7 times. It is worth noting that the models used for engine performance and mission profile were simplified to speed up the optimisation, i.e. the engine performance model didn't use any component maps and the mission model only used the take-off and cruise segments of the profile.

The formalisation and coining of 'TERA' occurred during the European Union's (EU) enVIronmenTALly friendly aero-engine (VITAL) project. This project ran between 2005 and 2007 (EU, 2006), and sought to investigate new direct drive, geared and contra-rotating turbofans to see if they could achieve the goals set out in the *European Aeronautics: A Vision for Europe 2020 (EC, 2001)* document, now administered by the Advisory Council for Aeronautical Research in Europe (ACARE). The project was carried out by a group of different companies, manufacturers, universities and organisations across Europe and it fell to Cranfield University to develop the 'TERA

2020' architecture for this project (Ogaji et al, 2007). This was done in order that these new technologies could be assessed to see if they meet the ACARE goals before any prototypes were built, ultimately to help lower overall design costs.

2.5.2 What is TERA?

Up to now the history and the application of TERA within large scale projects have been discussed, but what is TERA? The following section describes the TERA framework in more detail and outlines a typical approach used for aero-engine modelling.

TERA is a tool that can be used to assess mainly gas turbine engines (although there is no reason why this couldn't be expanded to other areas) with *"minimum global warming impact and lowest cost of ownership in a variety of emission legislation scenarios, emissions taxation policies, fiscal and air traffic management environments"* (Ogaji et al, 2007, p.1). TERA uses a modular, multi-disciplinary (in that several different disciplines are used such as gas turbine performance, noise modelling, emission modelling, aircraft performance e.t.c.) approach to optimise a particular 'goal' function, such as fuel burn, noise or global warming potential (ibid. p. 4). Figure 2.7 shows the TERA philosophy used in the VITAL project. The framework is explained in detail in Ogaji et al (2007) and is summarised below.

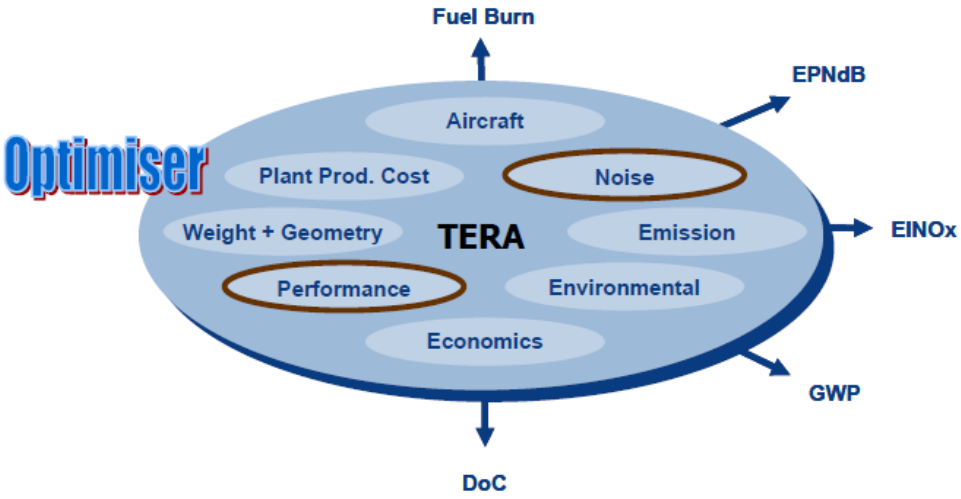

FIGURE 2.7: PHILOSOPHY OF TERA (OGAJI ET AL, 2007, P.4)

The TERA framework consists of several modules which are integrated together with an optimiser. The optimiser used for VITAL was a commercial optimiser called iSIGHT, although other user made genetic-algorithm optimisers have also been used, such as in Whellens et al (2003). The different modules are individual models that perform a specific function, such as an engine performance model or aircraft performance model. These are brought together within the optimiser, which can then give the 'optimum' result based on the end goal and individual parameters within the models that are set. Typical modules used for evaluating aero-engines are explained below.

Engine Performance Module: This can perhaps be considered the heart of the TERA framework, this is where the engine itself is modelled and simulated so as to give realistic results. Results given include gross and net thrusts, SFC, and exhaust gas temperatures (EGT). TURBOMATCH is Cranfield University's in-house code and was used for the VITAL project, although other engine performance models can be used, such as GasTurb (Colmenares Quintero, 2008 p.84).

TURBOMATCH was created at Cranfield University and uses 'bricks' to simulate individual components within a gas turbine such as compressors, turbines and nozzles. Bricks can also be used for arithmetic functions also. TURBOMATCH can and has been used to simulate various gas turbine engines from a simple cycle single shaft turbojets to more complex multi-shaft turbofan engines, to even more novel cycles such as wave rotors.

Aircraft Performance Module: The aircraft performance module contains the aircraft geometric and mission data. A programme such as Cranfield University's HERMES code can be used for this.

HERMES originally came from a way to assess more electric civil aircraft (Laskaridis, 2005) and has been adapted to simulate nearly any aircraft type. The code calculates lift and drag polars for the aircraft based on inputted geometric and empty aircraft weight details from the user. The code also simulates high lift devices such as flaps and slats at take-off and landing. The user inputs mission data such as taxiing time, take-off climb

rates, cruise altitude, cruise Mach number, diversion fuel, and descent data. The model interacts with TURBOMATCH via a program called 'Turbomatchcalls', which 'runs' the engine based on the thrust requirements and mission profile given by the user. HERMES then calculates a range of performance indicators such as fuel used, time taken and distance covered for the aircraft. HERMES can also give a maximum range for the aircraft based on the amount of fuel it has on board. Another example of an aircraft performance module used in TERA is given in Nalianda (2012).

Economics Module: The economics module used in VITAL comprises three different models - a life estimation model, an economics model and a risk model. The life estimation model is used to simulate the life of the hot section turbine discs and blades through a creep and fatigue analysis. This is combined with the economics model which utilises maintenance period, labour costs and capital costs of the engine to estimate the engine maintenance costs. The risk model studies the effect of changes in some of the input parameters on the net present cost (NPC) of the engine. Outputs of the module are (Pascovici et al, 2007, p.9):

- "*Direct operating cost (DOC k€)*
- *Engine maintenance cost (k€)*
- *Net present cost*
- *Cost of taxes*
- *Cost of airframe maintenance*
- *Stresses of the blades and disk*
- *The cost of labour and materials used in the overhaul"*

Further details of this economics module are given in Pascovici et al (2007). A further economics model has been developed by Nalianda (2012) detailing operating costs over an aircraft mission, shown in Figure 2.8 .

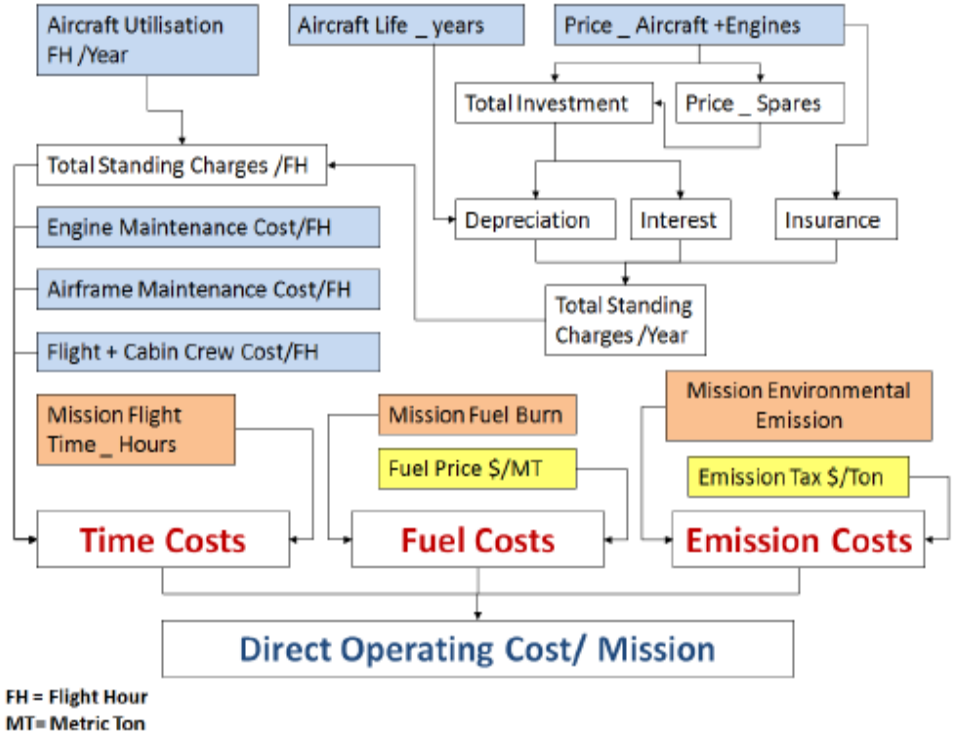

FIGURE 2.8: FLOW COSTS IN AN OPERATING COSTS MODEL (NALIANDA 2012, P.68)

Environmental Module: A parametric model was used in VITAL, which assesses the global warming potential (GWP) of the engine. The GWP index integrates the man-made emission radiative forcing effect along a pre-determined time period. This then gives an equivalent mass of CO_2. While this approach is good for well mixed molecules (such as carbon dioxide, methane and nitrous oxides), it does not take into account ozone or contrails.

Noise Module: The aircraft noise model used in VITAL was called SOPRANO and is a proprietary code made by a company called ANOTEC. The software calculates the overall noise level for an aircraft based on data from the aircraft and engine performance modules (Colmenares Quintero, 2008). The noise module itself is concerned with noise at three points at landing and take-off: *"sideline, cutback (flyover) and approach"* (Ogaji et al, 2007, p. 7), as these are required for certification. These points are time integrated to give the 'Effective Perceived Noise Level" (EPNL), for which there is a do not exceed limit.

Emissions Module: The emissions module output is by the economic module to estimate emission taxes, and the environmental module to provide the data for the GWP. In VITAL, an empirical approach was used, which used the work of Rizk and Mongia (1994, cited in Ogaji et al, 2007) to develop prediction equations to determine the emissions index for pollutants such as NOx, carbon monoxide and unburned hydrocarbons.

HEPHAESTUS, developed by Cranfield University, is another code that could also be used for this task. This code assesses the environmental emission performance of different combustor designs from a suite of different emission prediction software (Celis, 2009). The software uses empirical, semi-empirical and a partially stirred reactor model within the suite. HEPHAESTUS uses thermodynamic data from TURBOMATCH to predict emissions for the landing and take-off phase and data from HERMES to predict emissions during the flight.

Weight Module: The weight module is used to predict the weight of novel engines which have yet to be built. The module used in VITAL called WeiCo (Weight, Dimensions and Costs) has a catalogue of materials, component weights and geometries that are used in the other modules such as the aircraft module to predict aircraft weight and hence lift and drag, plant cost for the estimation of cost of the engine and the noise module for the estimation of turbomachinery noise.

Plant Production Cost Module: This module estimates the production costs of manufacturing the novel engine. It is a very complex module that has a large number of factors affecting it such as materials availability, technology levels, varying wages, production numbers e.t.c. The module reflects realistic cost trending.

2.6 Other Multi-Disciplinary Optimisation Tools

A similar concept to TERA has been developed independently in the USA called 'Environmental Design Space' (EDS). This has been developed by the FAA, Georgia Institute of Technology and Michigan Institute of Technology (CAEP7, 2007). EDS has

been designed to assess noise, emissions and performance of current and future aircraft and engine configurations, taking into account different economic and policy scenarios. EDS uses five different modules, developed by NASA, to perform this.

The five modules are very similar to those used within TERA and consist of (Spindler, 2007):

- Numerical Propulsion System Simulation (NPSS) - Engine simulation software
- Weight Analysis of Turbine Engines (WATE) - Engine weight model
- Flight Optimisation System (FLOPS) - Aircraft mission and performance simulation model
- Aircraft Noise Prediction Program (ANOPP) - Noise prediction model
- Empirical relations emissions module

The five modules would work together to help inform policy making and even to assess the market for future aircraft. EDS has been assessed by Spindler (2007) using a current Boeing 777 and found that despite a few minor problems with some models, overall the EDS could perform with a relatively high level of confidence. It is unknown if EDS will be publicly available, but it is interesting to see that a framework similar to TERA is being developed independently to perform a similar function.

2.7 Environmental Policy and Targets Context

The issue of climate change is a topic with a lot of political impetus around the world and because current commercial passenger aircraft use engines which burn fossil fuels, aviation is an industry which is targeted for emission reduction. A report by the Intergovernmental Panel on Climate Change (IPCC), Aviation and the Global Atmosphere (IPCC, 1999), estimated that aviation contributes approximately 3.5% of all radiative forcing (measured in W/m^2, radiative forcing is a value of how important a particular mechanism is to climate change (ibid, p.3)) from anthropogenic sources (ibid p.8). This has recently been updated to approximately 3% (ICAO 2012). With a growth

in aviation, this contribution is expected to increase to about 5% in 2050 (IPCC,1999). Within this context, it is clear that environmental policies will likely play a role in the development of aircraft and engines. It is therefore necessary to examine some of these policies to see what impact they may have on future aircraft and engine development.

2.7.1 Global Policies

The major international policy on climate change is the *Kyoto Protocol* (UN, 1998). The protocol came into force on 16 February 2005 and requires the countries listed in Annexe 1 (which includes the UK) to reduce their emissions of certain gasses (carbon dioxide CO_2, nitrous oxide N_2O, methane CH_4, sulphur hexafluoride SF_6, hydrofluorocarbons HFC's and perfluorocarbons PFC's) by 5% of 1990 levels by the period 2008-2012 (ibid, Article 3, paragraph 1). Although international aviation is excluded from the targets (ICAO 2012), Annexe 1 countries are expected to reduce emissions from these sources, working with the International Civil Aviation Organisation (ICAO - a United Nations organisation) (ibid.).

The Kyoto protocol notwithstanding, there are as yet no firm global policies to limit aviation emissions. Instead, the ICAO is continuing with further research into aviation emissions and is developing firmer policy proposals to put forward to the UN Council at a later date (ibid.). The main policy proposals will likely be finding technical solutions to the problem, with market based measures also being considered (ibid.).

2.7.2 European Environmental Goals and Legislation

The main aspirations and goals for Europe are set by the Advisory Council for Aviation in Europe (ACARE). This organisation was set up in 2001 following the publication of 'European Aeronautics: A Vision for 2020' (EC, 2001) by the European Commission. This document set the following goals to be met by 2020 (ibid, p.14):

- A reduction in CO_2 and fuel consumption of 50% of year 2000 levels;
- A reduction of NOx emissions of 50% of 2000 year levels;
- A perceived reduction in external noise of 50%.

These goals have recently been updated to more ambitious ones to be met by 2050 with the publication of 'Flightpath 2050: Europe's Vision for Aviation' (ACARE, 2011 p. 15):

- A reduction in CO_2 and fuel consumption of 75% of year 2000 levels;
- A reduction of NOx emissions of 90% of year 2000 levels;
- A perceived reduction in external noise of 65%,
- Emission free aircraft movements when taxiing.

These goals are particularly important when it comes to the design of aircraft and the engines that power them. The normal approach of increasing the efficiency of jet engines has been to increase both the propulsive efficiency (by increasing the BPR of turbofans) and the thermal efficiency (by increasing the OPRTET). While these approaches can bring about a reduction in SFC in an uninstalled engine, they may not bring about the changes required to meet the ACARE goals. For example, by increasing the diameter of the fan in a turbo-fan engine, the propulsive efficiency of the engine may increase, however, this brings its own challenges: increasing the fan diameter also increases the overall weight of the engine and also may cause installation problems if the engine is installed under the wing. In addition, a bigger nacelle to house the engine would likely be required, likely increasing the overall drag of the aircraft. These issues may mean that the overall fuel burn of the aircraft is not reduced, despite an increase in uninstalled SFC.

In terms of increasing the thermal efficiency of the engine, although this may also bring a reduction in SFC (and hence CO_2 emissions), this would likely have an adverse effect on the production of NOx within the engine. Higher combustor temperatures encourage the dissociation of nitrogen and oxygen molecules within the air, which in turn encourage the formation of NOx molecules. There appears to be a slight paradox, then, in increasing the thermal efficiency of the engine in that it reduces CO_2 emissions, but increases NOx emissions at the same time. These may be overcome by using a different fuel (hydrogen, for example) or a better combustor design (such as a 'rich burn, quick

quench' three stage combustion chamber, lean direct injection or lean premixed pre-vapourised combustors (Singh, 2011 p.83))

The third target to be met by 2050, a reduction in external noise, is interesting because one of the engine technologies often touted as being a solution for better overall efficiency is the so-called 'open-rotor' engines, which is essentially a turbo-prop with a high speed propeller (Barnard & Philpott 2004, p.149). Although offering far better propulsive efficiency than current turbo-fans, they have the potential to be considerably noisier as there is no duct shielding noise from the propeller blades, which are likely to have supersonic flow over them at transonic cruising speeds (ibid.).

The final ACARE 2050 goal, emission free aircraft movements when taxiing, implies that there will be some form of electric propulsion system when the aircraft is on the ground. This would likely mean some form of a battery (therefore adding additional weight to the aircraft) or fuel cell, which will be used when taxiing. It is clear, then, that the ACARE goals would require some radical thinking when it comes to engine and airframe technology.

In terms of legislation, there is currently the 'National Emissions Ceiling Directive' (Directive 2001/81/EC), which limits the emissions of certain pollutants from aircraft in the landing and take-off cycle around airports. Each member state is required to form its own regulations in this regard. In the UK, total emissions of NOx, sulphur dioxide, ammonia and 'volatile organic compounds' are regulated at the following during the landing and take-off cycle (The National Emissions Ceiling Regulations 2002):

- 4 minutes for approach;
- 26 minutes for taxi/ground idle;
- 0.7 minutes for take-off; and
- 2.2 minutes for climb

The limit is contained with schedule 1 of those regulations.

2.8 Alternative Aircraft Engine Technologies

Several different technologies that may have the potential to provide additional benefits over the conventional gas turbine engine have been proposed over time. This section provides an overview of some alternative technologies that have the potential to provide a benefit for replacing conventional gas turbines for aircraft propulsion.

2.8.1 Pulse Detonation Engines (PDE)

A pulse detonation engine (PDE) uses detonation waves to burn combustible propellant mixtures within a combustion chamber (Coleman, 2001). This produces an increased pressure within the combustion chamber and as such, PDEs are closer to a constant volume combustion process than constant pressure devices like gas turbines. The requirement for propellant mixture renewal after each detonation cycle creates pulses high pressure flow, giving the engine its name.

Operation:

A single cycle of a PDE is shown in Figure 2.9. The combustion chamber is open at the exit, while the inlet is controlled by a valve which regulates the timing of the process. At point 1, the inlet valve is opened and the propellant mixture enters the chamber. Once a sufficient load has entered the chamber, the inlet valve closes and an ignition source begins a deflagration at the closed inlet (point 2). This deflagration transitions to a detonation wave (Coleman, 2001) which propagates from the closed inlet through the propellant mixture towards the open exit (point 3). The detonation or shock wave travels supersonically through the unburnt mixture, while the sudden change in pressure and increase in heat from the shock wave initiates the combustion of the mixture behind the shock wave, increasing the pressure and temperature of the now combusted gas further (point 4). The speed of the flow immediately behind the shock wave is almost sonic according to the Chapman-Jouguet condition (Coleman, 2001 p7-10). The shock wave continues until it exits the chamber, followed by the high pressure and temperature moving gas (point 5). The flowing combusted gas creates an area of low

pressure between inlet valve and the exiting combusted mixture, which is used to draw fresh propellant mixture into the chamber once the inlet valve is opened to begin the cycle again.

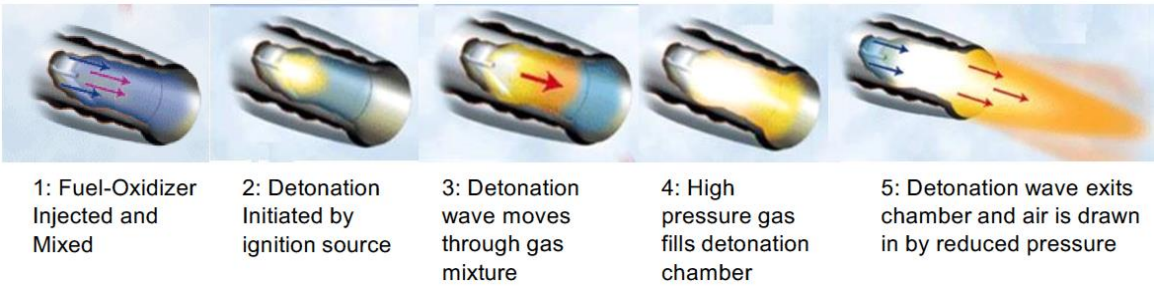

FIGURE 2.9: PULSE DETONATION CYCLE (MUSIELAK, N.D.)

There are three main concepts for using PDEs in aerospace applications: a 'standard' version where an inlet directly feeds into the detonation chamber and then exhausts through a nozzle (Figure 2.10); a pulse detonation rocket engine (PDRE) (Coleman, 2001) in which an oxidiser is also carried in the vehicle and used for low air and vacuum environments; and a hybrid version where a conventional combustor in a gas turbine or other air-breathing aero-engine is replaced with a pulse detonation combustor (Kailasanath, 2009).

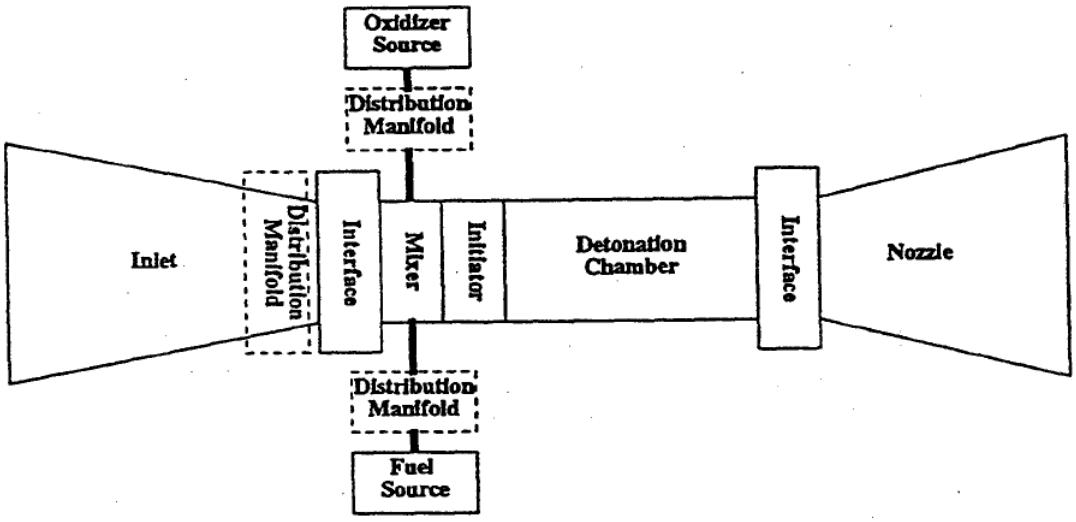

FIGURE 2.10: PULSE DETONATION ENGINE FOR AEROSPACE APPLICATIONS DIAGRAM

Potential benefits:

The interest in PDEs arises because of three main benefits they may have over other engine systems: good thermodynamic efficiency from the constant volume combustion cycle; the relative mechanical simplicity; and the potential ability to operate over a wide range of flight Mach numbers (between 0 and 5) (Coleman, 2001). The potential for PDEs to operate over a wide range of flight speeds is particularly useful for military applications, such as land and air based missile systems, while the relative simplicity which comes from not requiring pre-compression helps lower costs when used in such roles. It is the fuel efficiency gains that could potentially be achievable which make it a particularly interesting prospect for civil aerospace applications.

A PDE is based on the Humphrey cycle, which is more efficient than the Brayton cycle of a conventional gas turbine engine (Akbari and Nalim, 2006). This is because the combustion process in the Humphrey cycle also produces a pressure increase due to volumetric confinement (ibid.). This is demonstrated in Figure 2.11, which compares the two cycles on temperature-entropy chart with a fixed TET.

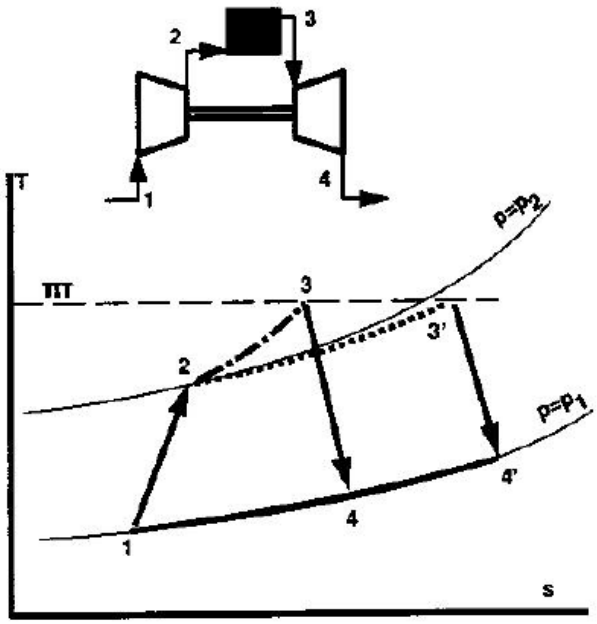

FIGURE 2.11: T-S DIAGRAM COMPARISON OF BRAYTON CYCLE (1-2-3'-4') AGAINST HUMPHREY CYCLE (1-2-3-4) (AKBARI AND NALIM, 2006, P.2)

As shown in the diagram, a pressure rise combustion process for the Humphrey cycle (1-2-3-4) replaces the slight pressure loss (for a real cycle) of the Brayton cycle (1-2-3'-4') combustion. Accordingly, for the same heat addition, the Humphrey cycle has lower entropy generation.

It is the greater inherent efficiency of the Humphrey cycle which has seen interest coupling a pulse detonation chamber within a gas turbine to create a hybrid engine. By replacing a conventional combustor with a pulse detonation chamber, the potential exists to achieve higher overall pressure ratios without needing to increase turbine entry temperature, and consequently gas turbines with higher thermal efficiency.

Although much research is ongoing for PDEs, some preliminary research as to the potential fuel benefits of a hybrid pulse detonation – gas turbine have been carried out. Rouser et al (2010) investigated experimentally a pulse detonation combustor coupled to a turbocharger under laboratory conditions. They found that pulse detonation driven turbine in a turbocharger delivered up to 41.3% improvement in specific power and 28.7% improvement in brake SFC compared to the same turbine driven from a constant pressure combustor. It should be noted that this was for a very low compressor pressure ratio of about 1.2.

Noppel (2011) developed a one dimensional performance model of a hybrid pulse detonation gas turbine to compare with a similar code for a conventional turbofan cycle. Over a range of different engine cycles (BPRs 15-30, OPRs 50-125, TETs 1700-2200K), the hybrid cycle was shown to have a better overall efficiency (57-61%) compared to the equivalent conventional cycles (47-51%). Noppel estimated that the hybrid pulse detonation cycle could achieve block fuel savings of between 10% and 40% compared to a conventional cycle.

Grönstedt et al (2013) undertook 2-dimensional CFD simulations of a hybrid pulse detonation/gas turbine engine with a maximum OPR of 53.81 and take-off BPR of 23.27 and estimated that fuel burn savings of up to 18.8% could be achieved compared to a comparable conventional cycle.

Challenges and difficulties:

There are several difficulties and challenges to overcome before PDEs and derivatives are ready to enter service.

One of the main challenges to overcome is reliably initiating and repeating the detonations (Roy et al, 2004). The ideal PDE performance is based on an assumption that detonation and the Chapman-Jouguet condition for the flow behind the shock wave occur quickly after ignition. However, the reality is that it takes some distance for the detonation to accumulate after triggering (ibid.) and consequently performance differs from the ideal cycle. Much research is ongoing to try and shorten the distance in which detonation waves transition from deflagration (see Roy et al, 2004, Cooper et al, 2002 and Lee et al, 2004).

Another issue is that it is clear from the operation of a single pulse detonation cycle that the timing of the inlet valve and ignition as well as the design of the combustion chamber is crucial. The detonation wave and propellant mixture should reach the exit of the chamber at the same time so that maximum energy can be extracted from one cycle and that no unburnt mixture escapes, lowering efficiency (Coleman, 2001). Under different flight conditions with different combustor entry temperatures and pressures, as well as different combustor exit temperatures, the local speed of sound and propagation rate of the detonation wave will change over these different conditions, so it is likely that the detonation chamber would need to be optimised for a particular condition, and other operating conditions may need to operate sub-optimally.

Several challenges would need to be overcome with respect to hybrid PDE-gas turbines. Homogenous, steady state flow is typically what gas turbines are designed for and introducing an unsteady, pulsed combustor would affect many components within the engine, including the turbines as well as installation of the engine on the aircraft. The cyclic nature of the PDE would introduce several new vibrations within the structure and may influence and increase the rate of fatigue damage on individual components

within the engine, but also on pylons attaching the engine to the airframe. Fatigue issues can be overcome by increasing the quantity of material in the affected components, however this would increase engine weight and could therefore potentially negate any performance gains.

Noise could pose a particular challenge to overcome, as a PDE would inherently create a distinctive noise from the cyclical detonations. This may not be as much of an issue in a hybrid engine as the bypass air and turbomachinery could help abate some of the noise.

Other issues are likely to be application specific and have different solutions based on how the engine would be used. These include heat transfer and cooling of the detonation chamber, structural loading, and physical arrangement of the detonation chambers within the engine.

Technology Maturity:

Aircraft have been flown using the pulse detonation concept in the 1940's with the German V1 flying bomb, while more recently in 2008 a manned Rutan Long-EZ aircraft powered by a pulse detonation engine flew a short, low altitude demonstration flight (Kailasanath, 2009). Despite these concepts, much research into the engines is analytical and laboratory work (Noppel, 2011), especially for the hybrid PDE-gas turbines and it is likely to be several decades before the challenges are overcome and engines of this type enter service.

2.8.2 Wave Rotor

A wave rotor is a non-steady pressure exchange device located within a gas turbine that consists of a rotating drum with a series of channels located within the circumference of the drum. The wave rotor forms a figure-of-eight connection between the compressor, combustor and turbine. The drum rotates between two stationary end plates that contain a number of ports, which control flow through the channels in the drum (Akbari et al,

2006). As the drum rotates, the ends of the channels are periodically opened closed, which exposes the channels to differing pressures, creating pressure (shock) waves within the channels.

Operation:

The wave rotor drum showing the channels is shown in Figure 2.12 while a schematic of a wave rotor situated within a gas turbine is shown in Figure 2.13.

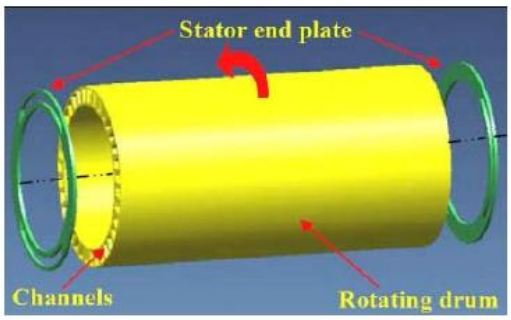

FIGURE 2.12: WAVE ROTOR DRUM SHOWING CYCLINDRICAL CHANNELS (AKBARI ET AL, 2006)

For a conventional wave rotor configuration, in the first step flow from the compressors enters one of the channels of the wave rotor. As the drum rotates, the channel connects with the combustor exit port. The sudden exposure of a high temperature and pressure gas causes a shock wave to travel along the length of the channel, compressing the relatively cooler gas within the channel and allowing some of the combustor exhaust gas to enter the channel. The drum rotates to the next port, the combustor entry. The freshly compressed gas in the chamber flows out into the combustor. Port timing is critical so as to avoid the gas/air interface between the fresh and exhaust gas in the channel reaching the exit of the port to minimise the exhaust gas recirculation rate. The drum then rotates to the final port, where the still high pressure exhaust gas can exit through the turbine and the cycle can begin again.

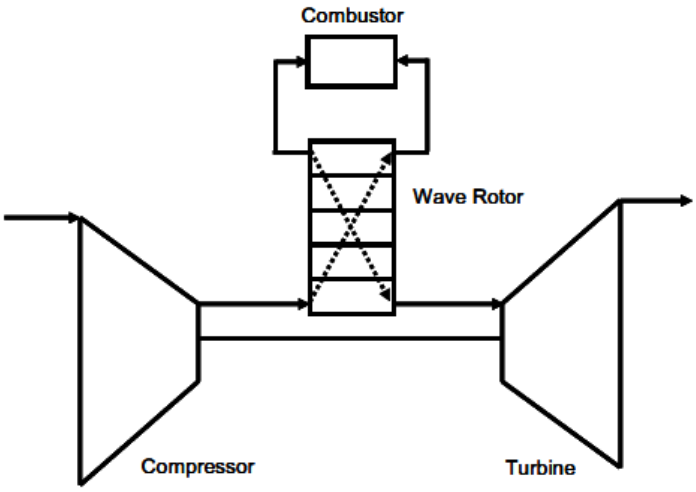

FIGURE 2.13: WAVE ROTOR LOCATED WITHIN A GAS TURBINE (NOPPEL, 2011)

Potential benefits:

The main advantage for a wave rotor is the same as a hybrid PDE - it allows for higher overall pressure ratios to be achieved while still having an acceptable compressor exit temperature. This is demonstrated in Figure 2.14, which shows a comparison of the temperature-entropy diagram of a conventional Brayton cycle and a wave rotor topped cycle. In both cases, the turbine entry temperatures and the pressure delivered by the high pressure compressor are the same. The wave rotor topped cycle gives increased power at a lower entropy rise due to the increased pressure from the wave rotor.

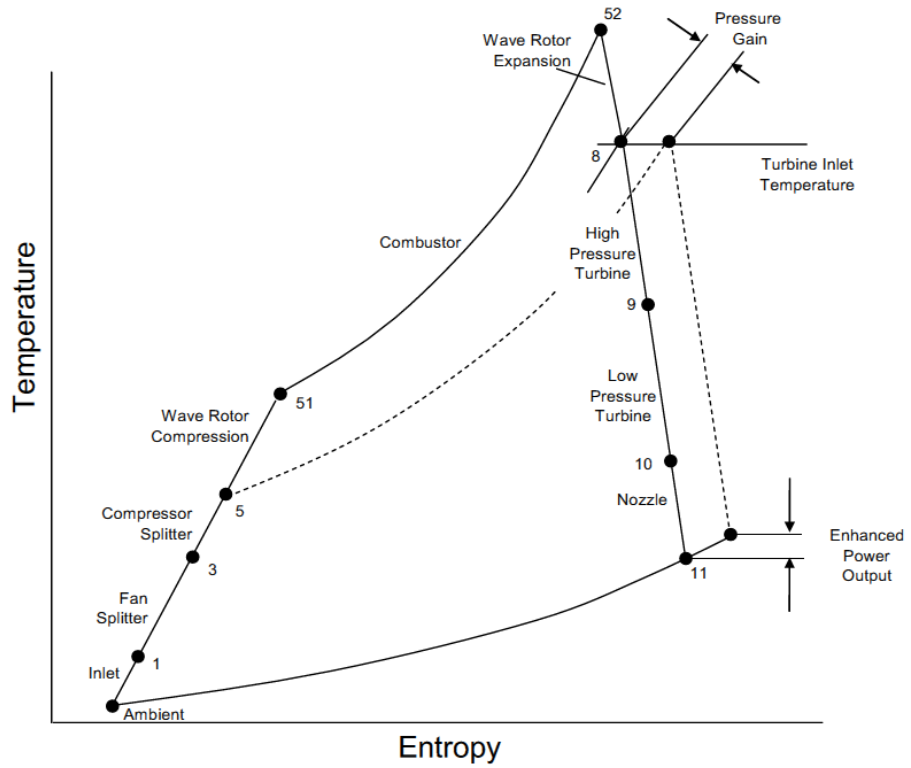

FIGURE 2.14: T-S DIAGRAM FOR GAS TURBINE TOPPED WAVE ROTOR CYCLE (BRAYTON CYCLE SHOWN DASHED) (WELCH ET AL, 1995)

Similar to the pulse detonation engine, Noppel (2011) developed a one dimensional performance model of a wave rotor topped gas turbine. The results, however, show that the wave rotor topped gas turbine engine is not as efficient as a conventional advanced gas turbine engine of similar cycle parameters. Over a range of different engine cycles (BPRs 15-30, OPRs 50-125, TETs 1700-2200K), the wave rotor cycle was determined to have worse overall efficiency (40-48%) compared to the equivalent conventional cycles (47-51%), giving a potential worsening of block fuel burn of between 14% and 34% compared to an advanced conventional gas turbine of similar cycle. The main reason for reduction in efficiency is that the compression and expansion processes within the wave rotor are less efficient than for the conventional turbomachinery, with a large increase in entropy across the shock waves. The increased overall pressure ratio and peak temperatures of the wave rotor are not sufficient to overcome this inefficiency. Noppel did, however, note that a niche could be found in applications where the overall size of the engine was an important factor, because a wave-rotor topped cycle would give more power compared to its size than a conventional engine. In addition, in

smaller, less efficient engines, with limited turbine cooling and lower efficiency compressors, wave rotors could offer an advantage (ibid.).

Challenges and difficulties:

Several challenges need to be overcome in order for wave rotors to become commercially available. The main issue is with sealing the plane between the rotor and end plates, which becomes a particular problem due to the high differential in temperature between the wave rotor and surrounding turbomachinery (Akbari et al, 2006). In addition, despite being largely self-cooling, with the hot gasses of the combustor exit being cooled by the compressor exit air, axial and radial temperature variations can still exist, which can cause thermal stresses and limit the strength of the rotor (ibid.). The unsteady nature of the device makes design and prediction of selecting an appropriate wave rotor configuration for a particular application difficult. Wave rotors have higher combustor temperatures which mean that there are significant challenges in developing material technologies for the combustor liner (ibid.).

Technology Maturity:

Much of the work carried out on wave rotors for aviation purposes has been laboratory work with NASA carrying out and continuing with much of the research (Akbari et al, 2006). The recent NASA work has been on sealing technology, which is a critical challenge. An experimental, prototype 36 channel wave rotor was built and operated by Asea Brown Boveri between 1989 and 1994 which found several design challenges to be overcome such as low pressures reached, inhomogeneous mixtures within each channel, thermal stresses on the ignition ring as well as sealing issues and rotor support bearing problems (ibid.).

Other research and simulation work has been carried out by Rolls-Royce Allison, ONERA as well as several universities around the world. The benefits of wave rotors as well as the challenges needed to be overcome to make wave rotors a reality are

understood, but it still needs serious research and will likely be a few decades before wave rotors become operational.

2.8.3 Intercooled, Recuperated and Intercooled & Recuperated Cores

The thermal efficiency of a gas turbine engine can be improved in two main ways: increasing the OPR and increasing the TET. In current conventional gas turbine cycles, OPR is limited by compressor materials and HPC delivery temperature at take-off (Kyprianidis, 2010), while a significant amount of heat is lost through the jet exhaust. Using an intercooler between compression stages can allow higher OPRs to be reached for a given high pressure compressor (HPC) delivery temperature, while a recuperator can recover some of the heat that would be lost in the exhaust.

Operation:

Intercooling involves the splitting of the compression process into multiple stages within the engine. Between the compression split(s), the air delivered by the first compression stage is cooled using a heat exchanger. This then lowers the work required for the second compression stage. For a given overall pressure ratio, the overall compressor work will be reduced (increasing specific work of the engine), while for a given HPC delivery temperature, the OPR will be higher.

A recuperated engine uses the hot gas temperature from the exhaust to preheat the compressor delivery air prior to its entry into the combustion chamber using a heat exchanger. For a given combustor exit temperature, less fuel would therefore be required to heat the compressed gas in a recuperated cycle compared to a simple cycle, thereby improving overall thermal efficiency.

Intercooled and recuperated cycles use a combination of both, combining the increased specific work output of the intercooled cycle with the increased thermal efficiency of the recuperated cycle. The combined cycle can also help to ameliorate the lower compressor delivery air of the intercooled cycle (Walsh and Fletcher, 2004).

Potential benefits:

The primary benefit of intercooling is that it gives a higher specific thrust in comparison to a similar sized engine without intercooling (ibid.). For modern aero-engine design where compressor delivery temperatures are reaching compressor blade temperature limits, it allows for the potential of higher OPRs than may be achievable through conventional means. As the trend of increasing OPRs in aero-engines continues in order to seek better thermal efficiencies, the gas delivery temperatures from the HPC are increasing further. This gas temperature has an impact on the engine in a number of ways.

For a given combustor exit temperature, there is an optimum OPR to give the best efficiency (Colmenares et al, 2007). This is determined by materials used in the construction of the HPC blades and the need for a cooling flow to the high pressure turbine (HPT). The higher the HPC exit temperature, the bigger the thermal stresses on the HPC blades and potential reduction in life; and the larger the quantity of air required to cool the turbine blades meaning a reduction in cycle efficiency (ibid.). Intercooling allows for higher OPRs to be achieved while at the same time giving an acceptable combustor exit temperature. For a given technology level, intercooling on its own can improve thermal efficiency compared to a simple cycle, with the losses from heat exchanger pressure loss and additional fuel required to achieve the same TET recovered from a significantly higher OPR (Walsh & Fletcher, 2004).

An intercooler also has the potential to help lower NOx emissions: a lower combustor entry temperature can help to reduce NOx formation within the combustor (Colmenares et al, 2007).

The primary benefit of recuperation is recovering normally lost heat from the exhaust gas and reintroducing it at the entry to the combustor. For a given engine TET, this reduces the fuel required and reduces the overall SFC of the engine. Recuperation in aero-engine applications also has the side benefit of improving propulsive efficiency

(Walsh and Fletcher, 2004). This is caused by the pressure loss from the recuperator at the low pressure turbine exit reducing core jet velocities.

Intercooled and recuperated cycles can provide both of the benefits of intercooling and recuperation, namely a higher OPR and recovered exhaust heat, thereby providing a significant increase in fuel efficiency (Colmenares et al, 2007). Kyprianidis et al (2010) showed that NOx emissions for an intercooled-recuperated engine are similar to that of a conventional engine of similar technology level. The significantly higher OPR means that it is considerably better at meeting current landing take-off cycle legislation, however.

In terms of fuel burn benefits, a number of studies have been carried out to quantify the fuel burn benefits that heat exchanged cores could be able to give. MTU Aero engines has undertaken significant research into heat exchanged cores both alone and under different EU funded projects such as NEWAC, CLEAN and AEROHEX (Boggia and Rüd, 2005). Using pre-design concept studies of a 3 shaft geared turbofan engine with intercooling and recuperation, Boggia and Rüd (2005) estimated that up to 18.7% reduction in SFC could be obtained from intercooling and recuperation compared to a baseline 1995 engine. It should be noted, however, that this study did not necessarily compare like with like – the proposed intercooled-recuperated engine had a much higher bypass ratio – 26.5 compared to the baseline of 5.1 and a much higher TET of 1,944K compared to the baseline of 1,600K. Boggia and Rüd did note that intercooling and recuperation would be more suitable for long range aero applications, where the additional weight associated with the heat exchangers would be offset with the better cruise SFC. For shorter range applications where the aircraft spends a lower proportion of its time at cruise, intercooled and recuperated engines may not offer as much, if any, benefit.

Kyprianidis et al (2010) used the TERA 2020 optimisation tool to assess intercooled and intercooled-recuperated aero-engine cores. 3-spool engines and a long-range aircraft model with design range of 12,500km and able to carry 253 passengers were used for the study. With an OPR of 80 for the two intercooled cores, block fuel benefits of

approximately 3.2% over a mission of 5,500 km were predicted for the intercooled core and up to 22% for the intercooled recuperated core compared to a comparable conventional turbofan of similar technology. More recently, Xu et al (2013) updated this study of an intercooled-recuperated aero engine and found that an optimised intercooled-recuperated engine could deliver and additional 5.56% fuel burn savings for the same mission.

Challenges and difficulties:

Intercoolers and recuperators have been previously used for industrial and marine purposes, however a number of challenges need to be overcome before they are suitable for aerospace applications. These relate mainly to weight, installation and layout, and heat exchanger effectiveness issues.

Intercooled engines are primarily useful for larger aero-engines on longer missions. Although the additional weight of the heat exchangers can be overcome by improved cruise efficiency, shorter range missions would not benefit as much due to the proportionally shorter time spent at cruise for the whole mission. In addition, smaller aircraft and engines are normally used for short range missions. One benefit of intercooling is that higher OPRs can be achieved for a given HPC delivery temperature. However, the higher the OPR, the smaller the HPC duct becomes, leading to increased tip leakage losses and lowering component efficiency (Camilleri et al, 2015). Therefore intercooled engines are only feasible for larger engines with a larger core flow.

Weight is a significant issue in aerospace applications. Any additional weight carried by the aircraft requires additional thrust from the engine and results in an increase in fuel burn. It is important therefore that any gains in thermal efficiency from heat exchanged cores are not reduced by additional engine weight. In this regard, there is a relationship between heat exchanger effectiveness and weight. The more effective the heat exchanger, the heavier it is due to the additional cooling vanes. Rolt and Baker (2009) found that an optimal effectiveness was between 60-70% to keep the weight and size of the intercooler to an acceptable level.

Heat exchangers also introduce pressure losses within the main air flow, mainly through the skin friction and boundary layer build up within the heat exchanger vanes, but also through the additional ducts required to route the flow (Walker et al, 2009). Although in practice this is not too much of a problem, as industrial and marine heat exchanged gas turbines exist, in aero applications the installation of the heat exchangers and ducts is a particular challenge. Ducts are required to diffuse the flow before it enters the heat exchanger, as pressure losses are proportional to the square of flow velocity (ibid.), however overall length of the engine is important for drag and weight considerations. One way to overcome the length issue is with a reversed flow core (Camilleri et al, 2015).

Many of these challenges are being considered by various research programmes, including NEWAC and LEMCOTEC, as well as engine companies such as Rolls-Royce and MTU and research institutions such as Cranfield University and Chalmers University.

Technology Maturity:

While these cycles have long been used for industrial and marine purposes - most recently with the 25 MW Rolls-Royce WR-21 Intercooled Recuperated engine used on the Type-45 Destroyer (English, 2003) - they have yet to be used in commercial aero applications (Colmenares, 2009). In 1967, Allison used a Model 250-E3 recuperated gas turbine engine powering a Hughes YOH-6A helicopter in a successful test flight program to test the concept (Jensen and Leonard, 2002), which demonstrates that heat exchanged cores are feasible for aero applications. The main considerations to overcome are heat-exchanger pressure losses and weight. However, considering the research being undertaken, the author's opinion is that intercooled and intercooled recuperated cores could become available for long range applications within 20 years.

2.8.4 Open Rotors/High Speed Propellers

During the fuel crisis In the 1970's, the increased propulsive efficiency offered by propellers led many manufacturers to look at potential designs that were suitable at higher flight Mach numbers (Barnard & Philpott, 2004, p. 148). Despite there being interest in technology demonstrator 'propfans' being created by both General Electric and a consortium led by NASA in the mid to late 1980's (Flightglobal, 2007), the considerable reduction in the price of oil and concerns about noise stopped any further development (Sweetman, 2005). Interest in open rotor engine configurations has been rekindled in recent years due to more stringent emission regulations, and have been investigated in the EU projects Clean Sky (Clean Sky, 2016) and DREAM (EC, 2016).

Operation:

The open rotor engine is similar to a turbo-prop in that it combines a gas turbine with a propeller located externally on the engine. The propeller uses aerodynamically advanced rotor blades which are a larger diameter than the blades of a conventional turbofan engine, giving rise to higher BPRs and hence improved propulsive efficiency. The open rotor differs from a turbo-prop as the highly swept rotor blades are designed for higher flight velocities, approaching those of conventional turbofans (Barnard & Philpott, 2004). Single rotating and counter rotating open rotor configurations with or without gearboxes have been proposed (ibid.).

Potential Benefits:

The open rotor allows for much higher bypass ratios (BPR) while retaining the high cruising speeds of conventional turbofan engines. At cruise conditions, contra-rotating open rotors BPRs of up to 50 (Mikkelson, D. C et.al., 1984; Grieb, H. and Eckardt, D., 1986) are possible. These higher bypass ratios allow for a much better propulsive efficiency in comparison to conventional turbofans, without a significant increase in mission time like conventional turbo-props. This allows the potential for lower mission fuel burn and CO_2 emissions without additional flight time DOCs.

Different configurations of open rotor have been considered, including pusher and puller configurations, and single rotor and dual rotor counter-rotating configurations. The benefit of a contra-rotating configuration over a single rotor is that it is able to deliver an equivalent level of thrust using a reduced propeller diameter, which enables reduced propeller tip speeds. This offers the important advantage of recovering the swirl on the propellers exit flow (Bellocq, P., 2012), and keeping higher cruise speeds within acceptable noise limits.

In terms of fuel burn advantages, Guynn et al (2012) undertook an a preliminary aircraft system level study of an Airbus A320/Boeing 737 size aircraft with two open rotor engines mounted on the rear of the aircraft. They estimated that block fuel burn savings of 18% could be achieved over a 500 nm mission compared to an advanced geared turbofan engine with a BPR of about 15 and OPR of 42, while savings of up to 12% could be achieved over a 3,250 nm mission. They found that cruise fuel burn savings were of the order of 10%, while superior fuel savings were found during the climb phase.

Challenges and Difficulties:

Despite flying demonstrators of open rotors since the 1980s, there still remain several challenges to overcome before open rotors become ready for certification. Bellocq et al (2016 , p.2) list several of these challenges:

"At Aircraft Level

- *Cabin and community noise*
- *Fuselage and structures fatigue (at proximity of engine)*
- *Engine installation and weight*
- *Aircraft aerodynamics (mainly for rear mounted CROR)*
- *Public perception*

At Engine Level

- *Small core, high impact of cooling flows on performance*
- *Operation during thrust reverse*
- *Mechanical design of the pitch control mechanism*
- *Mechanical design of the blades*
- *Gearbox reliability and oil-cooling technologies*
- *Maintainability and acceptable maintenance cost*
- *CRT [Counter Rotating Turbine] seals and blade containment"*

However, since the global financial crisis and corresponding fuel price rises, engine manufacturers in both Europe and the USA, as well as national and supranational bodies such as the EU, NASA and the FAA, have created projects to address these issues. The FAA and General Electric have researched aero-acoustic technology as part of the Continuous Lower Energy, Emissions and Noise (CLEEN) program (Khalid et al, 2013), NASA are involved as part of the Environmentally Responsible Aviation (ERA) project (Van Zante, 2013), while in the EU, the large Clean Sky (Clean Sky, 2016) and DREAM (EC, 2016) projects have brought together engine and aircraft industry, as well as research institutions from across Europe to research these challenges.

In the author's opinion, the major problem faced with open rotors is the noise created from the tips of the fan blades travelling at supersonic speeds, from the rotational speed of the blades and the forward motion of the aircraft (Barnard & Philpott, 2004, p. 169). This noise causes problems both for passengers in the cabin and the noise in and around airports. In conventional turbofan engines, this noise is ameliorated to some degree thanks to the engine nacelle shroud, but for open rotor engines, the installation of the engine on the aircraft becomes more important.

To reduce cabin noise the General Electric UnDucted Fan (UDF) demonstrator in the 1980's, the engines were mounted at the rear of the fuselage of a McDonnell Douglass MD-80 aircraft. The placement of the engines, however, potentially restricts the number of engines available to be fitted on the aircraft, making this technology suitable for

shorter range aircraft rather than long range aircraft. Recent wind tunnel experiments carried out by General Electric as part of the CLEEN project, show that open rotors are capable of meeting current noise legislation while retaining good propeller efficiency (Khalid et al, 2013). Safran Aircraft Engines carried out wind tunnel tests in 2013 focusing on noise emissions and was confident that noise levels would be 10dB lower than current turbofan engines (Gubisch, 2014).

Additional challenges remain with the design of the engines themselves and their integration, however. The contra rotating open rotor design, even though very beneficial in terms of increased propulsive efficiency, is technically challenging. The blade pitch of the contra rotating stages must be varied in order to optimally match the aircraft speed and power/throttle setting through the flight envelope, similar to turbo-props. This would require the application of a pitch change/control mechanism for actuation and control of the blade pitch. The space available within the engine may also be problematic - there would need to be a gearbox for the contra-rotation of one of the rotors, another for the reduction from the turbine speed and also space for the pitch control mechanism. This would also have an impact on the engine weight.

The integration of the engines on the aircraft may also necessitate a complete aircraft redesign. The engines may not be able to be mounted under the wings for two reasons - lack of space from the increase BPR that the engines offer and the potential for an uncontained rotor blade-off severing the wing. To overcome this, rear mounted engines would be a feasible option, however this restricts the number of engines that could be carried, meaning that the aircraft would likely be more suitable for shorter range missions.

Technology Maturity:

Open rotor flight demonstrators have been flown in the 1980s with the General Electric/McDonnel Douglas UDF, while Safran Aircraft Engines is currently building a prototype counter-rotating open rotor engine with flight tests scheduled to begin in 2019 (Gubisch, 2014). Much research (as described above) is being carried out to solve the

remaining issues with open rotors and in Europe, open rotors are expected to enter service from 2030 (ibid.).

Open rotor engines are likely to be more suitable for short to medium range single aisle aircraft (Larsson et al, 2014), as although they are capable of cruising speeds equivalent to turbofans (about Mach 0.8), greater fuel saving benefits can be had at slightly lower cruising speeds (ibid.). The open rotor also gives better fuel burn savings during the climb phase of the mission, making them more attractive for shorter range missions (Guynn et al, 2012).

2.8.5 Turboprops/Conventional Propellers

While novel engine cycles and new technologies can in some respects be seen as the 'future' of aero-engines, in order to achieve the goals of fuel burn reduction and lower engine emissions, it can sometimes be beneficial to see if there any existing technologies that could also meet those goals. Propeller driven aircraft have been around since the inception of manned, powered fixed wing flight, and the better efficiency of propeller driven aircraft compared to jet aircraft at lower flight speeds is well known (Barnard & Philpott, 2004, p. 138). Combining a propeller with a gas turbine engine produces a 'turbo-prop', which have been found on many aircraft since the first such powerplant was tested on a Gloster Meteor in 1945 (James, 1987).

Operation:

The turboprop engine consists of a propeller which provides the main thrust of the engine and a gas turbine which provides the power to drive the propeller. Barnard and Philpott (2004) provide a good description of the operation of turboprops.

Potential benefits:

There may be scope, however, for turbo-props on slightly larger aircraft and longer range missions. Because turbo-prop aircraft fly at an altitude of approximately 25,000ft

(Kirby, 2011) compared to a typical turbo-fan aircraft of approximately 35,000ft, the time spent in the climb phase is comparatively less and the cruise phases begins earlier. The overall mission block time may therefore be the same between the turbo-prop and turbofan aircraft, dependent on mission length. Indeed, anecdotal comparisons (Kirby, 2011) between the Bombardier Dash 8 and Embraer ERJ-145 turbofan aircraft showed that the total block time was the same for missions up to an hour and a half. The Embraer ERJ-145 cruises at Mach 0.78 (Embraer, 2012), similar to that of the Airbus A320 (0.78 - 0.82), while the Bombardier cruises at approximately Mach 0.63 (Kirby, 2011).

The implications are that, for missions of up to even three hours duration, a turbo-prop powered aircraft may not significantly lag behind a turbofan aircraft. Indeed, the currently in production Airbus A400m 'Atlas' military transport aircraft is designed to cruise at Mach 0.72 at altitudes of up to 37,00ft (Airbus, 2012), which is much more similar to conventional turbofan aircraft. Parzani (2012) carried out a comparison between the A400m and a Boeing 737-800 and found that the A400m was less efficient overall than the 737. However, it should be noted that the A400m carries considerable extra weight not found in the 737 because of its application as a military transport, such as armour, electronic counter measure systems and loading winches. If the aircraft was optimised for passenger transportation like the 737, the result may well be different. The engine that powers the A400m, the Europrop T400-D6, produces 8,200 kW (Rolls-Royce, 2006) and four of them power the A400m. The A400m has a maximum take-off weight (MTOW) of 141,000 kg (Hoyle, 2011), which is approximately twice the MTOW of an Airbus A320 (73,500 - 77,000 kg, Airbus, 2010a). Two T400-D6 type engines could potentially power an aircraft of Airbus A320 size.

In terms of fuel burn, turboprop equipped aircraft currently in service demonstrate better fuel consumption characteristics than equivalent turbofan equipped aircraft. This is demonstrated in Figure 2.15, which compares three similar size aircraft – the turboprop equipped ATR 72 and Bombardier Q400, and the turbofan equipped Embraer CJ-700 regional aircraft used for Fly In/Fly Out operations for the mining sector in Australia (Walsh and Bil, 2015). Up to 75% less fuel can be used for the shortest range missions

for a turboprop compared to a turbofan. The differences in fuel burn reflect the different cruise speeds for the three aircraft – the ATR 72 has a maximum cruise speed of 275 kts, the Bombardier Q400 a maximum cruise speed of 260 kts, while the Embraer CJ-700 has a maximum cruise speed of 473 kts. This reflects that the savings in fuel burn also come from the lower drag encountered by the aircraft at lower speeds, and the trade-off between good efficiency and speed of the mission.

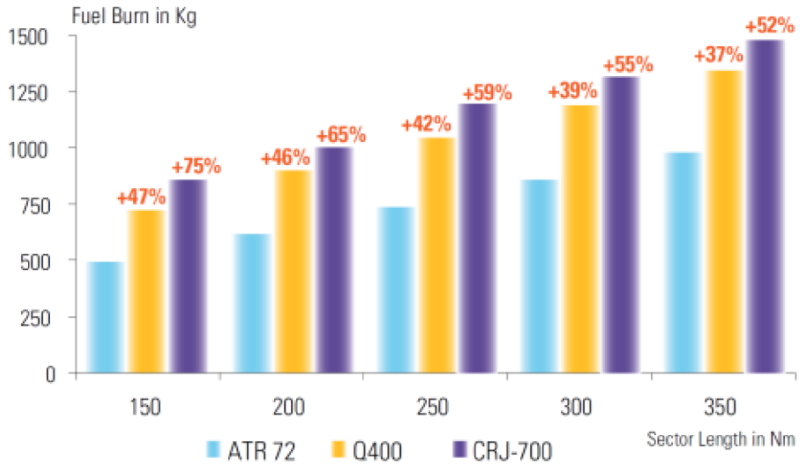

FIGURE 2.15: FUEL BURN COMPARISON OF TURBOPROP AND TURBOFAN EQUIPPED AIRCRAFT (WALSH AND BIL, 2015, P.6)

Challenges and difficulties:

The main two drawbacks with turboprops are speed - which makes them unsuitable for long distance routes - and noise - both in the cabin and on the ground (Barnard & Philpott, 2004, p. 163). Despite this, turbo-prop aircraft remain popular as regional aircraft (such as the Bombardier Dash 8 and ATR 42 & 72) where the short flight duration mean that the slightly lower top speed and greater noise than a conventional turbofan aircraft mean that these considerations are not so important.

Technology Maturity:

Turboprop equipped aircraft have been in service since 1945 and continue to be used for passenger and military applications to this day. Open-rotors, which are essentially

turboprops with higher flight speeds could be considered an evolution and next stage of this technology.

3.0 TERA Methodology and Models

This chapter describes the overall methodology used to investigate the quantitative element of the thesis, namely the search for an optimum conventional gas turbine engine suitable for use on short to medium range passenger jet aircraft. The chapter provides an overall description of the TERA methodology combined with the constituent models.

3.1 General TERA Methodology

TERA is a tool that can be used to assess gas turbine engines with *"minimum [environmental] impact and lowest cost of ownership in a variety of emission legislation scenarios, emissions taxation policies, fiscal and air traffic management environments"* (Ogaji et al, 2007). TERA uses a modular, multi-disciplinary (in that several different disciplines are used such as gas turbine performance, noise modelling, emission modelling, aircraft performance e.t.c.) approach to optimize a particular 'goal' function, such as fuel burn, noise or global warming potential (ibid. p. 4).

The TERA framework consists of several modules which are integrated together with an optimizer. The optimizer used for the EU VITAL project was a commercial optimiser called iSight, although other user made genetic-algorithm optimizers have also been used. The different modules are individual models that perform a specific function, such as an engine performance model, aircraft performance model or weight estimation model. These are brought together within the optimiser, which can then give a set of optimum results for a number of different objectives.

Figure 3.16 shows the TERA framework used to study the optimisation of aircraft engine technologies to reduce mission fuel burn. The figure shows the various models used within the framework and how they interact.

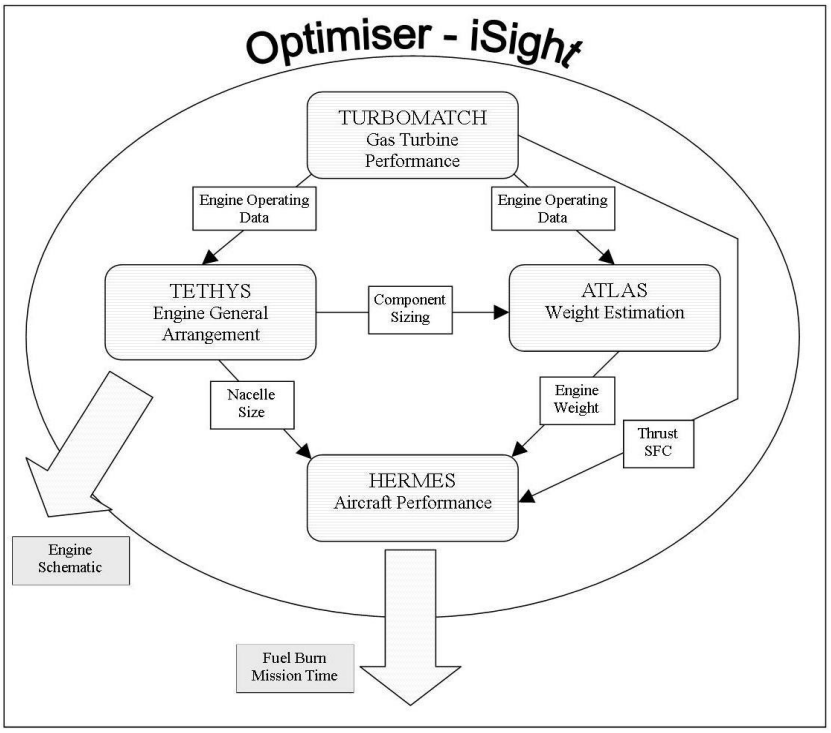

FIGURE 3.16: TERA FRAMEWORK

The overall TERA framework consists of four separate modules integrated within a commercial optimiser called iSight. The four modules are linked together using a separate Fortran code, which handle the inputs and outputs to and from each model. The four modules consist of the gas turbine performance code (using TURBOMATCH), the aircraft mission and performance code (HERMES), the engine sizing and general arrangement code (Tethys) and the engine weight estimation code (ATLAS).

3.2 Engine Performance Module

The engine performance module forms a fundamental part of TERA, particularly for this project where gas turbine cycles are being investigated. Several different gas turbine simulation tools are available, which will be discussed briefly.

The NPSS tool was developed at NASA Glen Research Center in 1995 (Follen, 2002), and is now available commercially through an industrial consortium managed by the Southwest Research Institute. NPSS is an object oriented code that is designed to allow

the user to assemble any type of engine using a plug and play concept. NPSS was created to try and simulate the whole flowfield through an engine, but to keep the simplicity of assembling pre-built components. The program allows multiple dimensionality (i.e. 0-D, 1-D, 2-D and 3-D) components to interact with each other through a process called ‘component zooming’ This allows a fan stage to be modelled for 3 dimensional flow while the rest of the components are modelled using 0-D or other dimensional codes. NPSS is also designed to integrate other disciplines, such as life estimation and economics to offer a full engine design suite.

GasTurb is a popular gas turbine performance simulation tool created by Dr Joachim Kurzke. It uses a set number of pre-defined engine configurations, which are able to be amended by the user to evaluate design point, off-design and transient performance (Kurzke, 2015). The program is designed to be user-friendly and offers three different levels of simulation, graded by user complexity. For the Basic Level, user input data is limited to simple properties such as component efficiencies, pressure ratios and combustor exit temperatures, while other details are set to default and hidden from the user. The Performance Level adds an extra layer of user inputs such as turbine cooling and internal air systems and is used to study gas turbine cycles. The final level, More, is used for preliminary engine design and can calculate a geometry and cross section as well as a weight for the engine.

The Project Object Oriented Simulation Software (PROOSIS) tool is another object oriented gas turbine simulation environment (Alexiou, 2014). It was developed as part of the European Union’s VIVACE project comprising research institutions, universities and industries across Europe as a European version of NPSS, which was not generally available to European industry (Bala et al, 2007). PROOSIS is able to perform not only steady state and transient gas turbine performance simulations, but additionally some system simulations, such as control, hydraulic and mechanical. PROOSIS is object oriented and allows a user to construct an engine graphically from a regularly updated Standard Components Library (SCLIB), or choose and modify an existing engine based on application from the Standard Engine Model Library (SELIB). PROOSIS is able to simulate individual components, either stand alone or coupled within a wider engine.

For this project, Cranfield University's own engine performance code, TURBOMATCH, was used. TURBOMATCH was chosen for three main reasons:

- Functionality – the code offers sufficient functionality for the project. The added functionality of the other codes, such as transient performance modelling, was not required for the project, where a large number of different cycles would be run.
- Availability – as TURBOMATCH is an in-house code, no licenses were required to be purchased and the expertise for any troubleshooting was easily available;
- Suitability – TURBOMATCH has been used for TERA and other multi-disciplinary optimisations in the past.

TURBOMATCH was created at Cranfield University by MacMillan (1974) and is a modular, '0-D' code where 'bricks' are used to simulate individual components within a gas turbine. These pre-programmed bricks, which mostly represent components in an engine such as ducts, compressors, intakes and mixers can be assembled by the user to create almost any type of gas turbine engine (Apostolidis et al, 2013). Other bricks are available within the code, such as the PERFOR brick, which collates the outputs of the other bricks to perform the overall cycle calculation. Each brick is a subroutine which calculates the thermodynamic process in the relevant component. Each brick requires specific user defined inputs, such as pressure ratio and isentropic efficiency for the COMPRE brick, which define the design point of the engine.

The bricks are arranged serially and are connected together using an interface called a station vector. Station vectors consist of eight different variables, although only five are required to describe the gas state:

- fuel to air ratio
- mass flow
- total pressure

- static pressure
- total temperature
- static temperature
- flow velocity
- area

The user defines a station number for the input and output of each brick (or two inputs in the case of a mixer, two outputs for a splitter) such that one station number is used for the output of one brick and the input of the next sequential brick. In this way, the individual components can be linked together to form a complete engine.

One other way of connecting components together which are not sequential in the flow path, such as the low pressure compressor and turbine, is the engine vector. Engine vector results, such as the compressor work can then be used as a brick data input into another component, such as a turbine in this instance. Figure 3.17 shows diagrammatically the flow to and from a brick.

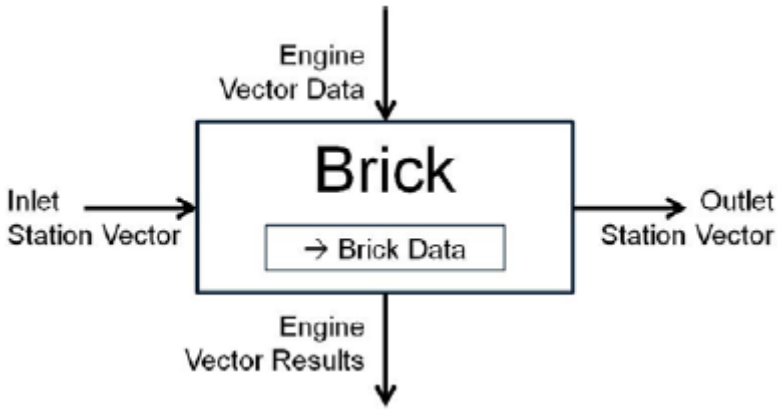

FIGURE 3.17: BRICK DATA FLOW (APOSTOLIDIS ET AL, 2013 P.4)

The user constructs the brick data and station vector items in a text input file[1], and then specifies the design point combustor exit temperature and inlet mass flow, followed by any off-design points. The design point calculation is the first to be determined, which

[1] A version of TURBOMATCH called Pythia with a graphical user interface allows a user to assemble an engine and generate the input text file automatically has also been created by Cranfield University.

sizes the engine, following the approach given in Walsh and Fletcher (2004). For off-design, TURBOMATCH is currently able to use two parameters as a handle - the combustor exit temperature and any shaft relative rotational speed (PCN).

TURBOMATCH uses a number of component maps to the model off-design behaviour of the engine. Five pre-defined maps[2] are available for each of the compressor and turbine, while there is one default map for each of the combustion chamber, intercooler and propeller bricks. The standard maps are based on real components and are derived experimentally, while the functionality exists for the user to upload other maps. The maps are scaled based during the design point operation. For off design cases, an in iterative procedure takes place (up to 100 iterations in TURBOMATCH 2.0) to match the performance of the components. A number of parameters are guessed initially, and then the validity of those guesses checked. Checks are carried out on mass flow compatibility, work compatibility, shaft rotational speed and the power law for driving generators (Apostolidis, 2013).

The outputs from the engine module are used in most of the other modules. The aircraft performance module uses thrust and SFC as its main inputs from the engine module, the engine sizing module uses component total pressures and temperatures along with mass flow values and splits which also feed into the weight model.

3.3 Aircraft Performance Module

The aircraft performance module is an important part of the TERA module when investigating aircraft engines, as it allows for the investigation of fuel burn over a range of different mission profiles rather than just looking at specific fuel consumption of an uninstalled engine. This is useful because it allows further conclusions for novel powerplants to be drawn, such as economic viability from mission fuel burn and CO_2 emissions over the mission.

[2] One map here refers to the correlated pressure ratio (enthalpy drop) vs efficiency and pressure ratio (enthalpy drop) vs non dimensional mass flow maps for the compressor (and turbine in brackets).

For this project, HERMES, Cranfield University's in house aircraft performance code, was used. HERMES was developed by Laskaridis in 2004 and was designed to be integrated with TURBOMATCH for the engine performance data. HERMES has been designed for use with passenger jet aircraft in conventional configuration (i.e. with engines hung under the wings), although turbo-props have also been modelled. HERMES assumes international standard atmosphere ISA conditions (although deviations can be inputted manually) and assumes a typical take-off, cruise, land profile. HERMES has been validated against published aircraft performance data with less than 1% deviation in the payload-range chart (Laskaridis et al, 2005).

A HERMES input file is given in Appendix 1. The input file is split into a number of sections to make inputting the required data easier for the user. There are a wide range of inputs to describe the aircraft geometry and mission profile including engine settings for the whole mission. TURBOMATCH is integrated within HERMES, which uses the mission profile data (such as altitude, Mach Number and engine settings) to create a matrix covering the whole flight envelope.

The output file of HERMES gives details of mission fuel burn, block fuel burn (this also includes taxiing at the airport), total mission and block ranges, mission time, HERMES also gives details of fuel burn for each phase of the mission for deeper study.

HERMES has a modular form and consists of six different modules, although these are hidden from the regular user. They are (ibid.):

- Input data
- Mission profile module
- Atmospheric module
- Engine data
- Aerodynamic module
- Aircraft performance module

The input data module consists of the required data to define the geometry of the aircraft, such as wing span, fuselage length and nacelle diameter, as well as the aircraft empty weight. The user inputted data is then used to calculate the wetted areas, and is used by the aerodynamic module to calculate the drag characteristics of the aircraft.

The mission profile module defines the mission that the aircraft will fly. This include overall mission range, climb profile, cruise altitude(s) and Mach number(s) as well as an optional diversion mission. The overall profile is defined by the user in the input file and is split into several segments: take-off, climb, cruise, descent, hold, approach, landing as well as an optional diversion climb, cruise and landing. A typical profile is shown in Figure 3.18.

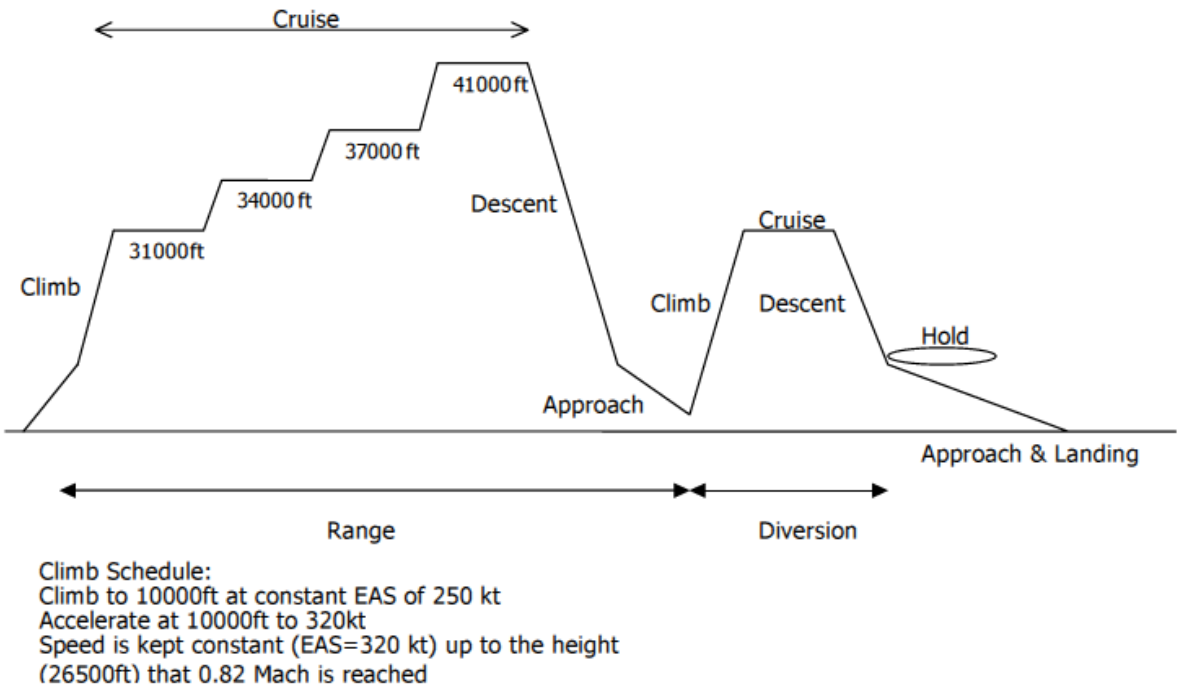

FIGURE 3.18: TYPICAL FLIGHT MISSION PROFILE WITH STEPPED CRUISE (LASKARIDIS ET AL, 2005, P4)

The atmospheric data module calculates the pressure and temperature of the air along the mission profile according to the ISA characteristics. The module also allows user to deviate from the standard temperatures and pressures from user defined deviations in the input file.

The engine data module provides the engine thrust and SFC data for the code. It also provides TURBOMATCH the appropriate mission data (altitude, Mach number, ISA deviation) so that the engine performance data can be calculated. The overall profile is specified by the user in the input file

The aerodynamic module computes the drag coefficients and drag polar profiles of the aircraft using data from the input, atmospheric and mission modules. This data is then used to obtain a thrust requirement for each stage of the mission, allowing the aircraft performance module to select the appropriate engine setting from the engine data module. The drag polar is made up of two main components: one dependent on aerodynamic lift and the other independent of lift. This is shown in the equation below:

$$C_D = C_{D0} + KC_L^2 \qquad \textit{equation 3.1}$$

Where C_D is the total drag coefficient, C_{D0} is the zero lift drag coefficient, C_L is the lift coefficient and K is the lift dependent factor.

The zero lift drag coefficient is estimated in HERMES using a component build-up method (ibid.). This estimates the subsonic drag of each component using a skin friction coefficient (C_f) that can be calculated, a component form factor (φ) which estimates viscous pressure drag, and a 'Q' factor which estimates interference drag effects. The total component drag is determined as a product of the wetted area (Swet). The general equation is (ibid.):

$$(C_{D0}) = \frac{\sum (C_{fc}\varphi_c Q_c Swet_c)}{Sref} \qquad \textit{equation 3.2}$$

Where subscript c refers to the individual component and Sref is the reference wing plan area.

The lift dependent drag factor, *K*, is calculated using the equation below:

$$K = \left(\left(\frac{C_1}{C_2 \pi AR} \right) + C_3 + C_4 C_{D0} \right) \qquad \textit{equation 3.3}$$

Where C_1 and C_2 are associated with the wing planform geometry, dependent on wing taper and aspect ratio, C_3 is the non-optimum wing twist and C_4 is used for viscous effects. *AR* is the wing aspect ratio. Full details of coefficients C_1 to C_4 are given in Jenkinson et al (2009).

The final module is the aircraft performance module. This module uses data from all the previous modules to calculate the total fuel burn for the mission. The mission is divided into different segments as described for the mission module and fuel burn calculated as follows.

On the ground phases of the mission, including taxiing and take-off fuel burn are calculated by simply using the SFC from the engine module produced at those conditions and combining it with a user-defined time period for those operations.

For the climb phase, the fuel burn, distance and time taken are calculated by splitting this phase into separate intervals of 1,500ft. The user specifies the equivalent air speed and any ISA deviations for each of these intervals (although standard values are included). The rate of climb (i.e. the rate of change of altitude with respect to time) and time taken to climb the segment is calculated for each interval using the following expression:

$$t = \int_{h1}^{h2} \frac{1}{V_{vertical}} dh \qquad \textit{equation 3.4}$$

Where *t* is the time taken to climb from altitude h_1 to h_2 and $V_{vertical}$ is the rate of climb. An iterative procedure is then carried out, which estimates a trial time and weight for the end of the segment and checks to see whether the drag, thrust and velocity of the

aircraft match. Once the estimation and check converges, the code moves to the next segment. The total time, distance and fuel burn of the climb are calculated by summing together the individual segments.

Cruise fuel burn is calculated using a modified integrated range technique. Essentially this technique breaks down the cruise into a number of small segments, each a user defined time interval. The code then calculates the small amount of fuel burnt and hence reduction in aircraft weight during that interval. This way the fuel burn over the whole cruise can be calculated. This technique starts with the Breguet range equation (Laskaridis et al, 2005) and assumes that cruise is at a constant speed and altitude:

$$Range = -\frac{V}{SFC}\frac{E}{g}\int_{m1}^{m2}\frac{1}{m}dm = \frac{V}{SFC}\frac{E}{g}\ln(\frac{m_1}{m_2}) \qquad \textit{equation 3.5}$$

Where V is the aircraft flight velocity, E is the aerodynamic efficiency (i.e. lift to drag ratio), g is gravitational acceleration and m is aircraft mass.

The cruise period is then divided into time intervals using the following formulae (Laskaridis et al, 2005). During steady level flight, the fuel burn reduced aircraft weight is given by (ibid.):

$$\frac{dW}{dt} = -\frac{SFC.W}{E} \qquad \textit{equation 3.6}$$

Where W is the aircraft weight.

The total fuel burn for the whole of cruise is given by (ibid.):

$$FuelConsumed = \int_{1}^{2} SFC\frac{W}{E}dt \qquad \textit{equation 3.7}$$

When the cruise time intervals are taken into account, the total fuel burn for cruise is given by (ibid.):

$$FuelConsumed = \sum_{i=1}^{n} \frac{SFC.W(t_i - t_{i-1})}{E} \qquad \textit{equation 3.8}$$

Descent fuel burn is calculated using a similar process to climb fuel burn. Descent is split into a number of segments and rate of descent, horizontal distance and time taken are iterated. The engines are assumed to be idle at these conditions as the aircraft trades height for flight speed, therefore very low power settings are used in TURBOMATCH.

For holding calculations, where the aircraft may be required to circle in a holding pattern prior to landing if the airfield is busy, a user inputted holding altitude and duration is used to calculate the fuel burn. It is assumed that the aircraft flies at a speed where fuel flow is minimised, i.e. its minimum drag speed. Using this information, the fuel burn for holding can be calculated straightforwardly.

HERMES then sums the fuel burn, segment duration and ranges of each of the phases to provide total results for the whole mission.

3.4 Engine Sizing Module - TETHYS

A vital step in the TERA framework is a way to estimate not only the overall size of a future engine, but also to have some idea as to the internal arrangements including number of component stages, component hub-tip ratios and internal sizing. This is required at a preliminary stage because it gives an indication as to the feasibility of a particular engine; that is whether it might be able to be built or used in the way intended. Real physical constraints, such as sufficient space under a wing to mount an engine, or the diameter of engine shaft limit possible engine designs.

Several methods are available that aim to predict the overall size and layout of an engine, however the author couldn’t find a suitable existing method that could offer a

reasonable cross-section of a gas turbine engine using data from a gas turbine performance code that isn't based on correlations and doesn't require several iterations to check through detailed compressor and turbine aerodynamics to help keep computational time down.

Sargerser et al's (1971) method to determine the size and length of aero engines is based on lightweight Vertical Take-Off and Landing (VTOL) engines that were available or in development during the 1960's and 1970's. As such, many of the correlations may be out of date (this is discussed in the weight module section) and without any contemporary information to update the correlations, this method is unsuitable.

Lolis (2014a) created a gas turbine sizing tool as part of the development of ATLAS, Cranfield University's weight estimation tool. The method employed offers good accuracy, with a gas path analysis to size not only the annulus, but also compressor and turbine stages and blade count. The method employs an iterative process to check component DeHaller numbers, velocities and pressures and as such requires some amount of computational time.

The author was searching for a method that would give an overall size of an engine with an idea of component stage count and critical parameters such as HPC exit hub-tip ratio that didn't require an iterative procedure or analysis of the compressor or turbine aerodynamics. Essentially, a method to give a reasonable prediction of engine size and layout that gave sufficient information to the other modules that could operate on a single pass (i.e. without iterations), so that computational time could be kept low for optimisation purposes.

Accordingly, a preliminary engine sizing and layout model called *Tethys* was created. Tethys fills the gap between a correlation based method such as Sargerser et al's and a more detailed method such as employed in ATLAS (Lolis 2014a). It is designed to be able to give an engine size from the outputs of a gas turbine performance code such as TURBOMATCH, with appropriate assumptions for stage loading and compressor/turbine stage length. *Tethys* is useful because it can predict the number of

component stages required within the engine (Booster, HPC, HPT, LPT) based on thermodynamic data from TURBOMATCH, and give an idea of engine size and layout without detailed information from the user.

Tethys was programmed using Fortran by the author in conjunction with Endara Mayorga (2015) and using the principles from Cranfield University's turbomachinery design course.

The structure of the model is shown in Figure 3.19. *Tethys* is based on the Cranfield University turbomachinery design course and uses thermodynamic data from TUBOMATCH, including pressures, temperatures, and mass flow to establish annulus areas, while user inputted details such as blade aspect ratios, stage loadings and hub-tip ratios are used determine the final schematic of the engine. The initial engine was sized based on the CFM56-5B4, and the assumptions used to size this engine were used on the final code.

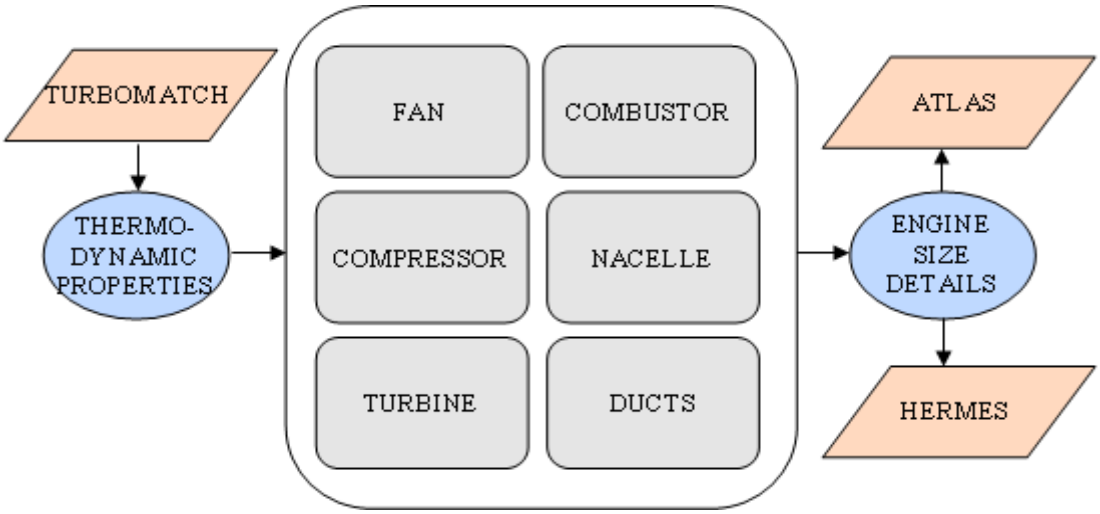

FIGURE 3.19: *TETHYS* STRUCTURE

Tethys calculates the overall size of a gas turbine by breaking down the engine into various components and calculating the individual size of each based on thermodynamic outputs from TURBOMATCH and various assumptions as to blade aspect ratios, flow velocities and blockage factors. Tethys sizes the engine based on a 2-dimensional flow

using a mean-line. The code assumes steady state flow conditions. Cp and gamma values stages are calculated according to the methodology in Walsh and Fletcher (2004) for each stage within each component. The method for sizing each component is given below.

3.4.1 Fan

The fan stage in Tethys consists of the fan rotor and stator, fan bypass duct and fan core duct. Currently, Tethys can only calculate a single stage fan (i.e. one rotor and stator).

The first step in calculating the fan size is to determine the annulus area of the fan face. The absolute diameter of the fan is known and is an input into the program, however the actual flow area is smaller due to the spinner. The inlet temperature and mass flow are known from the outputs of TURBOMATCH. An inlet axial velocity is chosen in order to be able to calculate the fan face Mach number using equation 3.9.

$$\frac{V_a}{\sqrt{T}} = M_a\sqrt{\gamma R}\left(1+\frac{\gamma-1}{2}M_a{}^2\right)^{-1/1} \qquad \textit{equation 3.9}$$

The values for component axial velocities are left to the user to input via the Tethys input file. Next, the value for the flow function, Q, is calculated using equation 3.10.

$$Q = M_a\sqrt{\frac{\gamma}{R}}\left(1+\frac{\gamma-1}{2}M_a{}^2\right)^{\frac{-(\gamma+1)}{2(\gamma-1)}} \qquad \textit{equation 3.10}$$

The inlet area can then be calculated using equation 3.11.

$$A = \frac{w*\sqrt{T}}{K_B*Q*P} \qquad \textit{equation 3.11}$$

The fan exit annulus is then calculated using the same equations, updated with the fan exit flow conditions from TURBOMATCH and a user input exit flow velocity.

Once the fan inlet and exit annulus areas have been calculated, the fan rotor can be sized. The inlet diameter of the fan tip is an input into the program and is known, while the fan outlet tip diameter is a user-defined reduction of the fan inlet tip. The hub diameters are determined from the tip diameters and the inlet and outlet annulus areas. The axial length of the fan rotor is determined by a user-input aspect ratio.

Next, the size and positioning of the fan stator is determined. The axial location of the stator is determined to be two fan blade chord lengths behind the rotor trailing edge. This value was chosen according to the guidance given in Sargerser et al (1971) for low noise designs. The length of the stator is calculated using a user input aspect ratio. The stator tip diameter is already known from the previous fan annulus sizing, while the hub radius is calculated using the bypass mass flow split and scaling the bypass split area accordingly.

The final part of the fan stage calculation in Tethys is to determine the location of the first stage of the core compressor. The axial location of the first core compressor blade is 0.5 fan blade chord lengths behind the fan blade trailing edge. This value has been determined based on scaling the CFM56-5B/4 engine schematic from Janes Aero Engines (Janes, 2011). The tip diameter of the first core compressor blade is determined by assuming that there is a 10^{o} slope from horizontal from the start of the splitter to the first core compressor blade tip. This has once again been determined from the schematic given in Janes (ibid.).

Main assumptions

Several assumptions have been made within the fan component calculation for simplification of the problem, to speed up computational time and also because of the limits of outputs from TURBOMATCH. The first major is assumption is that the pressure ratio along the span of the fan blade is constant. In reality, this will not be the

case. The core of the fan blade travels at a slower speed in comparison to the tip, which would generally result in lower pressure ratios at the core (McKenzie, 1997). This results in designers changing the shape of the blade, further affecting spanwise pressure ratio distribution. Ultimately this may mean that there are different flow pressures in the bypass and core streams, however TURBOMATCH is unable at present to consider this and therefore unable to be integrated into Tethys at this point.

Continuing with blade spanwise distribution assumptions, the isentropic efficiency and temperature rise is also considered constant along the blade, which in reality it would not be, however blading considerations are not considered in Tethys and in addition they are not required to determine the weight in Sargerser's model.

A further assumption is that for annulus sizing purposes, the fan rotor and stator are considered as one unit with no space between them, which are then split up later. This may mean that annulus sizing between the rotor and stator may not be absolutely accurate, however this approach has been used successfully before in Costi (2012).

Also included within the fan section is the spinner, which sits at the front of the engine. The spinner has been sized based on the CFM56-5B schematic in Janes (2011) and is the same for all further engines. For the purposes of this study this approach should be adequate, as the spinner size does not feature in any performance or weight calculations in any other models, and is included for the sake of completeness.

3.4.2 Compressors

Tethys assumes that the gas turbine engine is a two-spool engine with two sets of core compressors. It first calculates the size of the low pressure compressor and then the high pressure compressor. The user is able to input whether the each set of compressors mean, rising or falling line.

The first step that Tethys carries out in respect of the compressors is to determine the number of stages within each compressor set. This is done either by the user inputting

the number of stages in the input file, or calculating it based on an estimation of the stage loading through the set.

Number of Stages Calculation

To calculate the number of stages within the compressor set, the stage loading coefficient (equation 3.12) for the whole set is calculated based on the total temperature rise across the whole compressor set (with inputs from TURBOMATCH), with Cp and mean blade speed calculated for the compressor inlet. This stage loading for the whole set is then divided by a user determined maximum stage loading to estimate the number of stages required for the compressor set.

$$L = \frac{Cp\Delta T}{U^2} \qquad \textit{equation 3.12}$$

A second approach to estimate the number of stages required was also trialled by the author which was to divide to the total pressure ratio across the compressor set by a maximum pressure rise per stage (this approach is also given in Walsh and Fletcher (2004)), however, this approach fails to take into account differences in spool rotational speeds and inlet temperatures, while using stage loading it is possible to have some control on determining the number of stages based on efficiency.

Compressor Sizing

Once the required number of compressor stages has been estimated, Tethys sizes the first stage of the compressor. The inlet annulus area is sized the same way as for the fan, with user inputted inlet axial flow velocities required. The first stage of the low pressure compressor (LPC) is sized using the LPC inlet tip diameter from the fan program and using the annulus area, the LPC blade diameter can be determined. For the high pressure compressor (HPC), a user inputted inlet hub-tip ratio is used to size the first stage.

Once the first compressor stage has been sized, the mean blade speed can be determined by using a user inputted rotational speed (in revolutions per minute, RPM) and using equation 3.13.

$$N = \frac{U_M}{2\pi * r_M} \qquad \textit{equation 3.13}$$

The next step is to determine the stage outlet annulus area. The total compressor set temperature rise is known from the outputs of TURBOMATCH, as well as the set pressure rise once efficiencies have been taken into account. The temperature rise per stage is calculated by dividing the total set temperature rise by the number of stages, while the pressure rise per stage is calculated using equation 3.14.

$$\Delta P_{Stage} = \left(\eta_{Stage} \frac{\Delta T_{Stage}}{T_1} + 1 \right)^{\frac{\gamma}{\gamma - 1}} \qquad \textit{equation 3.14}$$

The stage polytropic efficiency is calculated by first determining the isentropic pressure rise for the set using equation 3.14 and calculating $\int Cp/TdT$ using the fully rigorous approach given in formula F3.28 and F3.29 given in Walsh & Fletcher (2004, p.116-117). The polytropic efficiency is then calculated using formula F3.43 (ibid, p.118).

$$\int \frac{Cp}{T} dT = R \ln\left(\frac{P_2}{P_1} \right) \qquad \textit{equation 3.15}$$

A stage outlet axial velocity is assumed (within Tethys, it is assumed to be 99% of the stage inlet velocity - this figure was determined from experience of lecturers at Cranfield University and during the sizing of the baseline engine given in Endara Mayorga (2015)), which is then used to determine the stage outlet Mach number and hence the stage outlet annulus area, following the methodology from the fan section. Once the outlet annulus area has been calculated, the stage outlet radial dimensions can be determined. The user can select whether the compressor set is mean, rising or falling

line. Depending on the choice, either the blade mid height, tip or hub is kept constant from the first stage, meaning the rest of the annulus radial dimensions can be calculated. This procedure is then looped by the number of stages within the compressor set.

There are two methods in Tethys to determine the axial dimensions within the compressor. The first is to calculate blade and stator lengths, and separation using user defined aspect ratios. As the blade heights are calculated during the annulus sizing operation, the blade and stator lengths can be determined. Typical blade and stator aspect ratios can be found in Saravanamuttoo et al (2008). The individual axial lengths can be summed to determine the total compressor length.

The second method to determine axial distances is to input an absolute initial stage length and subsequent stage length reduction factor. This was implemented in Tethys as it was found during testing that as compressor pressure ratio was increased, the reduction in annulus area was causing the compressor length to shrink. Subsequently, increasing pressure ratio would cause a reduction and size and weight of the engine.

Main Assumptions

As with the fan, several assumptions have been made for the compressor to simplify the problem and speed up calculation time. The first is that the annulus walls have straight sides and that there is no curvature in the walls. In real engines, this may not be the case, however for preliminary sizing purposes this simplification should be reasonable. The flow is also assumed to be adiabatic (although inefficiencies are determined by the engine performance module).

A major assumption made within the program is that no assessments are made with respect to blading, and whether individual rotors are able to give an acceptable DeHaller number. Tethys calculates the annulus inlet and outlet areas based on a user inputted axial velocity and output velocity based on the number of stages. The number of individual stages required within the compressor set is estimated based on the stage loading of the inlet conditions and the users input of max loading per stage. There is no

iterative process within the program to then determine whether the number of stages is acceptable. This assumption is in place because ultimately Tethys will be used to give an estimation of the size of a large number of potential engines through an optimiser, meaning computational time is important. Any potential optimal engine found could then be taken for further study to determine the final design. Tethys does, however, give the user an opportunity to input sensible values for inlet axial velocities and also able to monitor outlet hub-tip ratios so likely unfeasible designs can be discounted. It is dependent on the user, therefore, to perform a verification exercise prior to using the program to ensure that sensible values are used.

The blockage factor, K_B in equation 3.11, is an empirically derived correction used by Ramsden et al (2013) to account for the reduction in effective annulus area cause by the build-up of boundary layer along the annulus walls. The HPC is assumed to have a fully developed boundary layer so the value is constant, while the value for the LPC progressively increases. Values can be found in Ramsden et al (2013), Table 1, page A1.4. In reality, the boundary layer build-up will be dependent on several factors such as stage loading, pressure ratio, tip clearances and other flow features that cannot be determined easily at the preliminary stages of engine design.

3.4.3 Turbines

The process for calculating the size of the turbines is similar to that of the compressors. First, the inlet annulus area is calculated using thermodynamic inputs from the engine performance code as well as a user defined axial velocity. The blade inlet radii are then calculated using a hub-tip ratio defined by the user. An estimation of the required number of stages is then carried out by dividing the stage loading based on inlet conditions and turbine set exit temperature by a user defined max stage loading.

For the turbines, a slightly different approach is taken to calculate the inter-stage annulus areas. The Euler equation shown in equation 3.16 is used to calculate the total whirl of the stage, ΔV_W (see Figure 3.20 for nomenclature), and by assuming a 50% stage reaction and the same blade speeds at inlet and outlet (which are calculated from

the inlet radius and user inputted rotational speed), the exit whirl speed, V_{W3}, can be determined.

$$\Delta H = Cp\Delta T_{Stage} = \left(U_{IN}V_{Wo} + U_{OUT}V_{W3}\right)\Omega \qquad \textit{equation 3.16}$$

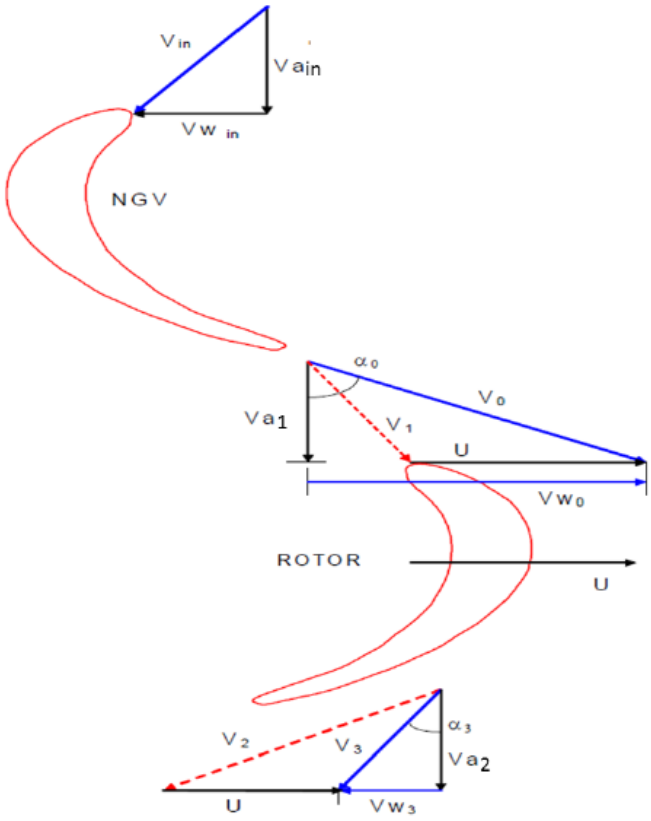

FIGURE 3.20: TURBINE VELOCITY TRIANGLES AND NOMENCLATURE (RAMSDEN ET AL. 2013)

The turbine complete stage set inlet and outlet axial velocities are user defined, with individual stage axial velocities determined by assuming these velocities follow a linear trend using the number of individual stages. These values are then used to determine the exit angle, α_3, and absolute exit velocity, V_3. By assuming that the temperature drop per stage is the total temperature drop divided by the number of stages, and calculating the polytropic efficiency in a similar method to the compressor, the pressure ratio of the stage can be calculated using equation 3.17. There is now sufficient information to calculate the annulus area.

$$PR = \left(1 - \frac{\Delta T_{stage}}{\eta_{stage} T_{in}}\right)^{\frac{\gamma}{(\gamma-1)}} \qquad \textit{equation 3.17}$$

The turbine radial dimensions can the be determined by a user inputted mean, rising or falling line option, the same as for the compressor.

The length of the turbine stages is calculated in the same way as the compressors, with a choice of either specifying rotor and nozzle guide vane (NGV) aspect ratios, or an absolute length for the initial stage with an increase factor.

Main Assumptions

As for the compressor, the turbine calculation assumes that the walls are straight and that the flow is adiabatic. A work done factor, Ω, is used instead of a blockage factor to take into account the boundary layer buildup. This corrects the specific work done by the stage and takes into account the non uniform radial profile of the axial velocity, rather than adjust the annulus area. A user inputted value of Ω, with a default of 0.98 given, is kept constant for all stages. This is because in the turbines, the flow faces a favourable pressure gradient which helps to keep the boundary layer build-up small

3.4.5 Nacelle

The nacelle is an important part of the design of a modern jet aircraft and engine. The main design criterion is a streamlined shape to reduce aerodynamic drag. The nacelle design used in Tethys is based on a long-cowl design with separate exhausts, similar to that of the CFM56 (Figure 3.21).

FIGURE 3.21: CFM56 ENGINE ON AIRBUS A320 AIRCRAFT (COLLINS 2006)

The sizing of the nacelle is carried out in accordance with the guidance given in the Cranfield University Propulsion System, Performance and Integration course notes (Williams 2014). For the purposes of Tethys, the nacelle design is based on the top-of-climb condition of the engine performance model at ISA conditions. The throat area of the intake is the primary dimension that starts the design of the nacelle, which must meet the maximum air flow demand of the engine. This is typically top-of-climb in a cold climate condition (ibid.). The resulting nacelle design in Tethys may be slightly smaller than a final design, but should be adequate for preliminary design purposes.

The design of the nacelle is split into four different components, as shown in Figure 3.22. The design of the nacelle is also assumed to be symmetrical, which is not often the case, but is a reasonable assumption for preliminary design. The design of the pylon is not carried out. This, however, is not a requirement for the aircraft performance code, HERMES. The nacelle is also designed assuming a zero degree incidence to the flow.

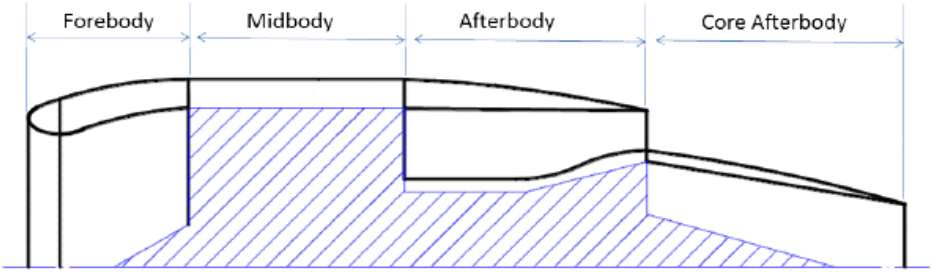

FIGURE 3.22: NACELLE DESIGN COMPONENT SPLIT (SUN, 2012)

This method assumes that the forebody follows a NACA-1 profile, while the afterbody is based on a circular arc. The profiles of a real nacelle will likely not follow these profiles, however, for the purposes of this study, where the aircraft performance code only requires a maximum diameter and length for the engine, this approach is more than adequate.

Intake Sizing

The sizing of the nacelle begins with the intake. Figure 3.23 shows a diagram of the intake and the nomenclature used. The first step is to determine the static temperatures and pressures at each of the stations (0- freestream; 1 - highlight; 2 - throat; and 3 - face). The total values are known from the engine performance program, while the Mach No. is known for the freestream and fan face. A Mach No. of 0.75 is assumed for the throat for high bypass ratio turbofans (Farokhi, 2009).

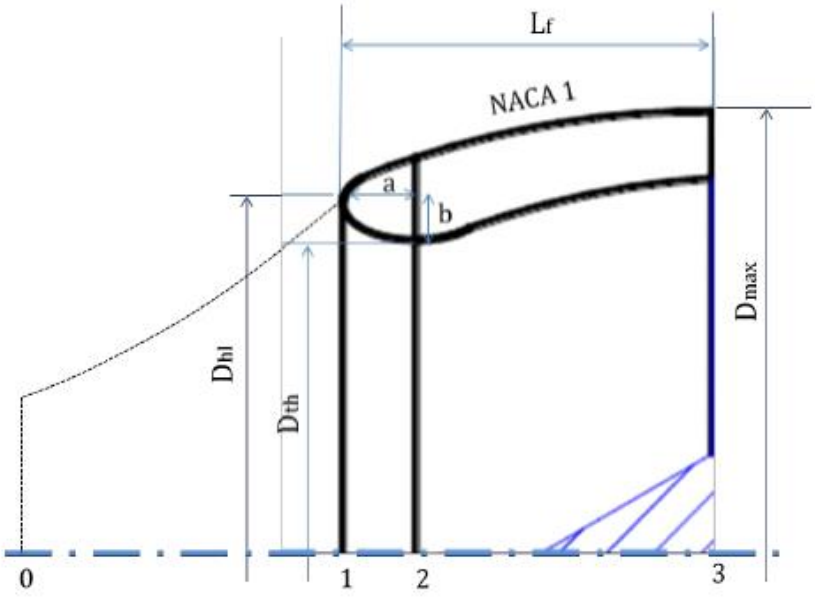

FIGURE 3.23: NACELLE INTAKE DIMENSIONS AND NUMBERING(ENDARA MAYORGA 2015, P.43)

With the Mach Nos. for stations 0, 2 and 3 known, the static temperatures and pressures can be determined, followed by the air density and flow velocity. This allows for the freestream area, A_0 and the throat area A_3 to be calculated. To calculate the highlight area, A_1, equation 3.18 is used. The user inputs a contraction ratio (CR), typically between 1.2-1.35, allowing for M_1 and A_1 to be found.

$$CR = \frac{A_1}{A_2} = \frac{\overline{M}_2}{M_1}\left(\frac{1+\frac{\gamma-1}{2}M_1^2}{1+\frac{\gamma-1}{2}\overline{M_2^2}}\right)^{\frac{\lambda+1}{2(\gamma-1)}} \qquad \textit{equation 3.18}$$

Finally, A_{max}, the nacelle maximum area can be found using equation 3.19.

$$\frac{A_{max}}{A_1} = 1 + \left(2\frac{A_0}{A_1}\left(\frac{M_1}{M_0}\sqrt{\frac{1+\frac{\gamma-1}{2}M_0^2}{1+\frac{\gamma-1}{2}M_1^2}} - 1\right) + \frac{2}{\gamma M_0^2}\left(\left(\frac{1+\frac{\gamma-1}{2}M_0^2}{1+\frac{\gamma-1}{2}M_1^2}\right)^{\frac{\gamma}{\gamma-1}} - 1\right)\right) / \left(-\overline{Cp}\right)$$

equation 3.19

where the pressure coefficient, $\overline{Cp}$, can be substituted with the critical pressure coefficient, Cp_{crit} using equation 3.20:

$$\overline{Cp} \approx Cp_{crit} = \frac{2}{\gamma M_0^2}\left(\left(\frac{1+\frac{\gamma-1}{2}M_0^2}{\frac{\gamma+1}{2}}\right)^{\frac{\gamma}{\gamma-1}} - 1\right) \qquad \textit{equation 3.20}$$

With the intake areas all found, the intake diameters can be calculated straightforwardly.

Nacelle Forebody

With the intake diameters calculated, the axial length of the forebody can be calculated. This is done using equation 3.21. A drag rise Mach No., M_D, is chosen by the user, which should be slightly higher than flight Mach No.

$$M_D = 1 - \frac{1}{8}\left(\frac{\sqrt{1-\left(\frac{D_1}{D_{max}}\right)^2}}{\frac{L_f}{D_{max}}}\right) \qquad \textit{equation 3.21}$$

Forebody Lip

The nacelle lip comprises the internal section of the forebody. A quarter ellipse with a major to minor axis ratio of 2:1, was assumed for the internal lip shape following the guidance in Williams (2014). For the internal sections beyond the lip, a simple conical shape is used.

Nacelle Midbody

The mid-section of the nacelle, called the midbody, is assumed to be a cylinder with a constant diameter of D_{max}. The midbody length is calculated once the positions of the forebody and afterbody have been found (it is a simple subtraction).

Nacelle Afterbody

The nacelle afterbody, which includes the core and bypass nozzles, are assumed to be circular arcs, following the guidance in Williams (2014). Figure 3.24 shows a diagram and nomenclature for the afterbody. The core and bypass nozzle areas are known as outputs from the engine performance code, while the boat-ail angles, B_f, are chosen by the user.

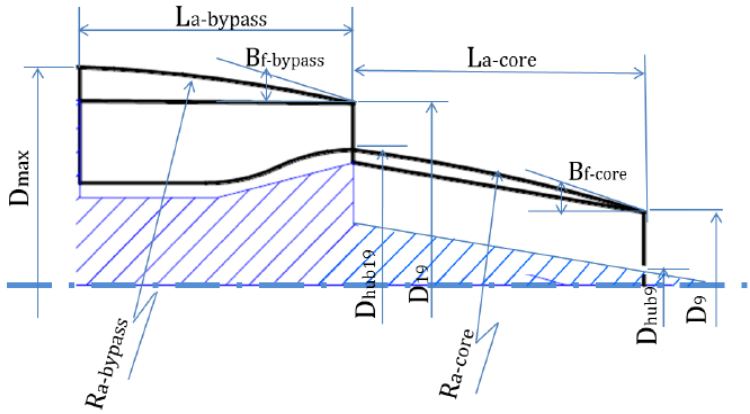

FIGURE 3.24: NACELLE AFTERBODY DIMENSIONS AND NOMENCLATURE (ENDARA MAYORGA 2015, P.48)

To begin the sizing, the D_{hub19} and D_{hub9} diameters need to be chosen. D_{hub9} is inputted by the user, while D_{hub19} is assumed to be 0.2m larger than the LPT maximum exit radius, following the advice by Jackson (2009). This allows D_9 and D_{19} to be calculated.

The afterbody lengths, $L_{a\text{-}bypass}$ and $L_{a\text{-}core}$ can then be calculated using equation 3.22, with β_c being half the boat-tail angle, β_f. The circle radii can finally be calculated using equation 3.23.

$$\tan \beta_c = \left(\frac{D_{\max} - D_9}{2L_a} \right)$$ *equation 3.22*

$$R_a = \frac{L_a}{\sin \beta_f}$$ *equation 3.23*

3.4.6 Ducts

Several inter-component ducts exist within a gas turbine engine, generally to overcome differences in annulus radii between turbomachinery, which come about as a result of trying to achieve good performance with differing rotational speeds, pressures and temperatures. Ducts can be used to accelerate the flow by altering the cross-sectional annulus area along the flow path, which would also affect the static temperatures and pressures. Pressure losses from slowing the flow and increasing the static pressure would ideally be minimised through a low duct angle, but in practice this is a compromised due to overall weight and sizing concerns (Walsh and Fletcher, 2004). Ducts are also a source of loss, due to boundary layer build up along the walls and heat loss through the walls.

Within Tethys, however, the losses are not taken into account. The engine performance program provides thermodynamic data for each engine section, therefore these factors will have already been taken into account. There is no feedback loop between Tethys and the engine performance program, Tethys provides the engine size based on the data given. The duct inlet and outlet annulus areas and diameters are already calculated from the components the ducts connect, so all that is required is a determination of duct axial length.

The axial length of the ducts is determined from the user inputting an absolute value for duct length. A default value scaled on the CFM56-5B engine schematic in Janes (2011) is included within Tethys. A suggestion for further improvement to the model would be to include a duct angle parameter. Duct angle usually has to be limited so that excessive losses due to turning and slowing down of the flow are minimised, but as discussed

earlier, this is often a compromise in real engines due to size and weight constraints (Walsh and Fletcher, 2004). With the duct angle, entry and exit velocities known and an assumption that the duct is 'straight' (i.e. with no swan necks or reverse flow), the axial length of the duct could be estimated.

3.4.7 Combustor

The combustor size is not currently calculated in Tethys mainly due to time constraints of establishing a working model. An absolute value for combustor length is entered by the user to provide an axial distance between the HPC and HPT. The default value in Tethys is the same as for the CFM56-5B/4 schematic given in Janes Aero Engines (2011), while the user can input any other value. According to Sargerser et al (1971) and Jackson (2009) it is reasonable to assume that combustor length does not play a big role in determining combustor weight, therefore given the time constraints, the author did not consider it critical that combustor length was calculated. For the combustor mean diameter, the mid blade radius of the HPT inlet is used.

In practice, however, the design of the combustor is an important consideration for gas turbine engines. Combustors have evolved from the first self-contained tubular combustor 'cans', to the tubular-annular design where ducts connect each of the combustor cans to the modern annular design, which is essentially two concentric rings of different dimeter producing an enclosed volume for the combustion process.

There are various factors that need to be considered for combustor design and sizing. The first is combustor height, which is influenced by various factors including the sufficient space to accommodate the mass flow, the speed of the flow (which is a compromise between a slow enough flow to reduce hot losses, but not to have a combustor that is too large and generates boundary layer losses) and sufficient space for cooling flows. For combustor length, the main factors to consider are sufficient length for flame stabilisation, mixing and residence time considerations for complete combustion and NOx emission minimisation (Mellor, 1990).

For the current project, as the different engines being studied would have the same application on the same aircraft, with similar thrust and core mass flow levels, it was considered that an absolute value of combustor length based on an existing engine would be adequate. To create a programme that is able to deal with different sizes and applications for engines, a recommendation for further work would be to incorporate some method of combustor sizing into Tethys, such as the empirical and semi-empirical single annular combustor design of Mohammed and Jeng (2009), or the slightly modified version of Lolis (2014a).

3.4.8 Verification

To verify the model and find values for the key assumptions that have been made, a verification exercise was carried out. A baseline engine, the CFM56-5B/4, was used as the existing engine for the model to be assessed against. As much of the inter-component thermodynamic data is not known for the real engine, the CUEJ56 performance model, itself based on the CFM56-5B/4, was used to provide the performance data. The CUEJ56 is described in detail in Chapter 4, while the full validation of the original sizing model is given in Endara Mayorga (2015).

Appendix 2 contains the Tethys input file, which provides the list of assumptions and variables used to match the engine size created in Tethys. Figure 3.25 shows the original matching of the CFM56-5B/4 carried out by Endara Mayorga, which was then used to match the CUEJ56 schematic created in Tethys, shown in Figure 3.26.

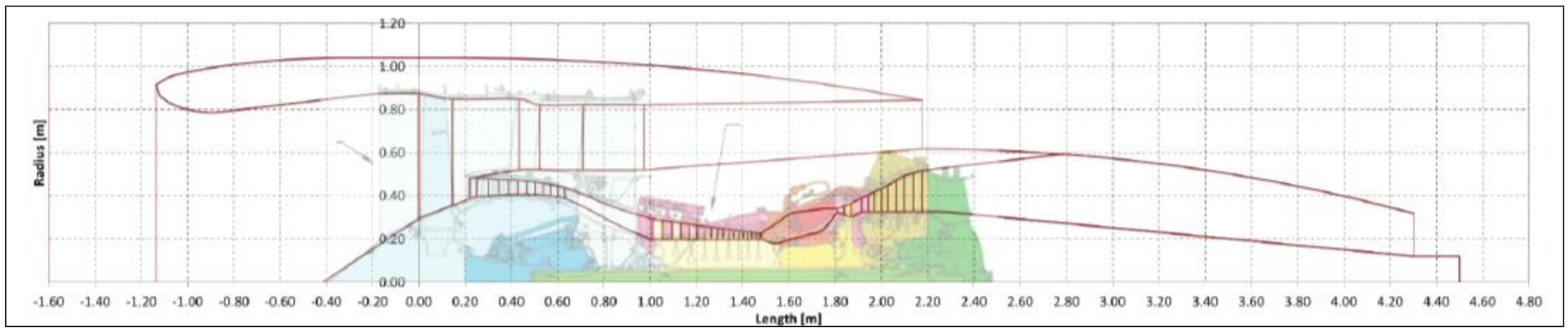

FIGURE 3.25: CUEJ56 VS. CFM56-5B LAYOUT (ENDARA MAYORGA 2015, P.100)

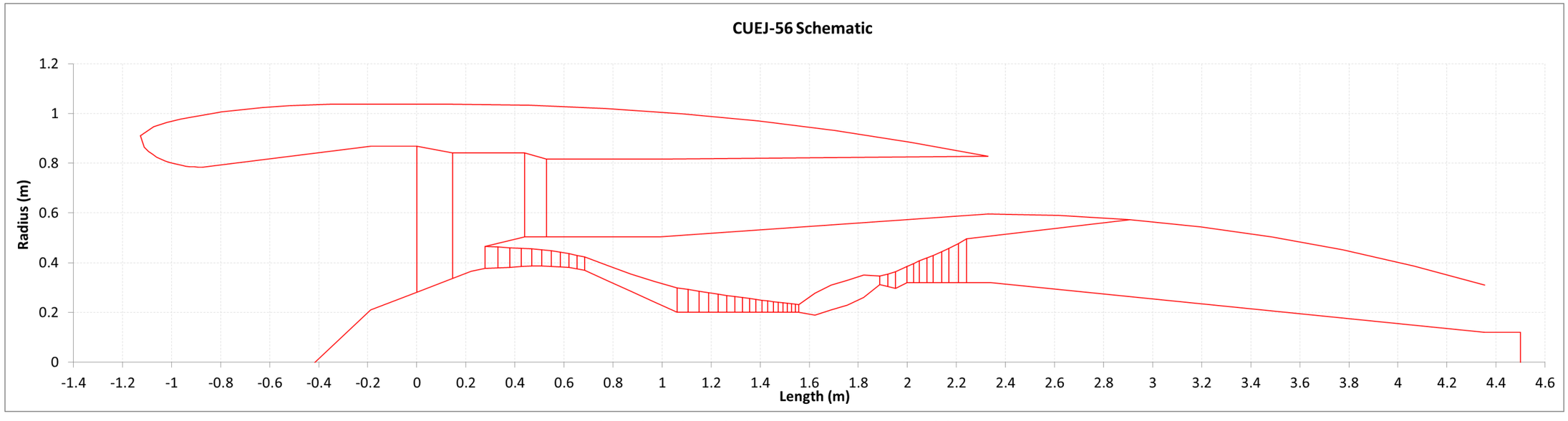

FIGURE 3.26: CUEJ56 LAYOUT USING TETHYS PROGRAM

3.4.9 Model Limitations and Potential Improvements

Tethys is a program that has been designed to predict the size and layout of a turbofan engine based on component performance data from an engine performance code combined with user defined variables and assumptions. The code has been designed to give a quick solution over a first pass (i.e. with no iterations) and as such requires the user to have some knowledge of gas turbine sizing to make reasonable assumptions.

Several improvements could be made to the code to improve the functionality, for which there was not sufficient time to implement. These are to include a gearbox sizing module, duct and combustor size modules, and a multi-stage fan module. Over the longer term, a propeller or open rotor module could also be included.

3.5 Weight Estimation Module

Weight estimation is an important part of assessing the viability of a future powerplant. An uninstalled powerplant may give a good SFC, however, once it is installed on an aircraft, its weight could mean that the overall fuel burn may be worse than a lighter engine with a worse SFC. A model that is able to provide an estimation of weight from engine performance characteristics is therefore required.

A number of different models and techniques for engine weight prediction have been developed over the years and can be split into two broad categories: whole engine based methods and component based methods.

Whole engine based methods primarily estimate the weight of an engine using a few easily obtainable variables, such as thrust or fan size and use statistical correlations from a database of engines to link those variables into an estimation of the overall engine weight (Lolis et al, 2014). The main advantages of this type of method are that they can provide a very quick estimation of engine weight with very few variables. This means that they are suitable at the very first stages of engine and/or aircraft development, where a broad picture of the problem is required.

The advantage of the method, requiring little information and few variables, also leads to the main disadvantage: accuracy. When so few variables are used to predict the weight, engines with similar variables would return very similar weights even though in reality they might be different. For example, if thrust is used as the main determinant of engine weight, then when optimising an engine for a particular aircraft where the thrust requirement remains broadly constant, the weight method would return the same weight for all engines, regardless of if they were different physical dimensions. This means no optimisation could occur using solely the engine thrust.

Additionally, if using data for engines from published sources, it is important that conditions are consistent between datasets. For example, if BPR is used as the main determinant of weight, then weight analysis between engines need to occur at the same condition (i.e. take-off). In published literature it is not often clear at what condition BPR is taken from, therefore weight estimation results could have some error.

Looking now at the potential error that is typical for some of the whole engine methods, Lolis et al (2014) carried out an analysis of some of the popular methods and their findings are displayed in Table 3.1. Lolis et al (2014) investigated a number of different engines (in the No. of Engines column) to find the error for each method (the Sargerser et al method is not a whole engine based method the accuracy will be discussed later). As can be seen from the table, the errors can be quite large, up to 50% for the Jenkinson et al method, despite claims from the authors of errors of up to 10% (Lolis et al, 2014).

Method	Year	No. of Engines	No. of Inputs	Error
Guha et al	2012	64	1	~ ± 30%
Svoboda	2000	64	1	~ ± 30%
Raymer	1989	64	2	~ ± 40%
Jenkinson et al	1999	64	2	~ - 50%
Torenbeek	1975	56	4	~ ± 25%
Gerend and Roundhill	1970	25	Min 8	~ ± 50%
Sargerser et al	1971	7	Min 45	~ ± 25%

TABLE 3.1: WEIGHT ESTIMATIONS SUMMARY AND ERROR (LOLIS ET AL, 2014)

Accordingly, to achieve lower levels of error, a different method of weight estimation, a component based method, may be more suitable, particularly for the type of work in this project where having a greater degree of accuracy is important.

Component based weight estimation methods may offer greater accuracy than whole engine methods due to the greater quantity of information and variables required. As the name implies, component based methods estimate the individual weights of the main components of the engine and sum them together to give the total engine weight. Despite offering greater accuracy, these methods are more complex, requiring additional information that might be difficult to obtain (such as compressor diameters and lengths) and require greater computational time to calculate.

One of the early component based methods was developed by Sargerser et al (1971), who investigated Vertical Take-Off and Landing (VTOL) engines and developed correlations to estimate the size and weight of these engines, as well as 'cruise' engines (i.e. jet engines designed for passenger aircraft), with certain limitations (the method generally estimates these engines to be light). Sargerser et al developed correlations for the main components of the engine, including fan & fan duct, compressor, combustor, turbine, accessories and the main structure, while neglecting ducts and support struts. Simple sizing parameters, such as length and diameter of the turbomachinery, as well as some basic thermodynamic cycle parameters were used to create the correlations, while different proportionality factors were used to differentiate between lightweight VTOL and heavier cruise engines, reflecting the different materials used. While Sargerser et al claimed an accuracy of ±10% for the weight estimation; they also stated that this could increase over time with new materials. This was found by Lolis et al (2014) and reflected in Table 3.1, with the error increasing accordingly. Jackson (2009) revisited Sargerser et al's correlations and thought that they were still the best correlations to use for preliminary design, and updated some proportionality factors to improve the accuracy.

Another component based tool is WATE (Weight Analysis of Turbine Engines) developed by Pera et al (1977) at Boeing for NASA and has a reported accuracy of 5-10%, confirmed by Lolis et al (2014). WATE is designed for use at a preliminary design stage, but requires more information than Sargerser et al's method. In addition to the basic sizing parameters, the code also requires material characteristics and structural loading information such as stress levels, shaft mechanical speed and material temperatures.

The search for better accuracy inevitably leads to more complex methods being created. Cranfield University is developing its own weight code called ATLAS, which is designed to have the accuracy of WATE with the ability to estimate the weight of novel engine configurations (Lolis 2014a)

For this project it was decided to use Jackson's (2009) updated version of Sargerser et al's (1971) component based method. The reason for this was because it offers a good balance of accuracy and complexity. Material information and stress levels which can be difficult to get hold of are not required and ATLAS was not yet available during the project period. Jackson's updates have helped improve the accuracy of the method. To update the method, Jackson re-evaluated Sargerser et al's original method using modern engines – a Rolls-Royce Trent 892 for large engines and a IAE V2500 for smaller engines. In this way he was able to provide new scaling coefficients for the core of the engine to match weights more accurately. Jackson also provided a method for calculating the weight of the engine nacelle. The methodology is described below.

3.5.1 Sargerser et al's Weight Estimation Method with Jackson's Updates

Fan

The equations for the fan are for a typical arrangement of a single rotor with downstream stator. The weight comprises the rotor and stator blades, support structure, casing and the front spinner. Two options for the equation are provided by Sargerser et al, with the standard equation being used and shown below. The second option also

includes terms for fan tip speed and fan solidity which were also suggested to influence the weight of the fan. However, as one of the assumptions for this study is that fan tip speed will remain broadly similar, and that the solidity of the fans is not known, the standard form of the equation has been chosen.

$$m_f = 135 D_t^{2.7} \frac{N}{AR^{0.5}} \qquad \textit{equation 3.24}$$

where m_f is the fan mass in kg, D_t is the fan tip diameter, N is the number of stages and AR is the fan blade aspect ratio.

Compressors

The compressor weight is a function of the average diameter and overall length of the compressor, the tip speed and number of stages. These details are all estimated by the *Tethys* general arrangement model.

$$m_c = 24 . D_m^{2.2} N^{1.2} \left(\frac{U_t}{U_{tref}} \right)^{0.5} \left(1 + \frac{L/D_{mi}}{(L/D)_{ref}} \right) \qquad \textit{equation 3.25}$$

$$\left(L/D \right)_{ref} = 0.2 + 0.0181 N$$

where m_c is the compressor mass, D_m is the average of the compressor inlet and outlet mean diameters, U_t is the compressor inlet tip speed while U_{tref} is a reference value (355m/s), L is the compressor total length, D_{mi} is the compressor inlet mean diameter and $(L/D)_{ref}$ is a reference value calculated by the second equation.

Combustor

The weight of the combustor is purely a function of its diameter. Difficulties in getting consistent data from manufacturers led Sargerser et al to assume that combustor length did not play a big role in determining combustor weight, a reasonable view according to Jackson (2009). Jackson found that the correlations were not consistent at larger

diameters and proposed a modified alternative for big combustion chambers. As the engines this study are dealing with are on the relatively small side of aero-engine sizes (in comparison with the Rolls-Royce Trent for example), the standard form of the equation has been chosen. Jackson also felt that a pressure term should be included for higher pressure ratios, however no modification was suggested. The author does not have the data to be able to make such a modification.

$$m_{cc} = 390 D_m^2 \qquad \textit{equation 3.26}$$

where m_{cc} is the combustion chamber mass D_m is the combustor mean diameter

Turbines

Similar to the compressor, the turbine input details come from the *Tethys* general arrangement model and include average diameter, number of stages and average blade speed of the turbine.

$$m_t = 7.9 D_m^{2.5} N U_m^{0.6} \qquad \textit{equation 3.27}$$

Where m_t is the turbine mass, D_m is the average of the inlet and outlet mean diameters, N is the number of stages and U_m is the average blade speed of the inlet and outlet at mean blade height.

Structure Weight

The additional parts of the engine (called ‘structure weight’ by Sargerser et al), including mounts, supports, shafts, bearings, inner fan wall duct and other transition sections. These have no specific correlations and were assumed to be dependent on the other engine components. Accordingly, an estimate of the structure weight is given by scaling each of the component weights by a factor of 1.18.

Nacelle

The nacelle weight is estimated using the method in Jackson (2009). The nacelle weight includes the intake, fan cowl and afterbody sections, shown in Figure 3.27. The nacelle is assumed to be made up of three sets of cylinders, with the portions of the nacelle exposed to the ambient free stream with double thickness skin. Underwing pylons are not included in the calculations, instead these are taken into account in the airframe weight portion of the aircraft performance model. Equation 3.28 shows how the mass is calculated.

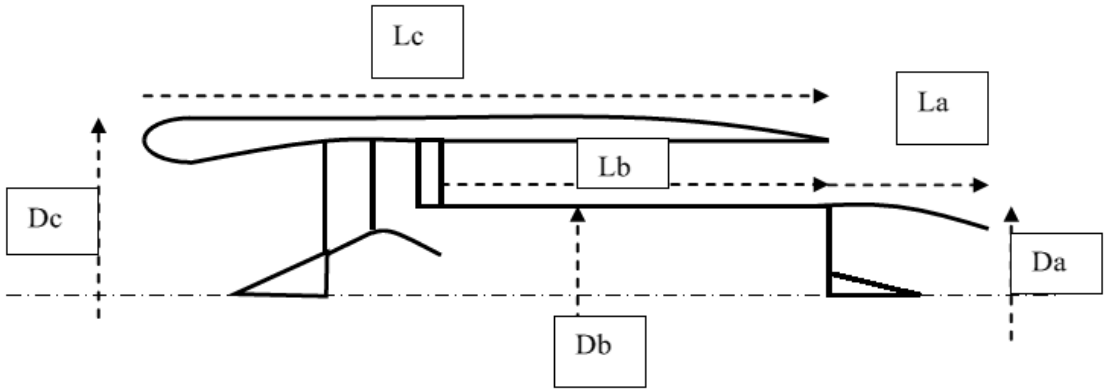

FIGURE 3.27: NACELLE DIMENSIONS USED FOR WEIGHT ESTIMATION (JACKSON 2009, P. 107)

$$m_{nac} = k\pi(2L_cD_c + L_bD_b + 2L_aD_a) \qquad \textit{equation 3.28}$$

The coefficient, *k*, in equation 3.28 is similar to *"... a density per square metre of nacelle in kg/m^2"* (Jackson 2009, p.107) and was calculated from a Rolls Royce Trent 892 engine. Jackson considered this acceptable to be used to calculate weights for different types of nacelle.

Gearbox

A simple method has been used to estimate gearbox weight, where an engine has a gearbox situated between the booster and fan on the low pressure shaft. Using this

method given in Pera et al (1977) and based on the work by Willis (1963), gearbox weight is a function of the input torque and gear ratio, demonstrated in equation 3.29.

$$m_{gbx} = k_{gbx} Q K_w \qquad \textit{equation 3.29}$$

Where k_{gbx} is the gearbox weight proportionality factor (a value of 0.000833 is recommended), Q is the input torque (lb-in) and K_w is the weight factor (a value of around 2 is recommended for a planetary gearbox with ratio of 3).

3.5.2 Model Structure

An overall structure of the model and where it fits into the TERA framework is given in Figure 3.28. The model itself is programmed in Fortran and is currently set up for a two-spool direct drive turbofan. The input and output files are simple text files, with the output file giving individual component weights, along with an overall dry weight and a corrected weight using a user defined correction factor, which will be discussed in the verification section.

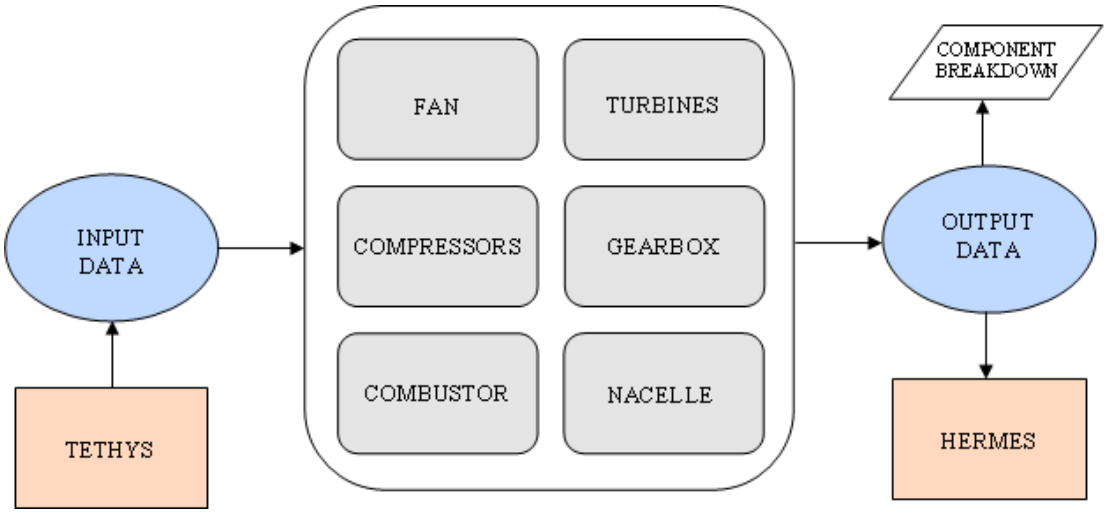

FIGURE 3.28: WEIGHT MODEL STRUCTURE

3.5.3 Model Verification

To verify the model, the baseline CUEJ56 engine was compared with the published value of 2381 kg (Janes, 2011) for the CFM6-5B/4 (Table 3.2). Using the geometric details from *Tethys*, the raw estimate of weight of the CUEJ56 is 1771.48 kg, some 28% less than the published figure. This is similar to the findings of Jackson (2009), who proposed to use a scaling coefficient for all weights to match the predicted model weight with the published engine weight. Using this method, a coefficient of 1.391 has been used to match the published weight with that of the model.

The discrepancy in weights shows the difficulties involved in predicting the weight of engines. Ultimately, it is the trend that is more important than absolute weights in this study, and this weight model should be able to fulfil this task acceptably.

Weights (kg)	**Raw Estimate Including Structure**	**Scaled Using Coefficient of 1.391**
Fan	380	529
Low Pressure Compressor	287	399
High Pressure Compressor	322	447
Combustion Chamber	115	160
High Pressure Turbine	141	196
Low Pressure Turbine	468	650
Total	**1713**	**2381**
% Difference of CFM56-5B/4	**28%**	**0%**

TABLE 3.2: WEIGHT MODEL COMPONENT BREAKDOWN COMPARISON

4.0 Baseline model setup and discussion

4.1 TURBOMATCH Model of CFM56-5B/4 Type Engine (CUEJ56)

The baseline engine model was created using TURBOMATCH, Cranfield University's in-house gas turbine performance code. The model, called the 'CUEJ56' (Cranfield University EasyJet 56), is a two-spool turbofan based on the CFM56-5B/4 engine. A schematic of CUEJ56 is shown in Figure 4.29.

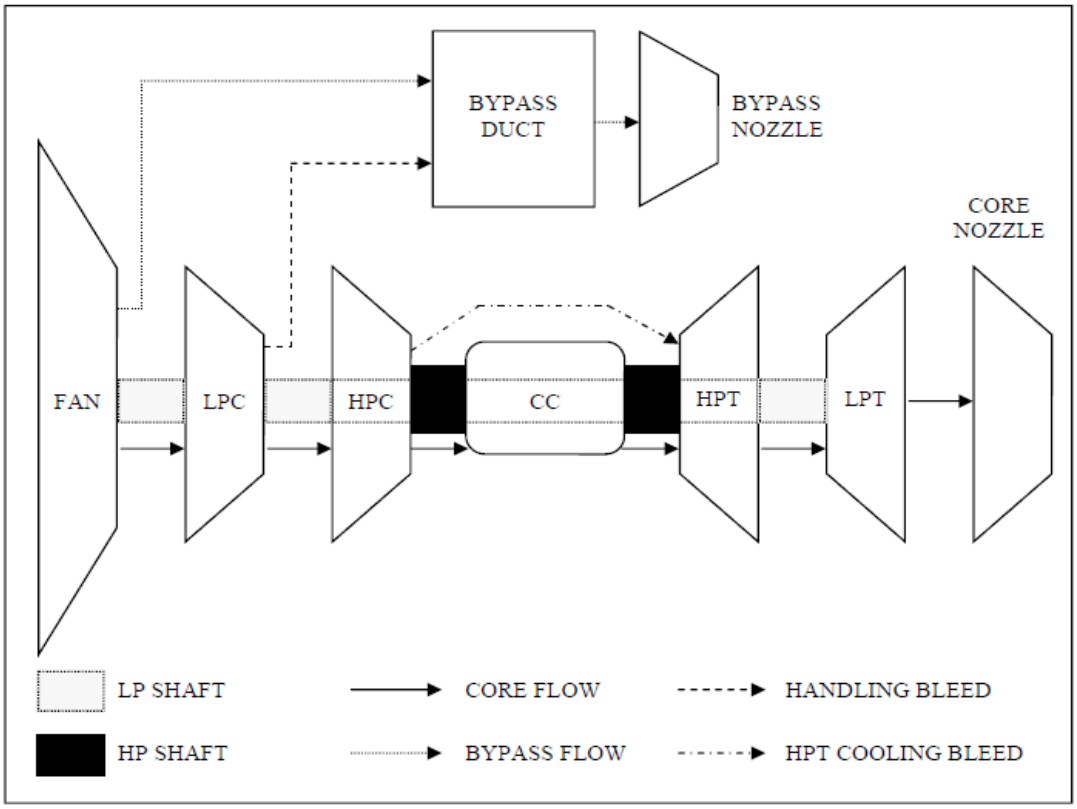

FIGURE 4.29: SCHEMATIC OF CUEJ56

The design point of the engine was selected as Top-of-Climb, where the aircraft has just reached the top of the climb phase and is about to throttle back and begin the cruise phase. This was chosen because the overall pressure ratio was given in Janes for this phase and therefore gave good information for starting point. A list of the parameters used for the design point of the engine are given in Table 4.3.

Parameter	Value
Design Point: Top of Climb (M=0.8, 10,668m, ISA)	
Mass flow rate (kg/s)	170
Overall Pressure Ratio	32.6
Fan Pressure Ratio	1.65
Fan Isentropic Efficiency	0.89
Booster Pressure Ratio	2.823
Booster Isentropic Efficiency	0.87
HPC Pressure Ratio	7
HPC Isentropic Efficiency	0.87
HPT Cooling Flow	13%
Customer Bleed (Cabin Pressurisation)	1%
Combustion Efficiency	99.9%
Combustion Fractional Pressure Loss	0.05
Turbine Entry Temperature (K)	1489
HPT Efficiency	0.91
LPT Efficiency	0.92
Flight Altitude (m)	10,668
Flight Mach Nº	0.8

TABLE 4.3: PARAMETERS AND ASSUMPTIONS USED FOR CUEJ56

The mass flow of the engine was initially calculated using the following formulae:

$$w = \rho A v \qquad \textit{equation 4.1}$$

$$v = M\sqrt{\gamma R t} \qquad \textit{equation 4.2}$$

$$\frac{T}{t} = 1 + \frac{\gamma - 1}{2} M^2 \qquad \textit{equation 4.3}$$

$$\frac{P}{p} = \left(\frac{\gamma - 1}{2} M^2 \right)^{\frac{\gamma}{\gamma - 1}} \qquad \textit{equation 4.4}$$

$$p = \rho R t \qquad \textit{equation 4.5}$$

First equation 4.3 was used to calculate the total temperature at the intake based on a flight Mach Nº of 0.8 and a static temperature based on the International Standard Atmosphere (ISA) at 35,000ft (10,668m). Then, assuming that the flow slows down through the intake and meets the fan blades at around Mach 0.5 (based on discussions with staff at Cranfield University), the static temperature on the blades can be recalculated. This can be used in Equation 4.2 to give the velocity of the flow on the blades (γ=1.4, R=287 J/kgK). The result can then be used in equation 4.1, combined with the air density calculated from equations 4.4 and 4.5, and the area of the fan, for which the diameter is given in Janes (2011 - Fan Diameter 1.735m). The final result was then modified once the model had been created in order to give a good match with publicly available data for the engine.

The pressure ratios were chosen so that the overall pressure ratio (OPR) matched with Janes and that the individual values for each component were roughly in line with what would be expected in real life (based on discussions with Cranfield University staff) - this extends to the component efficiencies also. Combustion efficiency was given as 99.9% as *"current emission regulations call for combustion efficiencies in excess of 99 percent"* (Lefebvre, 2010, p.135).

As compressor and turbine maps are not freely available for the CFM56-5B/4 engine, the library of maps within TURBOMATCH were used. The maps were chosen first based on having a good match for the pressure ratio that was being used and then secondly to give a stable code which converges consistently.

Once the input file was prepared and initial simulations run, it was then a case of adjusting the various parameters so that the model shows a good correlation with publicly available data. Table 4.4 shows how the CUEJ56 engine model compares with data for the CFM56-5B/4.

Parameter	CFM56-5B/4 Data	CUEJ56	Difference
At 35,000ft, M=0.8, ISA (DP)			
TOC Thrust (kN)	25.04	25.03	0.04%
TOC SFC (mg/Ns)	Unknown	17.03	-
TOC TET (K)	Unknown	1,489	-
Cruise Thrust (kN)	22.33	22.33	0.0%
Cruise SFC (mg/Ns)	16.98	16.98	0.0%
Cruise TET (K)	Unknown	1,430	-
At 0ft, M=0, ISA, SLS			
T-O Thrust (kN)	120.10	120.09	0.01%
T-O SFC (mg/Ns)	Unknown	8.81	-
T-O TET (K)	Unknown	1,634	-
T-O BPR	5.7	5.7	0.0%
T-O Mass Flow Rate (kg/s)	408.2	410.1	0.47%

TABLE 4.4: COMPARISON OF CUEJ56 WITH CFM56-5B/4 DATA FROM JANES (2011 P. 177-188)

As table 4.4 shows, the model CUEJ56 shows good correlation with public data for the CFM56-5B/4, with negligible differences between known parameters. The model should therefore be suitable for use within the TERA framework. However, in order to give further confidence with the model, it was run across a range of different scenarios in order to see if it agreed with the general trends for a turbofan engine.

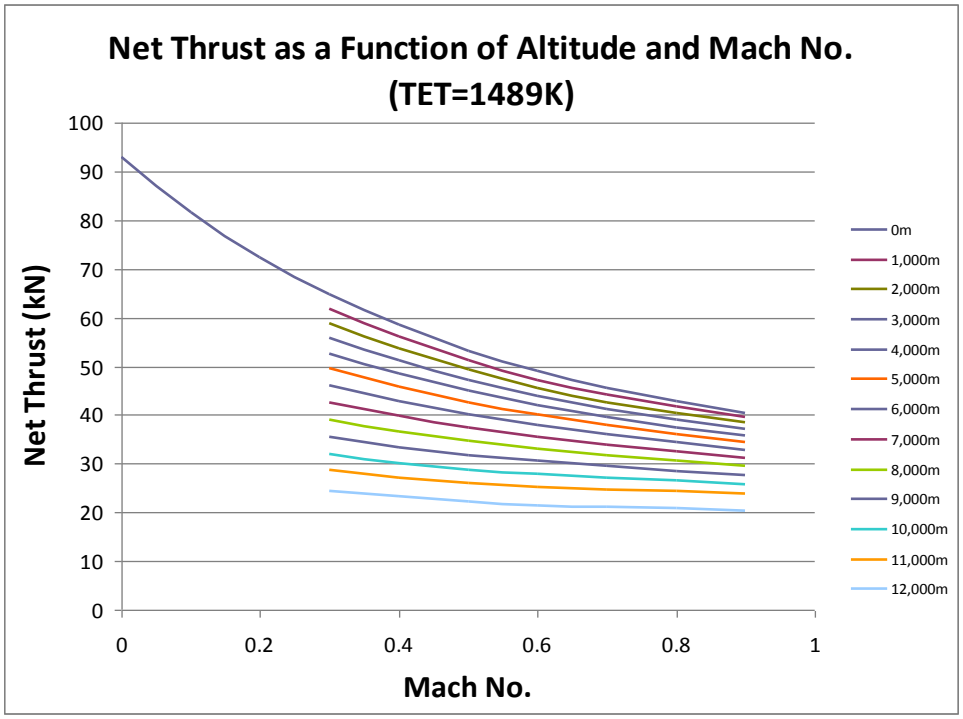

FIGURE 4.30: VARIATION OF NET THRUST WITH ALTITUDE AND MACH NO FOR CUEJ56 ENGINE MODEL

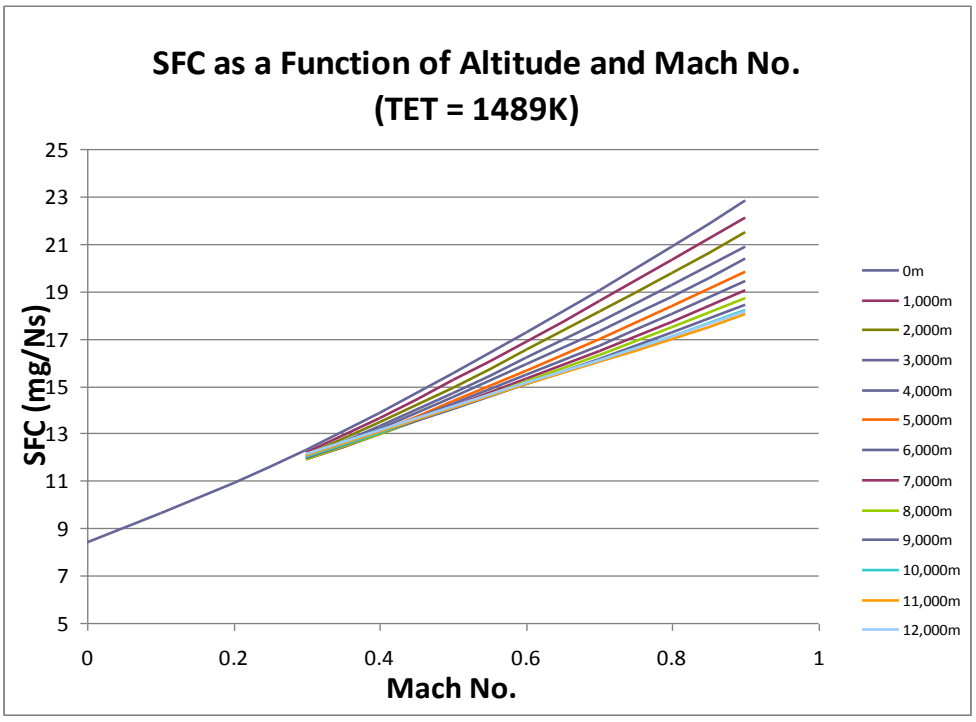

FIGURE 4.31: VARIATION OF SFC WITH ALTITUDE AND MACH NO FOR CUEJ56 ENGINE MODEL

Figures 4.30 and 4.31 show how the thrust and the SFC respectively of the CUEJ56 engine model vary with altitude and Mach number while keeping the turbine entry temperature constant at the design point value. The trends are as would be expected, with both net thrust decreasing and SFC increasing as the flight Mach number increases. Three factors influence the performance here (Pilidis et al, 2010, p.43): momentum drag, ram compression and ram temperature rise.

The main effect that can be observed in the graphs is that of momentum drag. As the flight Mach number increases, so does the momentum drag (*the drag due to the momentum of the air passing through the engine relative to the engine speed* Rolls-Royce, 1966, p. 181) which has the effect of reducing the net thrust and hence increasing SFC (SFC is fuel flow/net thrust). This is offset slightly as the Mach number increases beyond about 0.3 because of ram compression, which increases inlet pressure (and hence mass flow), and nozzle pressure ratio, which overall increases the gross thrust slightly. The third effect, ram temperature rise, increases the temperature of the air at the compressor, which overall reduces the thermal efficiency slightly.

As altitude increases, the net thrust decreases for all flight Mach numbers along with SFC. The main effect here is the fall in air density as altitude is increased, decreasing mass flow through the engine and reducing net thrust. A secondary effect is due to the reduction in ambient temperature as altitude increases is that for a constant shaft speed of the engine, the quasi non-dimensional shaft speed of the engine ($N/\sqrt{T}$) increases, giving an increased pressure ratio and TET. The effect of this can be seen with a slightly larger than expected drop in net thrust between 11,000 and 12,000m, where because of the constant temperature in the stratosphere (above 11,000m), this effect is no longer applicable.

Figures 4.32 and 4.33 show how net thrust and SFC of the model this time vary with ambient temperature and TET (power setting). The first effect on net thrust, increasing TET, is as would be expected - net thrust increases. To increase TET, more fuel needs to be added and greater thrust would be expected. The effect on SFC is interesting, however, and the phenomenon can better be seen on the coldest day. The distinctive

curve shows the trade-off between thermal and propulsive efficiencies of the engine. At low TET's, the overall thermal efficiency of the engine is low (thermal efficiency is proportional to TET), but the propulsive efficiency is high, due to a lower jet velocity. At high TET's, the jet velocity is increased greatly, meaning a lower propulsive efficiency but a higher thermal efficiency. At lower day temperatures, the rate of increase of net thrust can be seen at higher TET's. This is likely due to the compressors beginning to choke.

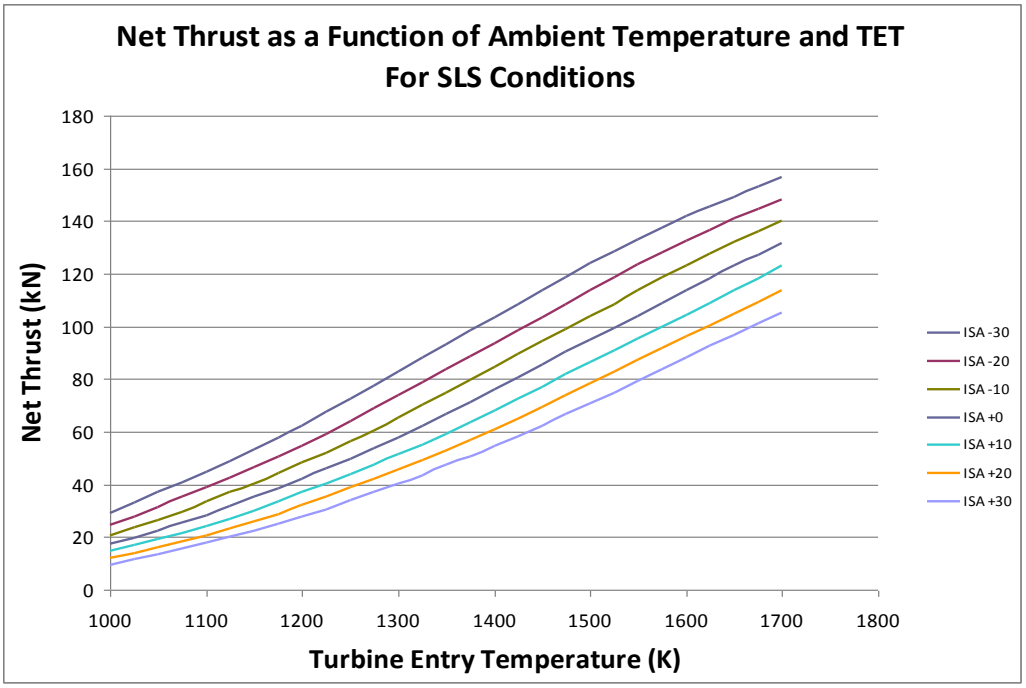

FIGURE 4.32: VARIATION OF NET THRUST WITH AMBIENT TEMPERATURE AND TURBINE ENTRY TEMPERATURE FOR CUEJ56 ENGINE MODEL

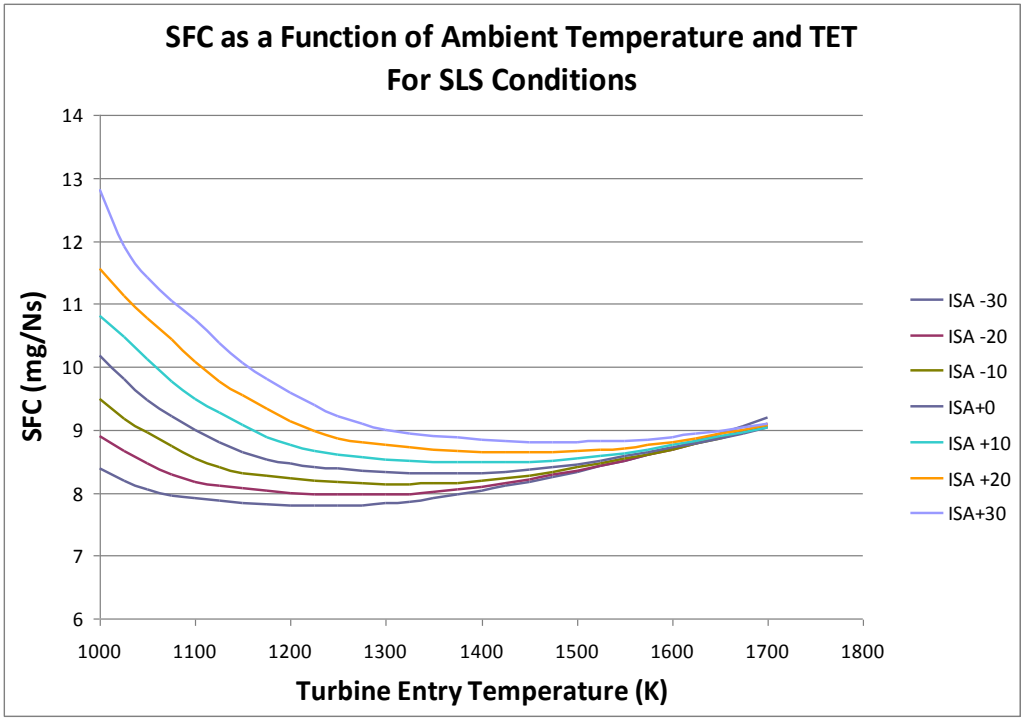

FIGURE 4.33: VARIATION OF SFC WITH AMBIENT TEMPERATURE AND TURBINE ENTRY TEMPERATURE FOR CUEJ56 ENGINE MODEL

The effect of ambient temperature is to reduce net thrust and increase SFC as the ambient temperature increases. The simple explanation for this is that the warmer the air, the more difficult (i.e. the more work required for the same pressure ratio) the air is to compress. Thus for a given TET, a greater proportion of the energy added to the engine form the fuel is required to compress the incoming air reducing efficiency and net thrust.

The figures show that the engine model behaves as would be expected, thereby increasing the confidence of the model.

4.2 Aircraft Model

The aircraft aerodynamic and mission model was prepared in HERMES, Cranfield University's in house aircraft performance code. HERMES calculates the lift and drag coefficients of the aircraft based on inputted geometric data and flies the mission using the engine model from TURBOMATCH and the mission profile that the user gives it. HERMES is able to calculate the maximum range of the aircraft based on the fuel and mission constraints given to it, or calculate the fuel burned for a set mission as well as

the flight duration (Cranfield University, 2009, p.18). The aircraft model is called the 'Cranbus EJ320'.

The first step was to find an appropriate aircraft to model. It had already been decided that the Airbus A320 would be modelled, however there are several weight variants available and the variant chosen should be the same as used in EasyJet's fleet. This was accomplished by reading the aviation media and finding a newly registered EasyJet Airbus A320. G-EZUL was an Airbus A320 registered in April 2012 (van der Mark, 2012). With the registration in hand, the variant of the aircraft and maximum take-off weight (MTOW) could be found from the Civil Aviation Authority's (CAA) website (CAA, 2012). The variant was given as an A3214 with a MTOW of 73,500kg. These details were cross-checked with Airbus' own details to ensure accuracy (Airbus, 2010a). Next, the aircraft geometric details were inputted. These were obtained from a scale drawing from Airbus (ibid. 2-2-0 p.3.) using dimensions where specified. There would be some inaccuracies when measuring, even using a computer tool, so these were checked with published data for a Boeing 737 (Brady, 2012), which although is a different aircraft, is similar to the A320 in many respects. The details such as thickness to chord ratio and aspect ratio were of the same order as the 737, so further confidence can be given to the model. The aircraft weights (operating empty weight (OEW), MTOW, payload, fuel) were all obtained from Airbus (2010a, 2-1-1 p.2) for the particular variant of the aircraft.

The aircraft mission profile used is the same as was used by Colmenares-Quintero (2008, p. 88-89) and has the following segments (ibid.):

- *"Start-up and taxi-out*
- *Take-off and initial climb to 1,500ft*
- *Climb from 1,500 ft to cruise altitude*
- *Cruise at selected speed and altitude including any stepped climb required*
- *Descent to 1,500ft*
- *Approach and landing*
- *Taxi-in"*

In order to check the accuracy of the model, a payload-range diagram was prepared using HERMES and compared with that given by Airbus. The following cruise data was inputted in order to correlate with that used by Airbus (2010a, 3-2-1 p.3):

- Cruise altitude 35,000/39,000ft (10,668/11,887m) (Cruise-Climb - gives the best range performance (Lawson, 2012 p. AVD0603/10))
- Cruise Mach number 0.76
- Temperature Deviation ISA +10^{o}
- Fuel Reserves 10% Flight Time Overshoot
- 200nm (370km) Diversion
- 30 minutes hold at 1,500ft

Finally, the model was run for maximum range at:

- Full payload, remainder fuel
- Full fuel, remainder payload
- Full fuel, no payload

to give the data for the payload-range diagram. This is shown in Figure 4.34. The diagram shows a fairly good correlation with the Airbus data at all ranges, with a maximum difference of 2%.

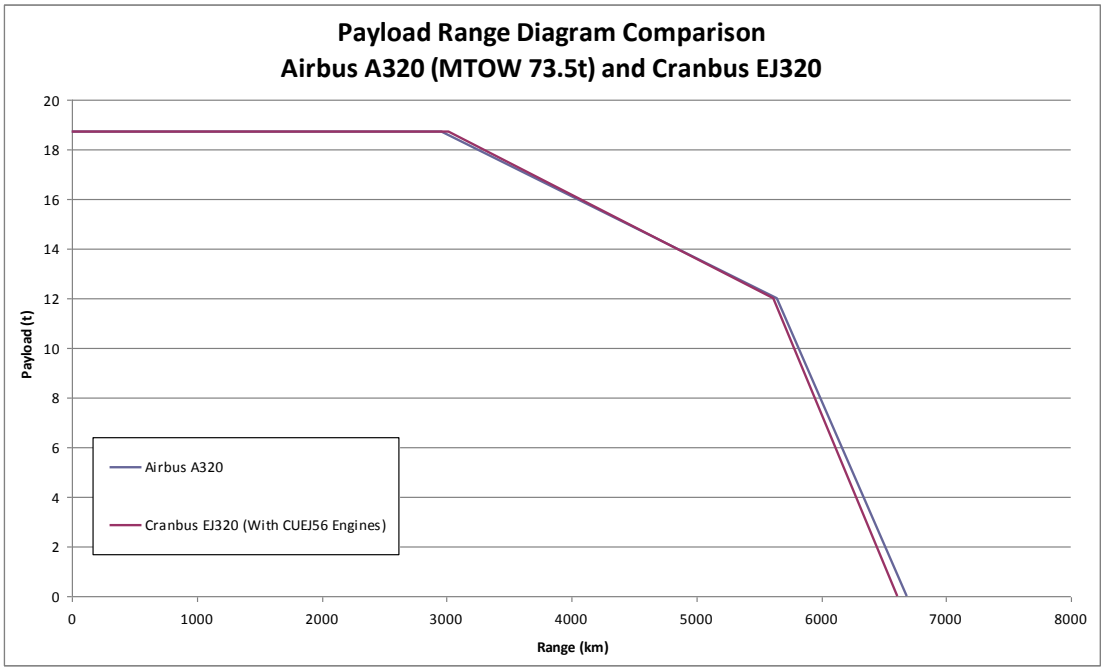

FIGURE 4.34: PAYLOAD RANGE DIAGRAM COMPARING CRANBUS EJ320 AND AIRBUS A320

4.3 Model Limitations

As the models created offer representations and simplifications of real engines or aircraft, there will inevitably be errors that mean they do not represent fully the real equipment. This is compounded by not having a complete set of data for the engine or aircraft, mostly because this data is proprietary and not released in to the public domain for competitive reasons. It is important, however, to look at the limitations in the models to see where they can be improved.

The engine model, although it shows good correlation with the performance data from Janes and behaves realistically, suffers from a lack of available data. Firstly, the component maps are from libraries within TURBOMATCH, which are very unlikely to be the same as those for the CFM56. Secondly, the overall pressure ratio is given in Janes, but not how this is distributed amongst each of the shafts, for which assumptions and judgements have to be made. Finally, the TETs were chosen so that the required thrust was met, however the real TETs may be different, which could affect overall efficiency.

5.0 Airbus A320 NEO Engines (Pratt and Whitney GTF & CFM Leap)

This section describes the two additional engine models that were created for the PhD project: the very high bypass ratio conventional turbo-fan based on the future CFM-LEAP, and a very high bypass ratio geared turbo-fan based on the proposed Pratt and Whitney PurePower engine. These two engines are proposed options on the Airbus A320NEO aircraft, due to enter service during the course of 2016. The engines were modelled based on information available during 2013 and 2014. The author is aware that these engines are currently undergoing certification and as such some information in this chapter may soon be out of date.

5.1 New Engine Context

5.1.1 A320 NEO

The A320NEO has been offered by Airbus to replace the A320 family of aircraft, as an interim between the current A320 family and an all new short to medium range narrowbody aircraft to be released sometime after 2030, once game-changing technological developments are available (Goold, 2012). The A320NEO is essentially an Airbus A320 with sharklets (wing-tip devices which help to lower drag by modifying the spanwise trailing vorticity distribution (Barnard & Philpott, 2004, p. 107) and new, more efficient, engines (Airbus, 2010), along with new, lighter, engine pylons (BreakingTravelNews, 2012). Airbus claim an improvement in fuel burn of up to 15%, resulting in either an additional 500 nm of range, or an extra 2 tonnes of payload (Airbus, 2010). In addition, the new aircraft would give lower noise and reduced NOx emissions.

Two engine manufacturers are offering engines for the A320 NEO: CFM with their LEAP engine and Pratt and Whitney with their PurePower PW1127G, a geared turbofan (Airbus, 2010).

5.1.2 CFM LEAP Very High Bypass Ratio Conventional Turbofan (“LEAP”)

The CFM-LEAP engine is a very high by-pass ratio 'advanced' turbofan engine (M'Bengue, 2010) with an entry into service of 2016. The engine is an evolution of the CFM56, with a bypass ratio of 11 (compared to the CFM56's 5.7 - Janes, 2011). The manufacturer claims up to 16% lower fuel burn than current engines, achieved through an increase in propulsive efficiency thanks to the increased bypass ratio; as well as an increase in HPC pressure ratio to around 22, double that of the existing CFM56 (M'Bengue, 2010).

The higher bypass ratio would normally mean additional weight due to the increase fan size, however the manufacturer claims that there would be no additional weight penalty due to a composite fan blade set and casing, in addition to further materials improvements (ibid.). It is also claimed that the engine would be quieter - up to 15 EPNdB lower cumulative margin against ICAO chapter 4; and lower NOx, with a 50-60% NOX margin against CAEP6 (ibid.).

5.1.3 Pratt and Whitney PurePower Geared Turbofan (“PPGTF”)

The PW1100G engine is one of the other options on the Airbus A320NEO aircraft. The engine uses a geared fan on a 2-shaft arrangement to try and optimise the fan speed, which due to its size, normally needs a slower rotational speed than the booster. The engine would deliver 27,000lbs of thrust, with a bypass ratio of around 12 (Pratt & Whitney, 2012). Pratt and Whitney claim that the engine would also deliver 16% fuel burn savings compared to current engines, with lower noise levels (15-20dB lower than ICAO4) and lower NOx (50% improvement over CAEP6) (Pratt& Whitney, 2012a).

5.2 Engine Performance Modelling

The first step in creating these engines is to create performance models using TURBOMATCH. Modelling these engines, which are still under development, can present some challenges: the lack of certified data allows for a freedom in modelling as

the author sees fit, whilst at the same time meaning that the models may not necessarily reflect real performance once the engines are established and flying on aircraft.

The literature available at the time of modelling for the CFM-LEAP and Pratt and Whitney GTF engines consisted mostly of documents produced by the manufacturers themselves and contained much information that was still not verified such as percentage fuel burn reduction. As the engines were still under development at the time, these figures were still subject to change and could not be verified. Accordingly, it was decided to only use whatever engine cycle figures (such as pressure ratios, bypass ratios, thrusts) were in the public domain and make reasonable assumptions for other information that was not available.

The following table describes the information that was available to the author at the time of modelling:

	CFM-LEAP	**P&W PW1127G**
Fan Diameter	78"[1]	81"[2]
Overall Pressure Ratio	~50:1 (TOC) [3]	~50:1 (TOC) [4]
Take-off Thrust	Unknown	26,250 lbs [2]
Bypass Ratio	~11:1[1]	~12:1[2]
Stage Count (F-LPC-HPC-HPT-LPT)	1-3-10-2-7[1]	1-3-8-2-3[2]

TABLE 5.5: A320 NEO ENGINES AVAILABLE DATA

Accordingly, many assumptions had to be made to model the engines. The main assumption was that as the A320 NEO is almost identical to the existing A320, save for new engines and the addition of sharklets, that the thrust requirements from the engines would also be the same. Accordingly, it was assumed that the thrust outputs of the models would be the same as for the published data for the CFM56-5B/4, as modelled by the CUEJ56.

The second assumption was that the component efficiencies would remain the same as for the previously modelled engine. This assumption was made because even though it

[1] CFM, 2013
[2] Pratt & Whitney, 2013
[3] Croft, 2011
[4] Flightglobal, 2013

is likely that component efficiencies would have likely increased through technological advancements, it was not feasible to quantify what this increase might be and therefore a more conservative approach was adopted.

A final assumption was that cooling flows and bleeds would be the same for all engines. A summary of parameters and assumptions is shown in Table 5.6. Please note that the model naming convention follows the previous Cranfield University EasyJet (CUEJ) followed by either 'LEAP' or 'PPGT' to refer to the LEAP and PWGTF engines respectively.

Parameter	**CUEJ56**	**CUEJ-LEAP**	**CUEJ-PPGT**
Design Point: Top of Climb (M=0.8, 10,668m, ISA)			
Mass flow rate (kg/s)	170	215	225
Overall Pressure Ratio	32.6	50	50
Fan Pressure Ratio	1.65	1.53	1.51
Fan Isentropic Efficiency	0.89	0.89	0.9
Booster Pressure Ratio	2.823	2.334	2.759
Booster Isentropic Efficiency	0.87	0.87	0.88
HPC Pressure Ratio	7	14	12
HPC Isentropic Efficiency	0.87	0.87	0.87
HPT Cooling Flow	13%	13%	13%
Customer Bleed (Cabin Pressurisation)	1%	1%	1%
Combustion Efficiency	99.9%	99.9%	99.9
Combustion Fractional Pressure Loss	0.05	0.05	0.05
Turbine Entry Temperature (K)	1489	1714	1725
HPT Efficiency	0.91	0.91	0.91
LPT Efficiency	0.92	0.92	0.92
Flight Altitude (m)	10,668	10,668	10,668
Flight Mach Nº	0.8	0.8	0.8

TABLE 5.6: ENGINE PARAMETERS AND ASSUMPTIONS COMPARISON

The mass flow rates for the engines were calculated by assuming that at top of climb the intake Mach No. was around 0.5 (Walsh and Fletcher, 2004, p.188) and using the fan sizes along with the ideal gas law, isentropic relations and mass flow equations , as described in Chapter 4.

The fan pressure ratios were determined by performing a fan optimisation process, seeking to find the lowest SFC at the engine cruise condition. Figures 5.35 and 5.36 demonstrate this for the two engine models. It was decided for the fan pressure ratio to be accurate two decimal places.

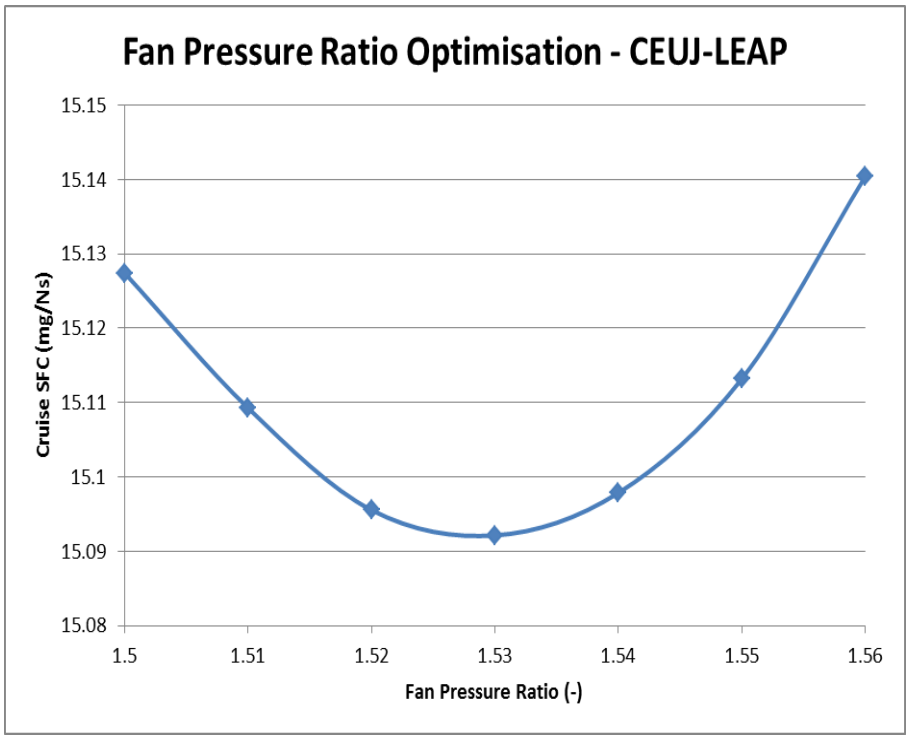

FIGURE 5.35: CUEJ-LEAP FAN PRESSURE RATIO OPTIMISATION

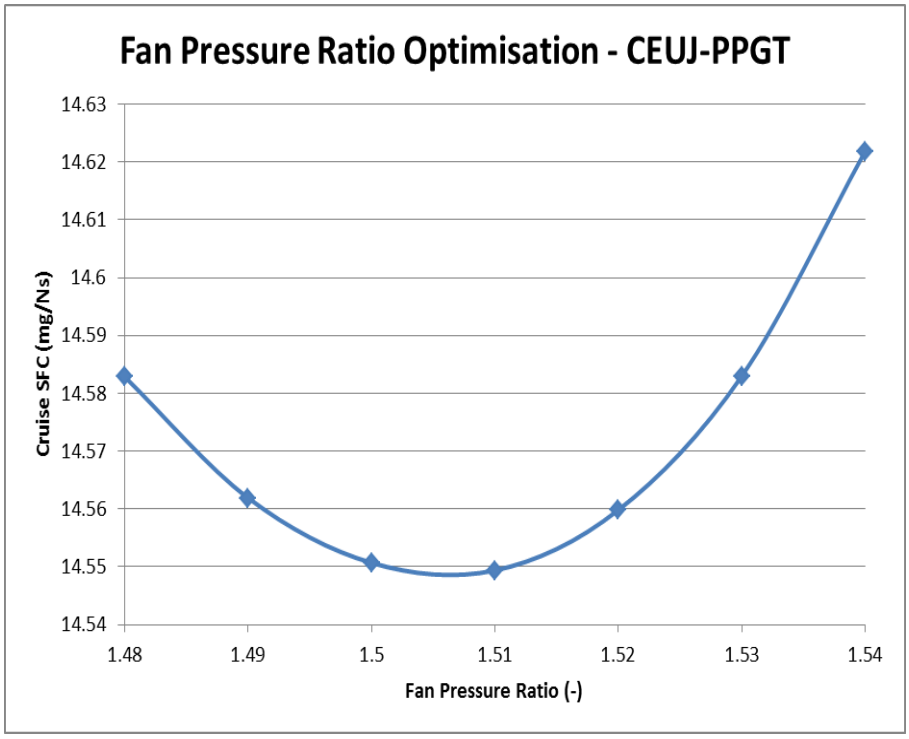

FIGURE 5.36: CUEJ-PPGT FAN PRESSURE RATIO OPTIMISATION

5.2.1 Gearbox Modelling in TURBOMATCH

The Pratt &Whitney GTF engine has a gearbox, with ratio 3:1, on the low pressure shaft between the fan and the booster (Pratt & Whitney, 2013). The gearbox allows for engines with larger fans and hence higher bypass ratios as there is less of a compromise between the fan, which needs lower rotational speeds to keep tip speeds down to an acceptable Mach number, and the booster and low pressure turbine, which need higher rotational speeds for an acceptable stage loading and efficiency (Kurzke, 2009).

In TURBOMATCH, which uses rotational speeds relative to the design point of the component, the gearbox is not directly modelled by the changes in rotational speed through the gearbox. The gearbox is a source of losses, however, and this is modelled by adding the losses of the gearbox as additional auxiliary work to the low pressure turbine. It was therefore decided to implement 2% of fan work as auxiliary work in the low pressure turbine. The value of 2% is based on work by Anderson et al (1984), who investigated gearbox efficiency for planetary gears within a turboprop gearbox, with a view to developing a model for future geared turbofan gearbox losses. Although

gearbox losses are not static and vary through the flight phases (Figure 5.37) due to there being a large ‘fixed’ component to the losses which proportionally lessens as engine power increases, the limitations of TURBOMATCH meant that a single value needed to be chosen. 2% represents the losses at cruise, which is generally where aircraft engines spend most of their time.

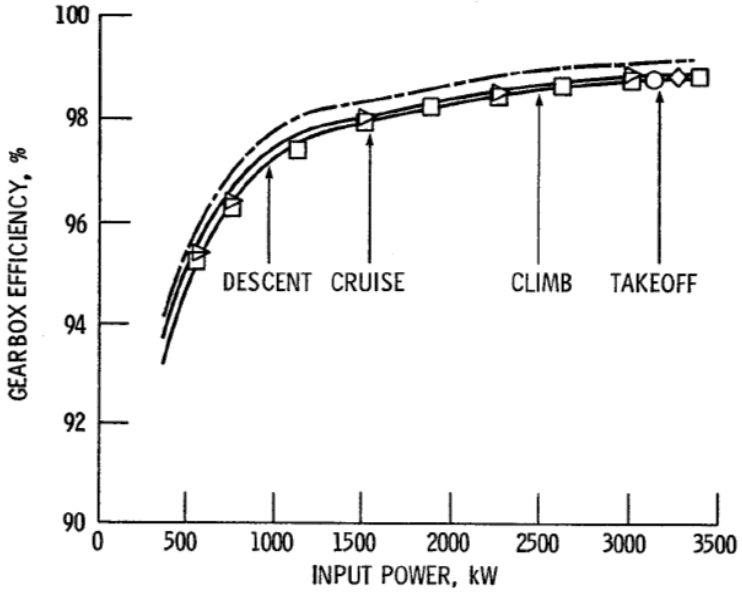

FIGURE 5.37: GEARBOX LOSSES ACROSS FLIGHT RANGE (ANDERSON ET AL, 1984, P.20)

5.3 New Engine Characteristics

As with the baseline engine model, the CUEJ56 which is described in Chapter 4, it is important to examine the behaviour of the new engine models to see if they behave as expected. Table 5.7 shows the comparison between key performance parameters of the new engine models and the baseline.

Parameter	CUEJ56	CUEJ-LEAP	CUEJ-PPGT
At 35,000ft, M=0.8, ISA (DP)			
TOC Thrust (kN)	25.03	25.04	25.03
TOC SFC (mg/Ns)	17.03	15.43	15.35
TOC TET (K)	1,489	1,714	1,725
Cruise Thrust (kN)	22.33	22.34	22.32
Cruise SFC (mg/Ns)	16.98	15.35	15.28
Cruise TET (K)	1,430	1,648	1,659
At 0ft, M=0, ISA, SLS			
T-O Thrust (kN)	120.09	120.16	120.4
T-O SFC (mg/Ns)	8.81	7.53	7.34
T-O TET (K)	1,634	1,819	1,826
T-O BPR	5.7	11.0	12.0
T-O Mass Flow Rate (kg/s)	410.1	484.2	500.0

TABLE 5.7: ENGINE PERFORMANCE COMPARISON

As can be seen from the table, for the three main operating points of the engine, where the thrusts were matched, the new models show improvements in SFC, as would be expected. TET also increases across the board, consistent with improving technology levels.

5.4 Aircraft Mission Performance

The next phase is to assess how the engines perform when integrated with the aircraft performance model, HERMES, and the improvements in fuel burn that can potentially be obtained.

The aircraft mode, the Cranbus EJ320, remains almost the same as for the baseline. The two new engines, the LEAP and GTF, are the options on the Airbus A320 NEO. The differences between the NEO and the original A320 are the addition of wing tip sharklets as well as the new engines. With the information available in the public domain, it is not possible to quantify the effect that the sharklets would have on their own, therefore a more conservative approach of using the original Cranbus EJ320 model is being taken. This then allows for the engines to be assessed in isolation.

The integration of the engines onto the aircraft model will have two effects, however. These are an increase in nacelle drag due to the larger physical size of the engines and a potential impact on the weight of the aircraft. These were accommodated by using the sizing program, Tethys and the weight estimation tool.

For the engine sizing, most of the inputs in Tethys were kept the same as for the baseline engine used in the validation, including blade aspect ratios, flow velocities and combustor size, as no information was available to inform these. However, as the fan size was changing, as well as the introduction of a gearbox in the CUEJ-PPGT engine, the rotational speeds of the fan, LPC and LPT, as well as the fan size needed to be updated. As the fan size was known, it was assumed that the fan tip speed would be the same as for the baseline engine, meaning the low pressure shaft rotational speeds could be calculated. For the geared turbofan engine, the shaft would rotate 3 times quicker than the fan. The maximum stage loadings allowed per stage were then adjusted to match the number of stages for each component to match literature.

Once the engine lengths were calculated, the weights of the engines could be estimated using the weight estimation tool. Table 5.8 summarises the CUEJ-LEAP and CUEJ-PPGT weights and dimensions.

Parameter	**Unit**	**CUEJ-LEAP**	**CUEJ-PPGT**
Dry Weight	kg	2,863	2,744
Total Weight Including Nacelle	kg	3,517	3,422
Nacelle Total Length	m	5.60	5.11
Engine Length (Fan to LPT Exit)	m	2.49	2.02
Nacelle Maximum Diameter	m	2.34	2.42

TABLE 5.8: CUEJ-LEAP AND CUEJ-PPGT WEIGHTS AND DIMENSIONS

The first step in assessing the engines on the aircraft is to calculate the new payload range diagrams. This is shown in Figure 5.38 below, and provides a comparison with the baseline.

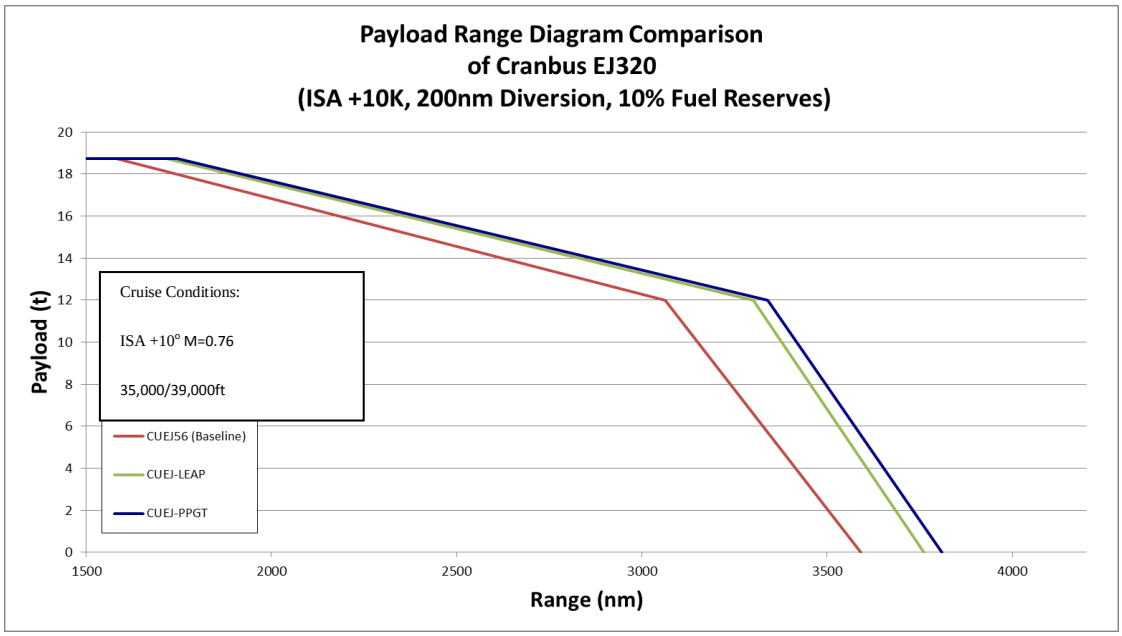

FIGURE 5.38: PAYLOAD-RANGE DIAGRAM COMPARISON FOR THE BASELINE AND ADDITIONAL ENGINES

The chart shows a significant increase in range for all payloads for both new engines compared to the baseline. At the zero payload, ferry range of the aircraft, the CUEJ-LEAP shows a 4.7% (169nm) increase in range while the CUEJ-PPGT shows a 6.1% (218nm) increase over the baseline. For the maximum fuel range, the improvements move to a 7.8% (229nm) and 9.0% (267nm) increase in range for the CUEJ-LEAP and CUEJ-PPGT engines respectively. Further improvements are made at the maximum payload point, with 8.6% (108nm) and 10.4% (138nm) increase in range for the CUEJ-LEAP and CUEJ-PPGT engines. While these figures are below the marketing figures of 15% reduction in fuel burn and 500nm increase in range (Airbus, 2013) for the payload range chart, this is likely explained by the conservative assumptions in efficiencies made for the engines.

Next, three typical missions were evaluated - short, medium and long range missions for the Airbus A320 aircraft. These are based on the mission length of flying from London to Amsterdam (short range), Rome (medium range) and Sharm el-Sheikh (long range). The destinations are based on existing easyJet routes and assume a payload of 16,350 kg, equivalent to 150 passengers with full baggage. It should be noted that the mission distances are typical, but may not reflect the day to day realities of flying these routes,

which may include waypoint and altitude changes from air traffic control The results are shown in Table 5.9 below.

Mission	**CUEJ56** (BASE)	**CUEJ-LEAP**	**CUEJ-PPGT**
	Block Fuel Burn (kg) (% improvement)		
Short Range (197 nm)	2,182	1,918 (11.65%)	1,913.63 (12.3%)
Medium Range (760 nm)	4,616	4,250 (7.9%)	4,181 (9.4%)
Long Range (2087 nm)	11,920	11,011 (7.6%)	10,881 (8.7%)

TABLE 5.9: ENGINE MISSION PERFORMANCE COMPARISON

The results also show a significant improvement in block fuel burn for the two new engines in comparison to the baseline CUEJ-56. The CUEJ-PPGT engine performs slightly better than CUEJ-LEAP and this would be due to the better propulsive efficiency from the higher bypass ratio engine, demonstrating that the losses through the gearbox can be recovered through better overall efficiency. As the mission length increases, although fuel burn improves for both engines, the scale of improvements progressively reduces suggesting that much of the efficiency gains are during the climb phase compared to the baseline.

It was then interesting to see what effect flight Mach No. might have on the overall mission fuel burn. The mission between Gatwick and Rome was chosen and the cruise Mach number varied, keeping all other factors the same. The results are shown in Figure 5.39, which has a number of interesting features.

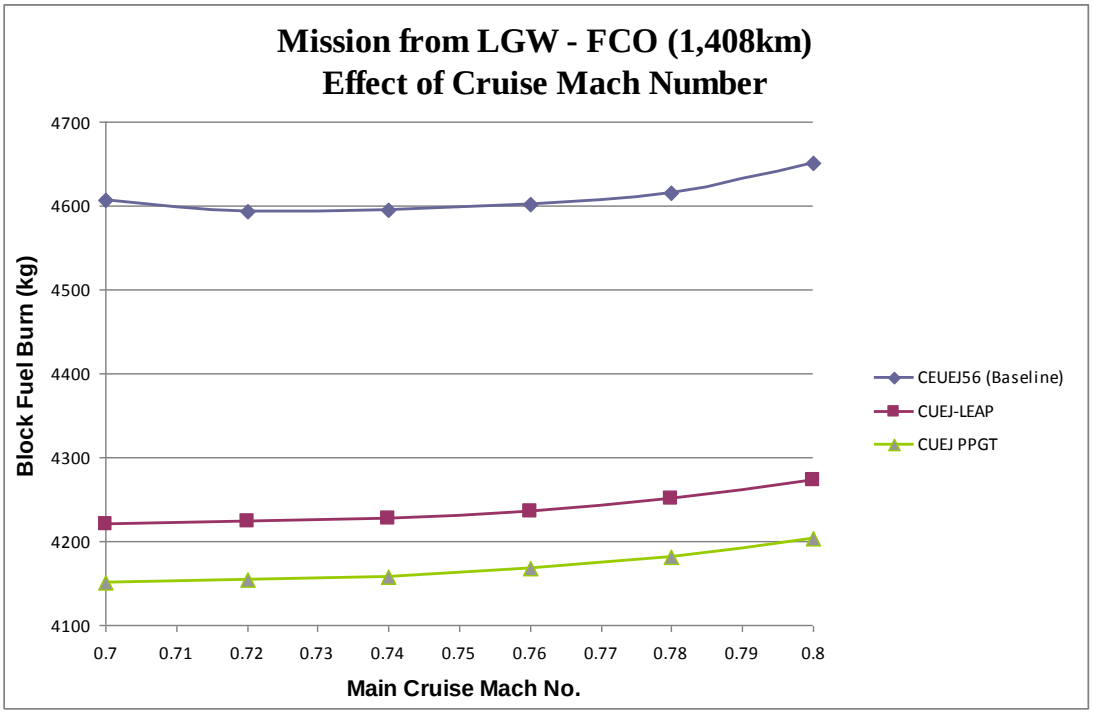

FIGURE 5.39: CRANBUS EJ320 CRUISE MACH NUMBER VARIATION

The first general feature is that as Mach number increases, the overall fuel burn increases. This is due to a combination of increasing drag on the aircraft (which increases proportionally to velocity squared), increased momentum drag in the engine intake and that the flight speed is increasing faster than the engine jet velocity, causing an increase in SFC. At lower Mach numbers and as cruise Mach number decreases, block fuel burn plateaus and then increases with further reduction in flight velocity. This shows the trade-off between the rate of reduction in SFC of the engine and the amount of time the aircraft spends during the mission burning fuel (i.e. the trade-off between fuel flow rate and mission time). As bypass ratio increases, the optimum cruise Mach number for minimum fuel burn shifts towards lower flight velocities, demonstrating the general trend that propulsive efficiency is improved at lower Mach numbers as bypass ratio increases.

6.0 Optimisation

This chapter describes the two engine models that were created for the purpose of finding mature conventional turbofans that would represent an upper limit in efficiency, which are able to fit on an Airbus A320 type aircraft in the typical configuration (an engine mounted under each wing); the optimisation method used and the results of the optimisation.

6.1 Engines for Optimisation

Two types of conventional turbofan were chosen for the optimisation. Conventional in this sense means a turbofan where the power and thrust are produced within the same unit (i.e. no distributed propulsion); the engine consists of a fan and bypass splitter, one or more axial or centrifugal compression stages, a constant pressure combustor, some turbine stages, and one or two expanding nozzles. In essence, the type of turbofan engines that have been available on passenger jet aircraft since around the 1960s. The two types of engine chosen were a direct drive turbofan, the CUEJ-DD1 with the fan attached directly on the low pressure shaft; and a geared turbofan, the CUEJ-GT1, with a 3:1 reduction gearbox between the fan and low pressure shaft. These types of engine were chosen because they represent a continuation of types currently available for purchase as part of the Airbus A320 NEO programme.

The CUEJ-DD1 direct drive engine is a two spool turbofan based on an updated version of the CUEJ-LEAP engine described in the previous chapter, while the CUEJ-GT1 shares the same basic performance model as the CUEJ-DD1, but with 2% of the fan work added to the low pressure turbine to account for gearbox losses, as described in Chapter 5.

6.1.1 Engine Initial Parameters and Assumptions

A number of assumptions need to be made in order to create models of hypothetical engines which would represent a limit in terms of fuel efficiency able to be

accommodated on an Airbus A320 type aircraft in conventional configuration. A summary of these assumptions is shown in Table 6.10, followed by a discussion of these parameters.

Parameter	**CUEJ-DD1**	**CUEJ-GT1**
Design Point: Top of Climb (M=0.8, 10,668m, ISA)		
Mass flow rate (kg/s)	265	265
Overall Pressure Ratio	67.2	67.2
Fan Pressure Ratio	1.4	1.4
Gearbox Efficiency	N/A	98%
Fan Isentropic Efficiency	0.89	0.89
Booster Pressure Ratio	3	3
Booster Isentropic Efficiency	0.88	0.88
HPC Pressure Ratio	16	16
HPC Isentropic Efficiency	0.88	0.88
HPT Cooling Flow	13%	13%
Customer Bleed (Cabin Pressurisation)	1%	1%
Combustion Efficiency	99.9%	99.9%
Combustion Fractional Pressure Loss	0.05	0.05
Turbine Entry Temperature (K)	1688	1688
HPT Efficiency	0.93	0.93
LPT Efficiency	0.93	0.93
Flight Altitude (m)	10,668	10,668
Flight Mach Nº	0.8	0.8

TABLE 6.10: PARAMETERS AND ASSUMPTIONS FOR ENGINES FOR OPTIMISATION

The main assumption made for the engines to be optimised is that the thrust requirement from the engines remains the same as for the baseline case. This is because the aircraft remains the same between the cases. The optimised engines will likely have a larger nacelle and heaver weight than the baseline case, however when taken as a whole and included within the total aircraft size and weight, the additional thrust required is likely to be relatively small and would not affect the convergence of the models.

With this main assumption made, the rest of the engine performance model is more straightforward to construct. The next step was to determine an engine mass flow. This was determined by assuming a future re-engining of the Airbus A320 in the same

configuration. There is a limited amount of space under the wings to fit the engines, therefore a maximum fan diameter that can be accommodated without re-configuring the aircraft. Using the drawing of the Airbus A320 (Airbus 2015a), a fan diameter of 2.2m has been assumed. Using the same method to determine mass flow as in Chapter 4, a value of 265 kg/s was calculated.

It was assumed that component efficiencies remain unchanged. This is a conservative assumption given the large amount of aerodynamic research into improving component efficiencies; however, by assuming these remain unchanged, a pessimistic view as to the cycle improvements can be gained, meaning that any potential improvements should be greater. It was also assumed that blade cooling flows remain at the same level as the baseline case, which assumes an improvement in blade cooling technology as per Birch (2000).

The rest of the engine cycle parameters such as bypass ratio; fan, booster and HPC pressure ratios, and turbine entry temperature are opened up during the optimisation, therefore broadly representative numbers are required in order for the optimisation to have a starting point. The OPR (and hence the individual FPR, Booster PR and HPC PR) is ultimately limited by the HPC delivery temperature, which is determined by the compressor material technology (Kyprianidis, 2011). Kyprianidis (ibid.) found that intercooling (which reduces the HPC delivery temperature) increases in benefit above an OPR of 50, and investigated OPR's of up to 80. It was decided, therefore to have an starting OPR of less than 80. The final choice of OPR was then reached after stability testing of the models. The starting BPR was chosen at slightly above that of the Airbus A320 NEO engines, while the TET was chosen to give the required thrust once the other assumptions had been made.

For the engine sizing model, the rotational speeds and stage loadings for the direct drive and geared engines were the same as used for the CUEJ-LEAP and CUEJ-GTF respectively.

6.1.2 Parametric Study

A parametric study has been carried out on a direct drive gas turbine engine model using the TERA framework described in chapter 3 as a precursor to optimisation. The parametric study is important as it establishes boundaries for the optimisation as well as identifying relevant trends and gives an idea of what an optimised engine might look like. Essentially, the parametric study is able to close the design space considerably and identify where an optimised engine is likely to lie. The parametric study can determine the extents and identify what the limiting factors are of a proposed technology.

For this parametric study, the DD1 direct drive turbofan model was used as the basis for. Several parameters were changed in order to study the effect that these parameters have on the overall fuel burn of the aircraft. Table 6.10 on the following page lists the parameters that were varied along with the magnitude of the variation. Each parameter was changed on its own, leaving the other parameters constant.

Parameter	Baseline Value	Change
HPC Pressure Ratio	16	-2.4, +2.4
Fan Pressure Ratio	1.4	±10%
Booster Pressure Ratio	3.0	±15%
Bypass Ratio (Top of Climb)	12.5	±10%
HPC Inlet Hub-Tip Ratio	0.63	±10%

TABLE 6.11: PARAMETERS ALTERED FOR THE STUDY

The parameters in Table 6.11 were chosen because they determine the overall cycle of the gas turbine. Turbine entry temperature (TET) is not considered within this particular parametric study because without changing other parameters at the same time, the thrust of the engine would change. The aircraft performance model would then ‘throttle back’ the engine to provide a required level of thrust, altering the TET once more.

The Effect of High Pressure Compressor Ratio

The first parameter to be investigated was the HPC compressor ratio. This was varied from between 13.6 and 18.4 (from an original baseline of 16), while keeping all other parameters the same. The effect on block fuel burn that varying HPC pressure ratio has

can be seen in Figure 6.40. The chart shows that generally as pressure ratio is increased, the block fuel burn decreases up to a point and then begins to increase. The main factor influencing this behaviour is that the thermal efficiency of the engine is increasing due to the increased pressure ratio. However, this does not continue indefinitely due to the relationship between propulsive and thermal efficiencies, particularly with bypass engines. As the thermal efficiency of an engine improves (while keeping bypass ratio and fan work the same), the exhaust velocity of the engine increases, thereby resulting in an overall reduction in propulsive efficiency. The gradient changes in the graph reflect that as HPC pressure ratio is increased, extra HPC, HPT and LPT stages are required increasing the weight of the engine.

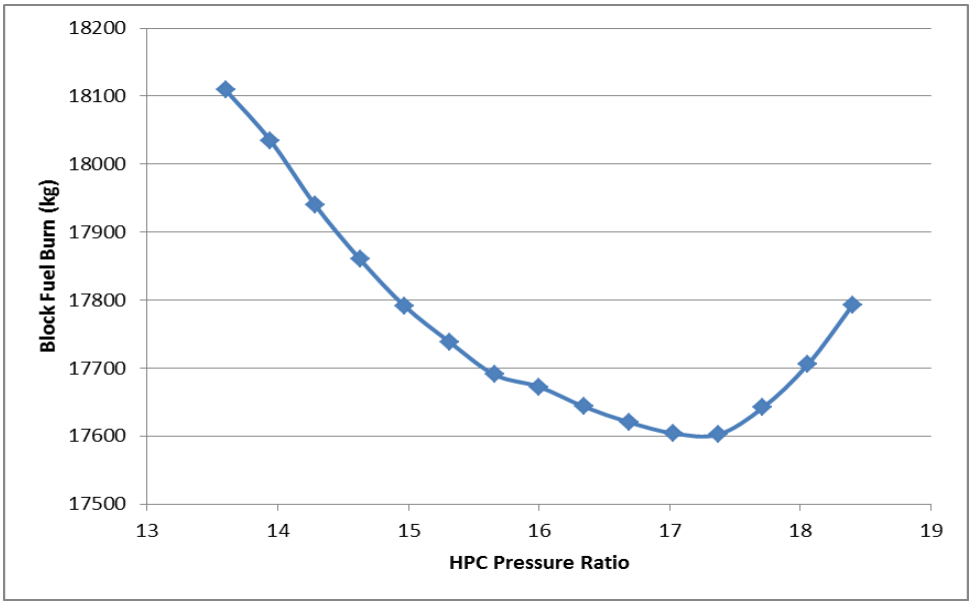

FIGURE 6.40: HPC PRESSURE RATIO VS BLOCK FUEL BURN

Although the chart shows an optimum HPC pressure ratio, this may be difficult to achieve in practice. Within the compression system, as pressure ratio is increased, the density of the air is increased and the cross sectional area along the axial flow path reduces, resulting in smaller blade heights. This is expressed in Figure 6.41 which shows how the HPC outlet hub to tip ratio varies as pressure ratio is increased.

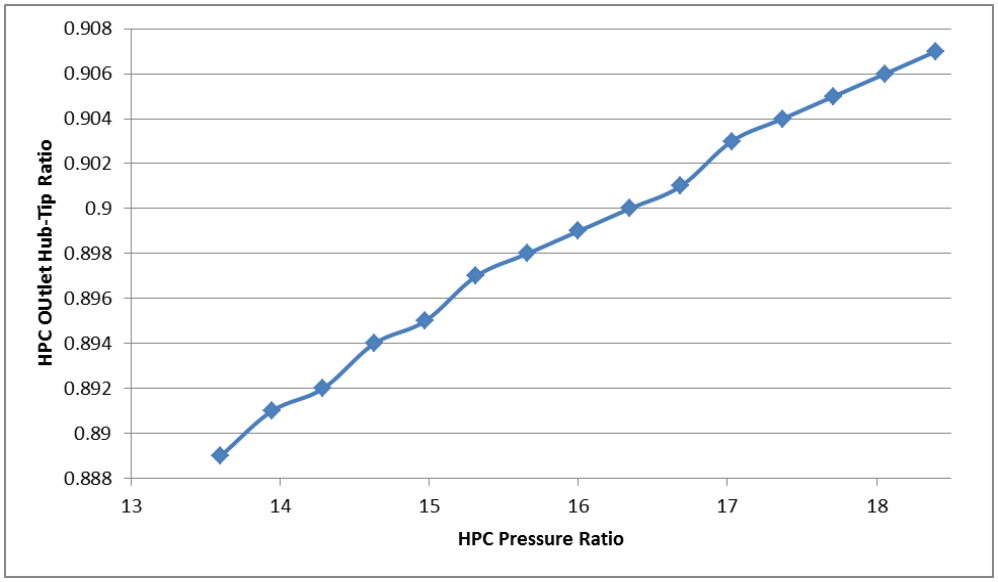

FIGURE 6.41:HPC PRESSURE RATIO VS HUB-TIP RATIO

Hub-tip ratio refers to the ratio between the diameter of the hub of a blade and its tip, and is a way of referring to blade height non-dimensionally. This ratio is important in considering the feasibility of an engine because it has a relationship with the efficiency of the component. The rotating blades within an engine cannot form a seal with the outer lining due erosion and rubbing issues so a small amount of flow is able to pass between the blade tip and casing (particularly from the higher pressure side returning back upstream to the lower pressure side) causing inefficiencies, referred to as tip loss (Ramsden et al, 2013). While measures are put in place to reduce this happening, a small amount of leakage always occurs. The size of gap is generally independent of blade height. In addition, a boundary layer builds up on the walls of the casing, its thickness determined by the Reynolds number of the flow within the compression system.

Accordingly, there will always be inefficiencies within the compression system that are more 'fixed'. While these inefficiencies are relatively small for a large blade, where the proportion of flow in the main blade is much larger than at the edges, as the blade height begins to reduce, these inefficiencies become more dominant. As such, there is a rule of thumb that a maximum hub tip ratio of 0.9 can be achieved before these losses become too great (although modern designs can allow hub-tip ratios slightly greater

than this). The TERA framework assumes a constant component efficiency, therefore these tip loss and boundary layer effects are not captured in Figure 6.41. It is important therefore to recognise that there is a limit on hub tip ratio that can be achieved.

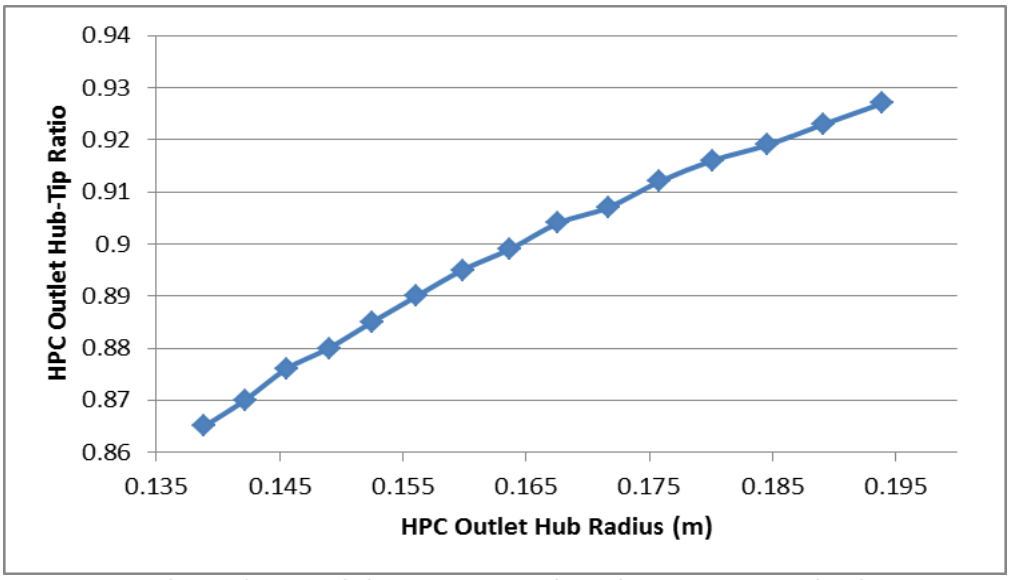

FIGURE 6.42: HPC OUTLET HUB RADIUS VD HUB-TIP RATIO

One way to reduce the hub-tip ratio is to reduce the radius at the hub of the blades. Keeping the pressure ratio constant, a reduction in hub radius would mean a relative increase in blade height. This is because for a particular pressure, the annulus cross sectional area will remain the same. If the hub radius is reduced, this would result in a proportionally lower reduction in tip radius. This would have the effect of reducing the hub-tip ratio. This effect can be seen in Figure 6.42 where the HPC outlet hub-tip ratio has been varied for a constant pressure ratio.

As can be seen, a smaller hub-tip ratio results in a smaller hub radius. This presents a challenge to the design of the engine, however, as the hub radius can only be reduced to a specific point, as multiple shafts, bearings and oil systems need to fit in an ever smaller space. As a result, there will be a limit on how small the hub radius of the high pressure compressor can be.

In conclusion, increasing high pressure compressor ratio can result in block fuel burn savings, however there exist physical limits into how much of these savings can be realised. The main limit demonstrated is that of the HPC hub radius.

The Effect of Fan Pressure Ratio

Figure 6.43 shows how block fuel burn varies with fan pressure ratio. The chart shows that there is an optimum fan pressure ratio for block fuel burn. This is as expected as there is an optimum fan pressure ratio for a given bypass ratio due to the relationship between core and bypass streams. For a fixed TET and bypass ratio with a low fan pressure ratio, the bypass thrust will be low, but the core thrust high, due to the relatively low quantity of work extracted in the LPT (Saravanamuttoo, 2008), affecting the overall propulsive efficiency. As fan pressure ratio increases, bypass thrust increases, the work extracted by the LPT increases and core thrust (and hence core jet velocity) decreases. Thus, there is an optimum relationship between the core and bypass jet velocities to give the best efficiency.

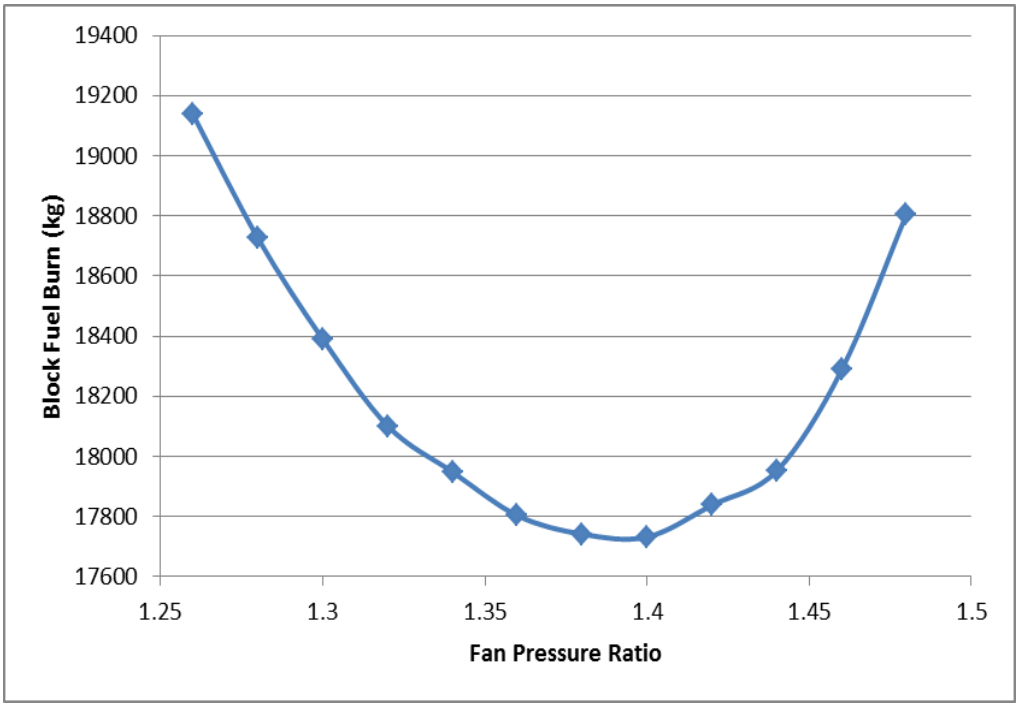

FIGURE 6.43: FAN PRESSURE RATIO VS BLOCK FUEL BURN

The chart also shows that the relationship is not symmetrical - the block fuel burn increases faster after the minimum point than before it. This is due to the increase in engine weight caused by additional LPT stages being created as a result of the extra work done by the fan.

The Effect of Booster Pressure Ratio

The effects of booster pressure ratio on block fuel burn are shown in Figure 6.44. The effects are a combination of the effects of the change in fan pressure ratio and HPC pressure ratio. As pressure ratio increases, block fuel burn improves as a result of increased thermal efficiency. There is a plateau and an optimum region for the booster pressure ratio, after which block fuel burn begins to rapidly increase. This is due to the combination of the reduction in propulsive efficiency, plus the additional weight of the engine from the creation of extra turbine stages on the low pressure shaft.

The increase in pressure ratio in the booster has the additional effect of the reduction of the hub diameter of the HPC (Figure 6.45). This is because the increase in pressure ratio results in a reduction in the cross-sectional area of the gas path at the exit of the booster. This reduction in area is carried on to the HPC, which for an acceptable hub-tip ratio means that the hub diameter must reduce. Accordingly, as for the HPC, there is real physical limit to booster pressure ratio that can be achieved.

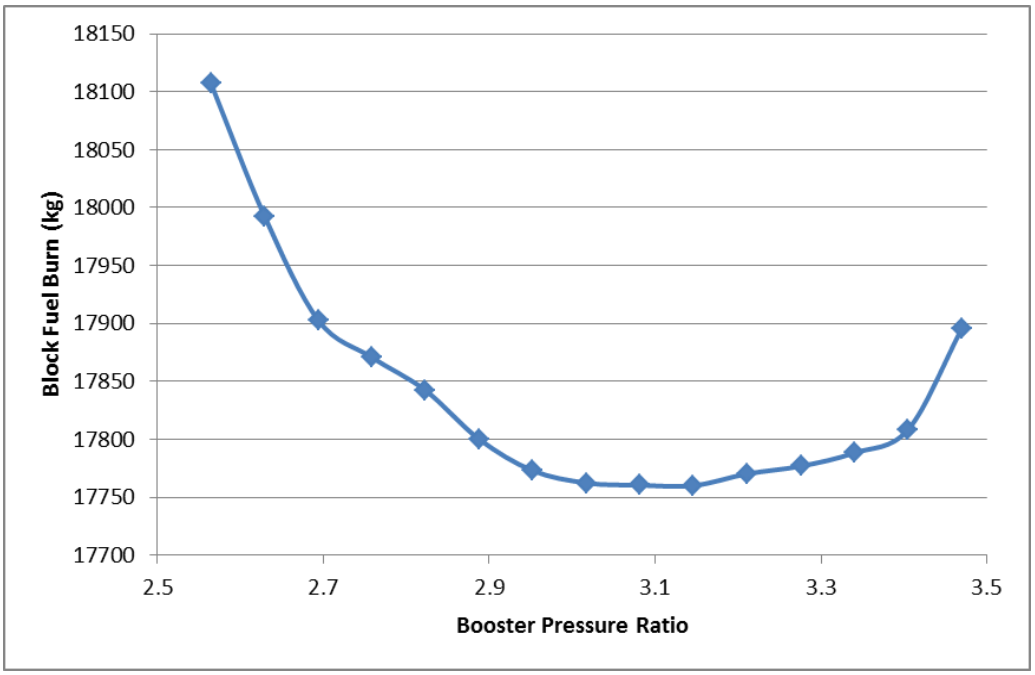

FIGURE 6.44: BOOSTER PRESSURE RATIO VS BLOCK FUEL BURN

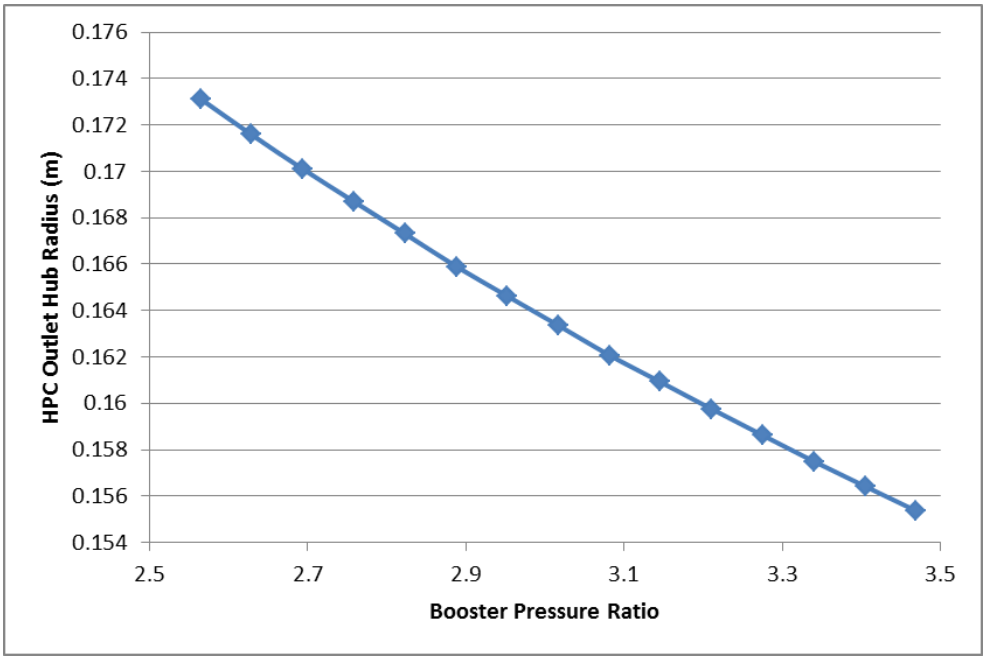

Figure 6.45: Booster Pressure Ratio vs HPC Hub Radius

The Effect of Bypass Ratio

The thermal efficiency of a turbojet engine increases by increasing overall pressure ratio and turbine entry temperature. However, this effect also increases the jet velocity of the engine which has the effect of reducing propulsive efficiency. To achieve better propulsive efficiencies, the jet velocity of the whole engine needs to be reduced (but high enough to provide sufficient thrust for the flight speed). This requirement has resulted in the development of turbofan engines, of which a portion of the inlet mass flow is bypassed around the core and exited through either separate or mixed nozzles. Therefore a large portion of the power generated in the core is used to drive the fan rather than be used to provide thrust directly by expansion through a nozzle. A way of increasing propulsive efficiency further, therefore, is by increasing the bypass ratio of the engine – increasing the proportion of air that bypasses the core.

Figure 6.46 shows how block fuel burn is affected by changes in bypass ratio of the engine at the design point (top of climb). In general, the block fuel burn should always increase as bypass ratio increases, due to the increased propulsive efficiency. However, the chart shows that the block fuel burn begins to level out. This is likely due to the structure of the models. Although bypass ratio is increasing, the fan pressure ratio, total mass flow and turbine entry temperature have been kept constant throughout. As has already been seen, there is an optimum fan pressure ratio for a particular bypass ratio, therefore increasing bypass ratio without altering the fan pressure ratio would result in increasing inefficiencies.

In addition increasing the bypass ratio means but also keeping inlet mass flow constant means that the mass flow through the core is decreasing. The work done by the fan is increasing meaning that additional work is required from the LPT in the core, increasing the number of stages and therefore the weight of the engine. This combines with the fan issue to start to reduce the benefit of additional bypass ratio. To get the benefit of higher bypass ratios and higher propulsive efficiency, the fan pressure ratio, inlet mass flow and turbine entry temperatures would need to change with it.

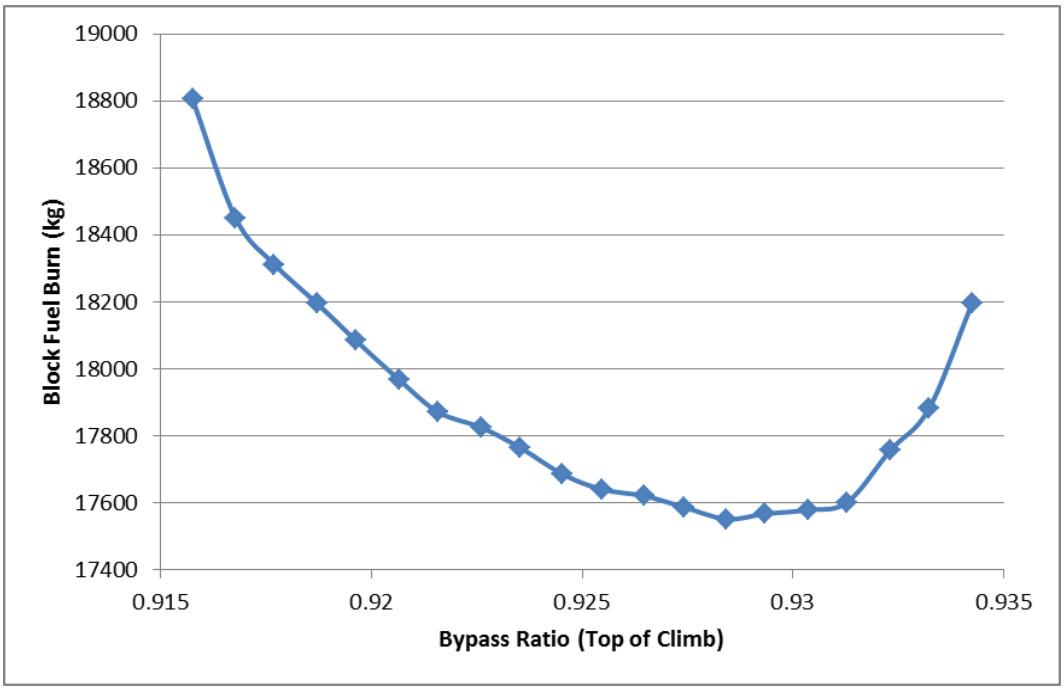

FIGURE 6.46: BYPASS RATIO VS BLOCK FUEL BURN

6.1.3 Optimisation Setup

The commercial software Isight was used to carry out the optimisation. Isight is made by Dassault Systemes and is a suite that provides a number of different automated optimisation techniques and speeds up manual design space exploration through 'design of experiment' techniques.

There are three main types of optimiser within Isight: Numerical gradient based algorithms, exploratory algorithms (i.e. genetic algorithms) and knowledge based, heuristic algorithms (Koch et al, 2002). The exploratory genetic algorithm was chosen for the optimisation as it provides the opportunity for a global search of the design space and is useful where the search space is poorly understood and/or irregular (Whellens, 2002). The genetic algorithm is useful for gas turbine optimisation as it has the ability to deal with failed solutions, which overcomes the difficulty that the governing non-linear equations often have no solution (ibid.). The genetic algorithm has been used in other TERA type optimisations, such as Whellens et al (2002), Colmenares (2009) and

Nalianda-Karumbaiah (2012). Goldberg (1989) and Machalewicz (1996) provide a good overview of genetic algorithm techniques.

Following the parametric study, the optimisation variable boundaries and constraints could be set up, which are shown in tables 6.12 and 6.13 respectively. As the study was to look at a potential 'best' conventional turbofan engine that could fit on an airbus A320 type aircraft, the main engine cycle parameters were relaxed as much as possible, subject to model stability limitations found through the parametric study.

The engine constraints are related to the sizing of the engine. The overall diameter of the engine is fixed through the fan diameter, therefore the only way to increase bypass ratio would be to make the core smaller. To reflect that there is a limit to how small the core of the engine can go, as there will need to be ample space for shafts, oil systems and bearings, a minimum hub radius of 0.15 metres was chosen. This gives room for further core size reduction from the CUEJ-LEAP and CUEJ-GTF engines. To respect the aerodynamic limits of the high pressure compressor stages, the HPC outlet hub-tip ratio was limited to just over 0.9, the ratio beyond which aerodynamic inefficiency through boundary layer build-up and tip leakage becomes too great.

	Units	Lower	Upper
Fan PR	-	1.3	1.45
Booster PR	-	2.5	3.5
HPC PR	-	13.6	18.4
BPR	-	11.2	13.7
TET Design Point	K	1520	1856
HPC Initial Hub/Tip Ratio	-	0.567	0.693

TABLE 6.12: UPPER AND LOWER BOUNDARIES FOR THE OPTIMISATION VARIABLES

	Units	Constraint	Min/Max
HPC inlet Hub Radius	m	0.15	Minimum
HPC Outlet Hub Radius	m	0.15	Minimum
HPC Outlet Hub/Tip Ratio	-	0.905	Maximum

TABLE 6.13: CONSTRAINTS APPLIED IN THE OPTIMISATION

Two missions were chosen for the optimisation of both engines, short and long range missions which represent typical missions flown by the Airbus A320 aircraft. The short range mission was based on a mission length equivalent to the distance between London and Amsterdam (365km, 197nm), while the long range mission is equivalent to the distance between London and Sharm El-Sheikh (3,869km, 2,089nm). Table 6.13 provides a summary of the main mission parameters. The missions are meant to be representative of the distance of the missions flown and include typical cruising altitudes, but do not include or take into account any directions from air traffic control such as waypoint or altitude changes.

Mission	**Short Range**	**Long Range**
Distance (km)	365	3,869
Payload (kg)	16,350 (Equivalent to 150 passengers with baggage)	16,350
Take-off Elevation (m)	62	62
Take-off Temperature ISA Deviation (K)	0	0
Cruise Altitude(s) (ft)	18,000	35,000/37,000
Cruise Mach No.	0.65	0.78
Cruise Temperature ISA Deviation (K)	0	0, +10
Landing Elevation (m)	-4	44
Landing ISA Temperature Deviation (K)	0	+10

TABLE 6.14: MAIN AIRCRAFT MISSION PARAMETERS

The optimisation was run as a single objective optimisation seeking to find the lowest block fuel burn through changing the variables listed in Table 6.12. A total of 2,700 iterations were run.

6.1.4 Optimisation Results

The results of the optimisation for the CUEJ-DD1 and CUEJ-GT1 engines for short and long range missions (the post script –SR and –LR are given for the engines optimised by each mission) and the comparison with the baseline and previous engines are summarised in Figures 6.38 and 6.39 respectively. These figures show the block fuel burn for each mission and demonstrate that there are potentially still fuel burn improvements to be made for gas turbine aero-engines in a conventional configuration.

The first trend that can be observed from the charts is that the geared CUEJ-GT1 engines offer slightly better performance at both mission ranges than the equivalent direct drive CUEJ-DD1 direct drive engines, despite both engines starting from the same base and having slightly higher SFCs. The reason for this can be observed in the schematics for the engines generated in Tethys (Figures 6.49, 6.50, 6.51 and 6.52),in Table 6.15, which gives a breakdown of the weight, stage count and sizes of each engine, and Table 6.16, which provides some key parameters of the engine during various flight phases.

As can be seen, both direct drive engines are significantly heavier and longer than two geared turbofan engines. This comes about largely because of the extra stages required in the booster and LPT. The fan is the main determinant of low pressure shaft rotational speed, as the absolute speed of tip of the fan needs to be limited to around or just above Mach 1 for noise and efficiency reasons. In the direct drive engine, the booster and low pressure turbine rotate at the same speed as the fan. As the fan in the optimised engines is larger than the previous engines, the shaft rotational speed is lower. This means that

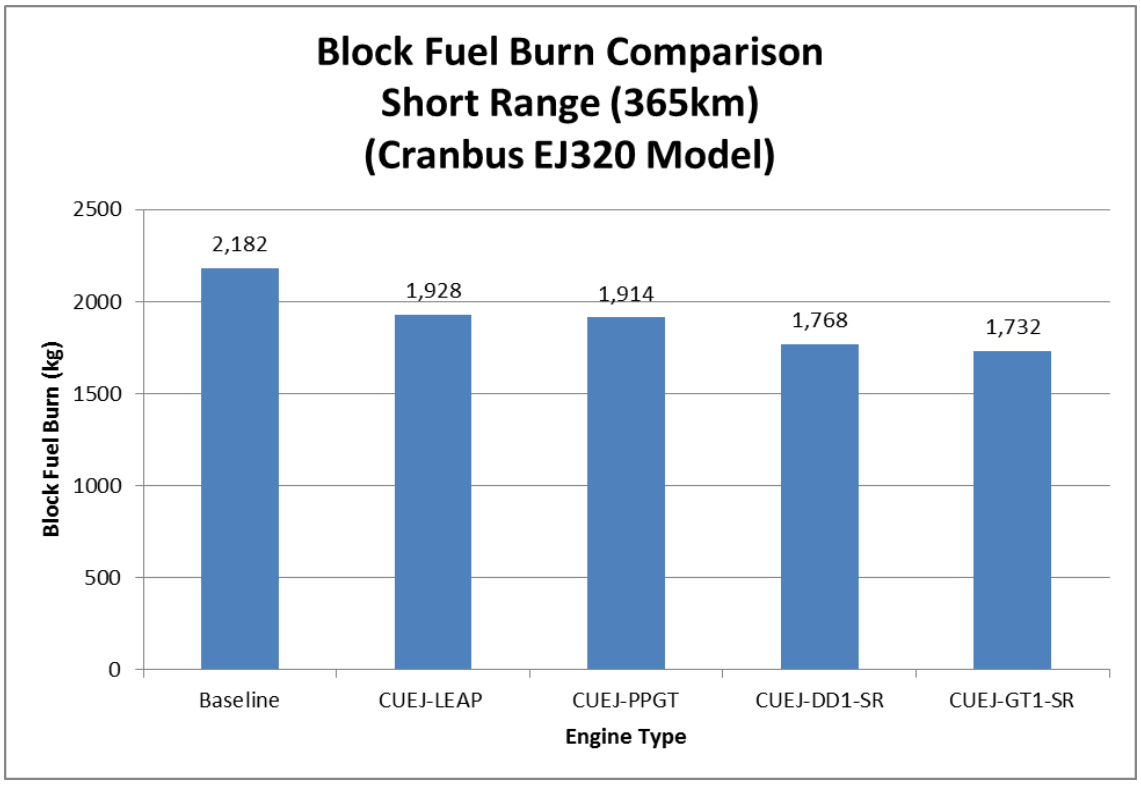

FIGURE 6.47: BLOCK FUEL BURN COMPARISON, SHORT RANGE MISSION

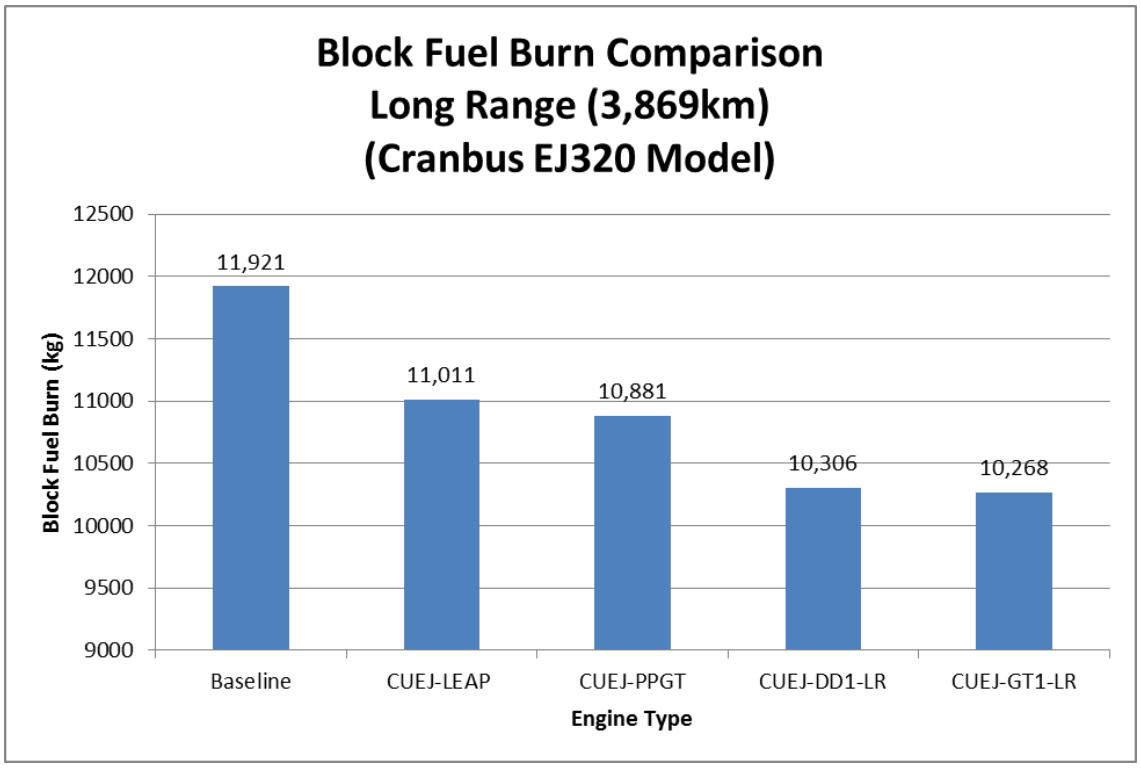

FIGURE 6.48: BLOCK FUEL BURN COMPARISON, LONG RANGE MISSION

Parameter	Unit	CUEJ-DD1-SR	CUEJ-DD1-LR	CUEJ-GT1-SR	CUEJ-GT1-LR
Total Weight	kg	3921.5	3872.5	3658.3	3480.3
Dry Weight (excl Nacelle)	kg	3282.4	3238.9	3026.9	2872.4
Stage Count	F-LPC-HPC-HPT-LPT	1-5-14-4-13	1-5-14-3-12	1-4-11-3-3	1-3-9-2-3
Length (Fan to LPT Exit)	m	3.84	3.54	2.36	2.15
HPC Hub Radius	m	0.155	0.153	0.150	0.154
HPC Exit Hub/Tip Ratio	-	0.902	0.896	0.904	0.898

TABLE 6.15: OPTIMISED ENGINES: ARRANGEMENT AND WEIGHT

Phase	Parameter	Unit	CUEJ-DD1-SR	CUEJ-GT1-SR	CUEJ-DD1-LR	CUEJ-GT1-LR
TOC (ISA) (18,000ft, 0.65M – SR) (35,000ft , 0.78M – LR)	Thrust	kN	30.9	30.9	25.1	25.0
	SFC	Mg/Ns	14.02	14.25	14.63	14.79
	TET	K	1,585	1,599	1,749	1,749
	OPR	-	52.9	55.8	70.6	64.6
Cruise (ISA) (18,000ft, 0.65M – SR) (35,000ft, 0.78M – LR)	Thrust	kN	26.1	26.2	22.3	22.4
	SFC	Mg/Ns	14.61	14.65	14.52	14.72
	TET	K	1,539	1,544	1,679	1,682
T-O (ISA) (SLS)	Thrust	kN	120.2	120.1	120.2	120.2
	SFC	Mg/Ns	6.44	6.56	6.47	6.58
	TET	K	1,818	1,847	1,801	1,802
	HPC Exit T	K	965	974	955	929
	BPR	-	13.76	13.74	13.63	13.71

TABLE 6.16: OPTIMISED ENGINES: PERFORMANCE SUMMARY

to stay within an acceptable stage loading limit for the booster and LPT, additional stages are required. Up to 13 LPT stages are needed for the CUEJ-DD1-SR engine, compared to only 3 for both of the geared engines. This shows the advantage gearboxes have in two spool turbofan engines with boosters, as fan sizes and bypass ratios get larger. By being able to run the low pressure shaft at a faster rotational speed, the amount of work that a single turbine stage can deliver is greater for a similar stage loading. Consequently, fewer booster and LPT stages are required, reducing the overall weight and size of the engine.

Even with the gearbox losses, which account for the slightly higher SFCs seen in Table 6.16 for the GT1 engines compared to the DD1 engines, the reduced weight and drag then translates into a fuel burn benefit over a mission.

The second trend that can be seen is that the optimised engines give a slightly better benefit in fuel burn for shorter range missions than longer range missions. This is a trend seen with higher bypass ratio engines, for example with the open rotor study by Guynn et al (2012). This is because there is a greater benefit in SFC reduction at lower flight speeds, representative of take-off and climb. This is due to the fact that in these cases, as bypass ratio increases, the inlet mass flow also increases. As inlet mass flow increases, it means that momentum drag also increases as velocity increases. This means that, proportionally, a slightly larger quantity of fuel is required to overcome the additional momentum drag at higher speeds than at low, or zero, forward speeds, for a given thrust level. This is also reflected in the greater convergence between take-off and top-of climb SFCs as bypass ratio increases, seen through this study. Therefore, while engine SFC reduces across all aspects of the flight regime, it reduces proportionally more at lower flight speeds than higher ones.

Accordingly, the shorter the overall mission length, the greater proportion of the mission the aircraft spends for take-off and climb. The fuel burn benefit of bypass ratio increases becomes more pronounced the shorter the mission.

An interesting trend is observed when comparing the results of the optimisation between the short and long range missions - the engines optimised for short range missions are heavier than their long range equivalents. At first glance this seems surprising - it may be expected that the trend should be the other way round as weight would likely be a considerable penalty during the climb phase for which the short range engines have as a proportionally greater length of their missions. However, the answer lies with the size of the engine. The longer range engines are shorter than the equivalent short range engines. The short range mission has a cruising altitude of 18,000ft and a cruise Mach number of 0.65, but due to the length of the mission, the cruise phase is very short. By contrast, the engines optimised for the longer range mission have cruise altitudes of 35,000/37,000ft with a cruise Mach number of 0.78 and spends a far greater proportion of its time at cruise. These higher speeds mean that aerodynamic drag, which increases with the square of flight velocity, becomes a much more influential factor. Thus, an engine with a shorter nacelle would be more beneficial to an aircraft with higher flight speeds, due to having a lower wetted area and smaller skin friction drag component.

By comparing the take-off data in Table 6.15, it can be seen that the engines optimised for the short range mission have slightly higher TET's and overall pressure ratios (inferred from the HPC delivery temperature) than the equivalent engines optimised for the longer range mission. Accordingly it can be seen that there is a trade of between better engine cycle efficiency and sacrificing some of that efficiency if it means a smaller engine, depending on the overall type of mission involved.

6.1.5 Fuel Burn Savings

Figures 6.47 and 6.48 show that potential fuel burn savings may be achievable for future conventional turbofan engines compared to the engines that are currently being released as part of the Airbus A320 NEO programme. The gains shown on those charts are between 5% and 9% for the best case scenario and reduce as mission length

increases. Figure 6.49 shows a payload range diagram comparison of all the engines considered in this study.

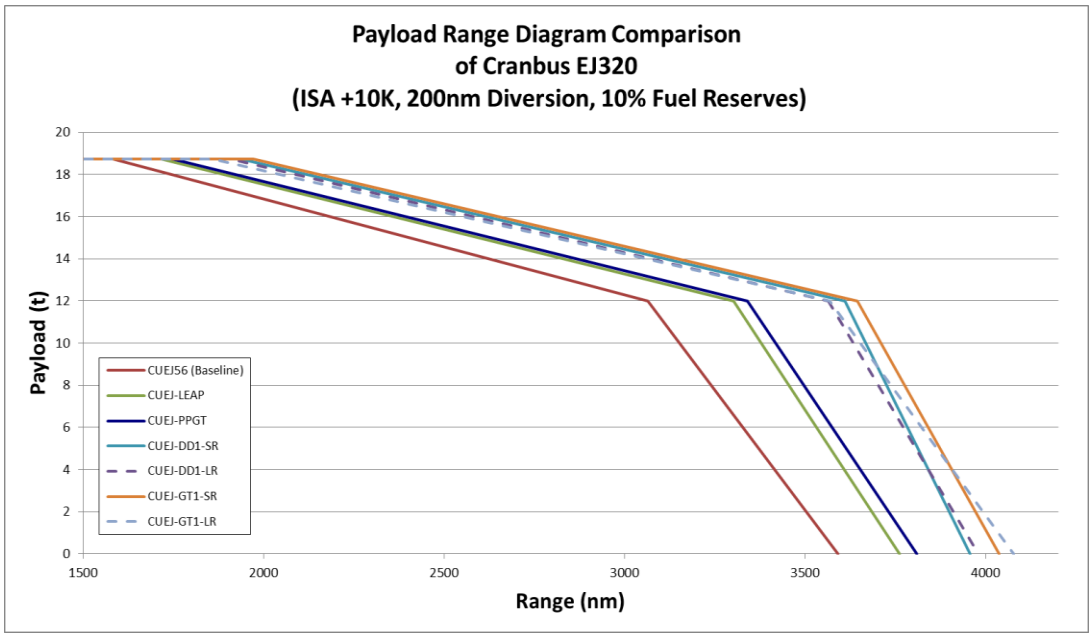

FIGURE 6.49: PAYLOAD RANGE DIAGRAM COMPARISON

The diagram reiterates that there is still some potential for gains from a conventional turbofan engine. In the best case, up to a 12% increase in range with full payload, lowering to up to 6% improvement at ferry range could potentially be achieved.

These gains come from two main places – better propulsive efficiency from a higher bypass ratio and better thermal efficiency from higher overall pressure ratios. These are reflected in the better cruise SFCs of the optimised engines (14.44- 14.73 mg/Ns, Table 6.15) compared to the CUEJ-PPGT and CUEJ-LEAP engines (15.28 and 15.35 mg/Ns respectively).

The take-off bypass ratios of the optimised engines have all finished at around 13.7:1, which is slightly larger than the CUEJ-PPGT at 12:1. The overall pressure ratios have all increased, with a range of between 65 and 77 at Top-of-climb. This is significantly more than the A320 NEO engines, with OPRs of around 50.

6.1.6 Limits to Achieving Gains

There are three main reasons why the potential fuel burn gains may not be realised. These are:

1. Core size
2. HPC delivery temperature
3. Turbine cooling requirements

The bypass ratio of a turbofan engine can be increased either by increasing the size of the fan, decreasing the size of the core or a combination of the two. For the optimised engines, the fan diameter was fixed to the size of engine that could potentially fit under a current Airbus A320 aircraft. To allow for an increase in bypass ratio, the allowable size of the high pressure shaft hub diameter was reduced to 0.15m. This was to allow for higher pressure ratios to be achieved with an acceptable hub-tip ratio. If this hub size reduction cannot be achieved, perhaps because of material stress limits, then it is unlikely that the bypass ratio and pressure ratios achieved could be met, unless a larger engine could be accommodated elsewhere on the aircraft.

As per Kyprianidis (2010), the interest in intercooling engines comes about because it allows for higher pressure ratios to be achieved due to HPC material considerations. As pressure ratios get higher, the HPC delivery temperature increases. This creates potential problems for the last few rows of HPC blades and discs, as these components are not cooled. Typically, titanium alloys used in compressor blades have a temperature limit of 540^{o}C (813K) (Leyens, 2004), which means that if temperatures higher than this are reached, Nickel based superalloys (with a limit of about 1,000^{o}C, 1273K), which are much heavier, need to be used. If temperatures higher than about 1,250K are used, then cooling would be required, which would be difficult to achieve.

The HPC delivery temperatures of the optimised engines at take-off are up to 973K, which is significantly hotter than the limit for current titanium alloys, although this temperature could be withstood by Nickel superalloys. Titanium aluminides are being

researched that have the potential to withstand temperatures of up to 800ºC (1,073K), which would help in achieving higher HPC delivery temperatures.

Turbine cooling requirements are always an item of consideration for new engine designs. The trend towards better thermal efficiency means higher OPRs and TETs. This places a double effect on the turbines. Firstly, higher TETs mean that turbines may require more cooling to keep the blades, as well as discs and annulus walls, at an acceptable temperature for creep and fatigue life, as well as oxidation requirements. The higher pressure ratios also result in higher HPC delivery temperatures, which is where turbine cooling flows are normally extracted from. A higher HPC delivery temperature would likely mean a greater turbine cooling flow is required, which would further impinge on efficiency.

For this study, it was assumed that turbine cooling flows remains the same as for the previous engines, which would therefore mean that turbine cooling technology advances. Although the absolute TET at take-off remains broadly consistent across the optimised engines compared to the A320 NEO engines, TETs have risen at top-of-climb and cruise, due to the larger engines requiring more fuel to overcome momentum drag for a given thrust. This could affect creep life as the engine spends proportionally more time at cruise than take-off. In addition, the higher OPRs and consequently higher HPC delivery temperatures could affect turbine cooling flows. Turbine cooling is a significant area of gas turbine research, and treatments such as thermal barrier coatings are seen as way to ameliorate the effects of high temperatures in the shorter term, with ceramic matrix composite blades over the longer term (Li et al, 2014), although significant challenges in fabrication, oxidation, corrosion and high stress region design need to be overcome. Accordingly, there remains some uncertainty as to whether the potential fuel benefits could be reached. TURBOMATCH does not currently have the capability to study the effects of turbine cooling flows, so this uncertainty could not be analysed. A recommendation for further research would be to analyse the effects of turbine cooling flows.

The issue of NOx formation should also be considered. NOx is an important issue for aviation, as it has effects both on the ground, where NOx emissions can cause adverse health effects, and higher up in the atmosphere where they can contribute to global warming and have an impact on the ozone layer (Schumann, 1997).

NOx is formed within an engine in four main ways: *"thermal NO, nitrous oxide mechanism, prompt NO, and fuel NO"* (Lefebvre, 2010, p.374). Thermal NO is produced within high temperature regions in the combustion chamber, through the oxidation of nitrogen within the air using the Zeldovich mechanism (ibid.). Thermal NO formation is generally low at temperatures below 1850K and is controlled mostly by flame temperature with an exponential relationship between NO formation and temperature. Residence time within the combustor is also important, with thermal NO production increasing with for a larger residence time, unless the fuel-air ratio is very lean. Increasing combustor inlet pressure and temperature also have an effect on increasing thermal NO production. Nitrous oxide mechanism refers to the reaction between N_2 in the air through to NO via nitrous oxide, N_2O.

Prompt NO can be found under some conditions in the very early flame region and can be a significant contributor to NOx emissions under lean premix conditions (ibid.). The role of inlet pressure on Prompt NO production is uncertain (ibid.). Fuel NO is formed through organically bonded nitrogen that exists is some fuels, and thus the quantity formed is largely dependent on the fuel used.

Current NOx legislation focuses primarily on local air quality issues and as such restricts NOx emissions around airports. It is determined by way of the ICAO landing and take-off (LTO) cycle. The LTO cycle is determined by running a test engine at different power settings to reflect different phases of the LTO cycle for different periods of time and measuring the total amount of gaseous emissions. The result is then divided by the gross thrust at sea level to give the so called 'NOx characteristic' (D_P/F_{oo}) which means that different engines can be compared. The components that make up the LTO cycle are:

- 4 minutes for approach (30% power setting);
- 26 minutes for taxi/ground idle (7% power setting);
- 0.7 minutes for take-off (100% power setting); and
- 2.2 minutes for climb (85% power setting)

Progressively more stringent NOx emission limits have been introduced over the years by way of the international Committee on Aviation Environmental Protection (CAEP) meetings, with the latest being CAEP/8. Goals for the future have also been introduced, although these are not yet mandatory. A chart detailing the CAEP NOx limits is given in Figure 2.4, Chapter 2.

The optimised engines have higher combustor inlet pressures and temperatures, as well as slightly higher TETs than the previous engines discussed in the thesis, which would push the production of NOx within the combustion chamber. A trade-off therefore exists between lower NOx production, and higher thermal efficiencies, which favour high OPRs and TETs.

The Lean Direct Injection (LDI) combustor, however, could be used to help lower NOx emissions in this case. The LDI injects fuel directly into the large quantity of air flow in the combustor (all combustor air except that used for liner cooling enters through the combustor dome (Tacina et al, 2014)), and uses multi element fuel/air swirlers to rapidly mix the fuel and air. This helps to eliminate local hotspots and keep flame temperatures lower, reducing the production of NOx within the combustor. This type of combustor has been tested by NASA and has been shown to reduce NOx emissions by up to 87% from CAEP/6 limits (ibid.). The design of the combustor in any future engine is therefore crucial to meeting NOx reduction goals, and one such as the LDI concept would help the optimised engines meet these limits.

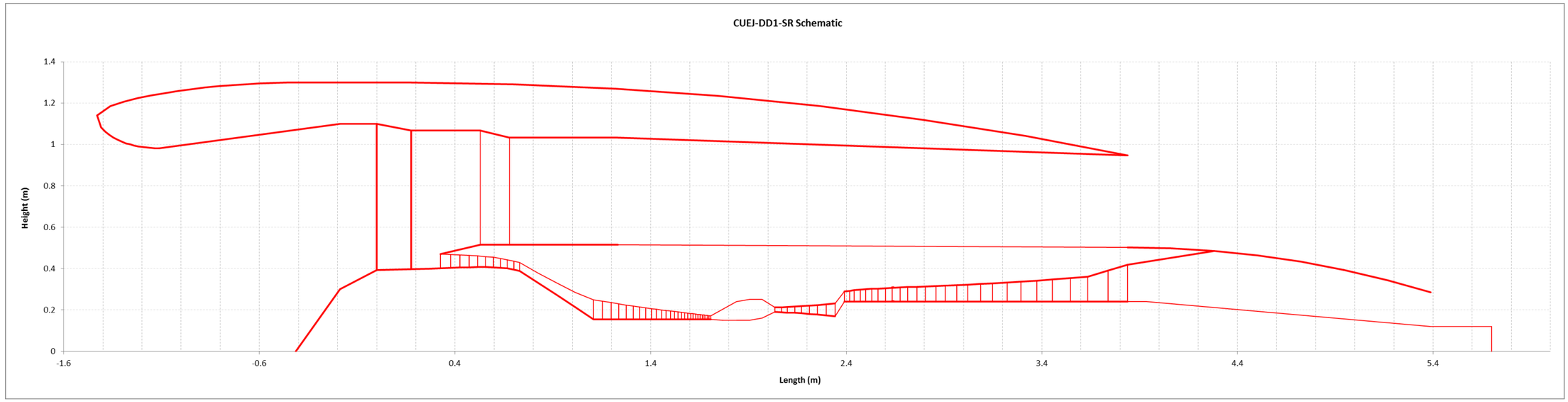

FIGURE 6.50: CUEJ-DD1-SR SHORT RANGE SCHEMATIC

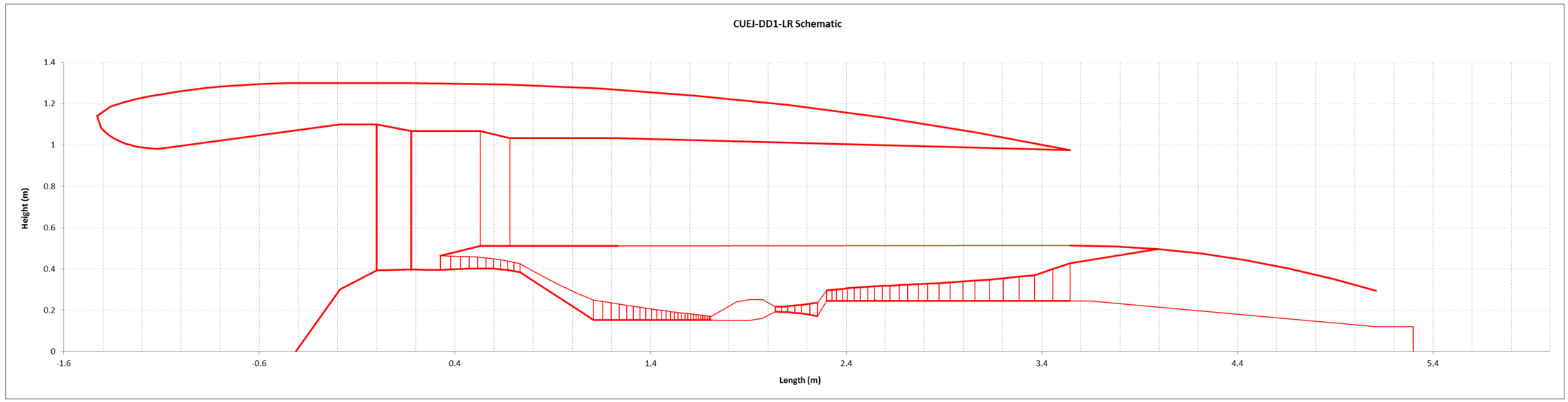

FIGURE 6.51: CUEJ-DD1-LR LONG RANGE SCHEMATIC

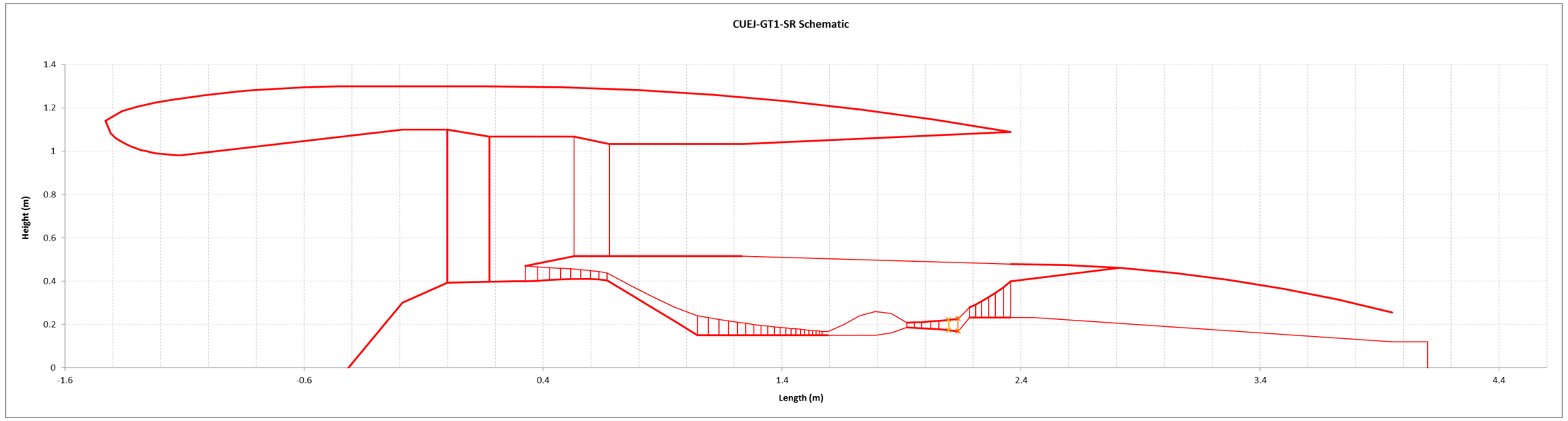

FIGURE 6.52: CUEJ-GT1-SR SHORT RANGE SCHEMATIC

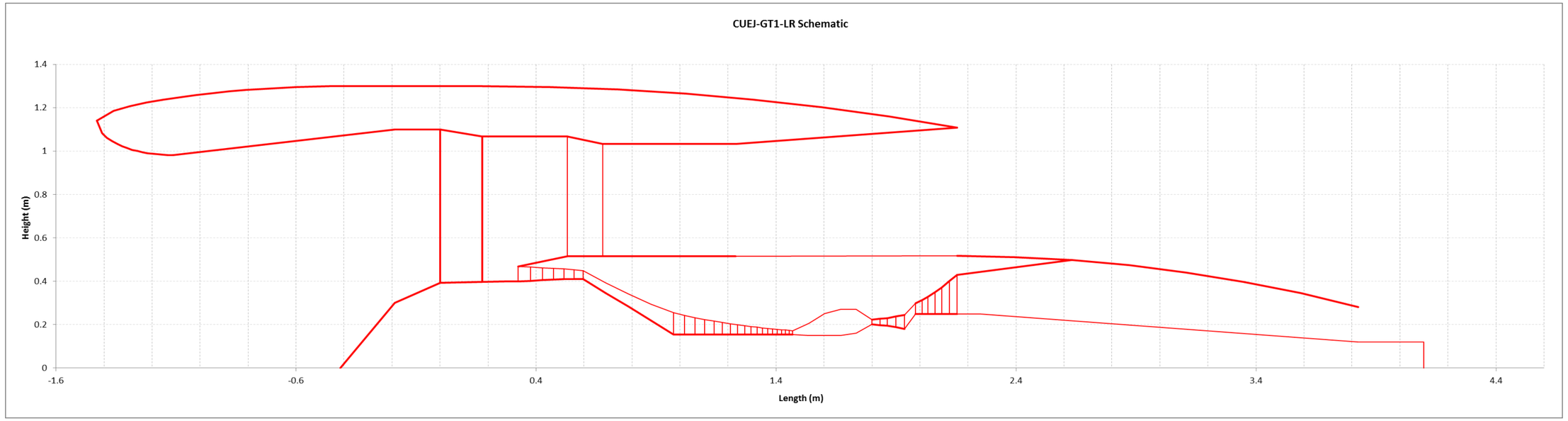

FIGURE 6.53: CUEJ-GT1-LR LONG RANGE SCHEMATIC

6.1.7 Economic Analysis

This section describes an economic analysis that has been carried out comparing the two optimised CUEJ-DD1 and CUEJ-GT1 engines with the baseline CUEJ56 engine as well as the CUEJ-LEAP and CUEJ-PPGT engines for the short and long range missions. This is in order to evaluate the trade-off between potential savings from mission fuel burn reduction and potential additional direct operating costs (DOC). The economic model used was based on the work of Goldberg et al (2015) and is shown in Figure 6.54.

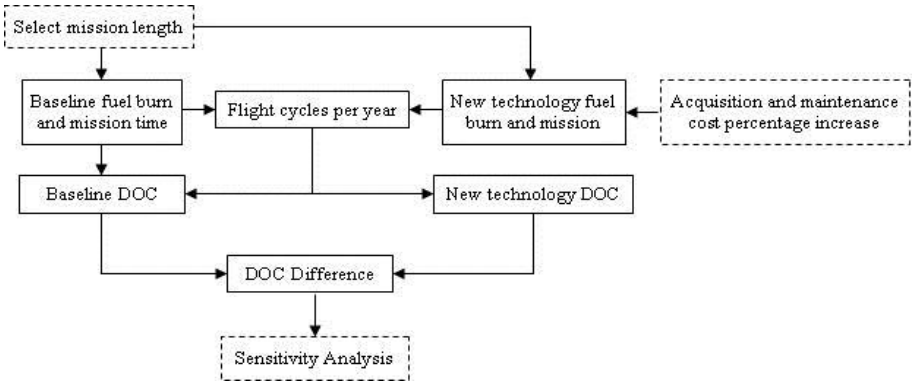

FIGURE 6.54: ECONOMIC SENSITIVITY ANALYSIS MODEL STRUCTURE

When an operator is making the decision whether to buy a particular aircraft or engine technology, an investment cost analysis is performed. A simplified total of the expected income minus costs over the life of technology can be used, however it is more common to use the Net Present Value (NPV). NPV also takes into account the fact that additional incomes or expenditures in the future may not be as valuable as those today (because of inflation, or investing cash into a different venture). NPV makes use of a discount factor, commonly the interest rate, or the weighted average cost of capital (WACC), a value which weights the costs a company attributes to debt and equity.

The technology that offers the highest NPV is the one most likely to be selected when comparing different options that can be invested in. Another way of assessing the suitability of a new technology is to calculate the Internal Rate of Return (IRR). This is the rate at which the new technology just breaks even, i.e. expenditures exactly cancel

out revenue. The higher the value of IRR, the higher the return on investment provided by the new technology. The investment should ideally exceed the minimum required return rate (the WACC) in order to be considered (Raymer, 2006). In the aviation industry, the WACC typically lies at around the 7% mark (Morrell and Dray, 2009).

Here, the NPV assessment is made in terms of the difference in operating cost between the baseline aircraft and engine and the proposed new technologies. The project IRR is then calculated in order to assess whether it exceeds the WACC.

As accurate prediction of the costs of a new engine and airframe can be very difficult, a sensitivity analysis may be performed which assesses the impact of maintenance and acquisition costs on the potential fuel cost savings of a new engine configuration. The model creates a map which can be used to determine the sensitivity of acquisition and maintenance costs for a new aircraft/engine to determine whether it remains profitable in comparison to the technology it replaces, over the lifetime of the aircraft from an investment analysis perspective.

In order to carry out the analysis, an assessment needs to be made of how the aircraft and engine combination is used over its lifetime, the typical acquisition and maintenance costs of the aircraft and engine and an understating of the fuel costs.

To determine the typical aircraft operation over its lifetime, the number of yearly flight cycles has to be determined. This was calculated by using the average aircraft utilisation figure of 11 block hours per day from the 2014 easyJet annual report. The short range mission takes approximately 50 minutes, which works out at a daily cycle of 12 and a yearly cycle of 4,380. The long range mission takes a little over 5 hours, which means a daily cycle of 2 and a yearly cycle of 730.

The aircraft acquisition costs are based on the average list price for the A320 given by Airbus of $97m (Airbus 2015). The aircraft and engine maintenance costs were obtained from Aircraft Commerce (2006), updated to 2015 prices, of $788 and $393 per flight hour respectively. DOC’s are heavily influenced by fuel prices, so two fuel price

scenarios have been carried out of $69 per barrel (average jet fuel price for 2015) (IATA 2015) and the all-time high jet fuel price of $140 per barrel (ibid.). Flight and cabin crew costs are not taken into account, as the crew requirements are identical for this aircraft using alternative engines.

A comparison of the CUEJ-DD1-SR and CUEJ-GT1-SR engine models were made against the baseline CUEJ-56 equipped on an A320 aircraft for the short range missions at a fuel price of $69 per barrel. The two maps are shown in Figure 6.55.

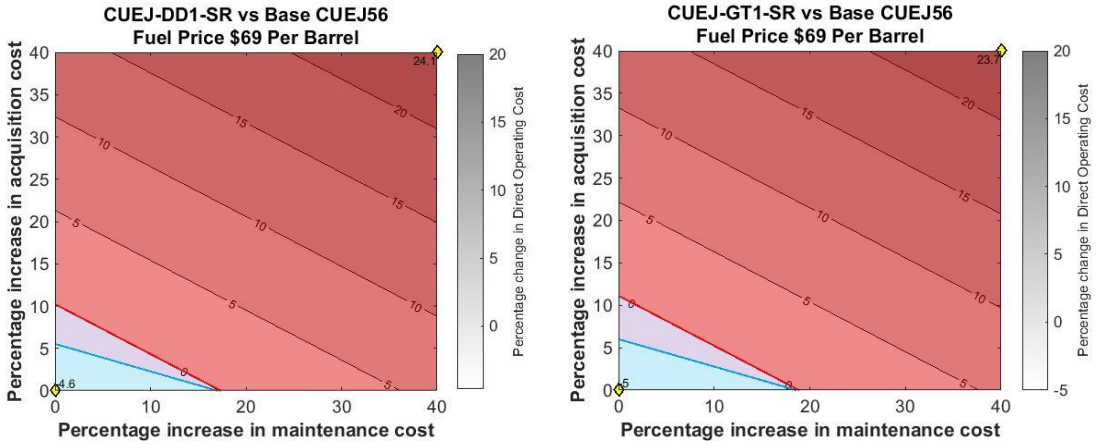

FIGURE 6.55: SENSITIVITY ANALYSIS FOR SHORT RANGE CEUJ-DD1 AND CUEJ-GT1 MODELS AT A FUEL PRICE OF $69 PER BARREL IN COMPARISON TO BASELINE

The charts can be read as follows:

- The red shaded area is the unprofitable area – here the proposed technology is less profitable over its lifetime compared to the baseline. The benefits from improved fuel efficiency are outweighed by the increased ownership costs;

- The red line is the equal DOC line - the operating costs for the proposed new technology are equal to that of the baseline technology;

- The cyan shaded area below the blue line is the profitable, suitable IRR area - here the new technology offers lower operating costs over its lifetime in comparison to the baseline and offers a higher rate of return than the minimum value determined by the WACC;

- The small grey wedge between the cyan and red lines is the profitable, inadequate IRR area – although the DOC's of the new technologies are lower than the baseline, the technology does not offer a suitable rate of return;

- On the axes, a value of 0 represents aircraft and engine acquisition and maintenance costs that are the same as the baseline. Moving away from the origin represents percentage increases in maintenance and acquisition costs of the new technology compared to the baseline.

The maps show that for a $69 per barrel fuel price, there is a significant profitable margin for both engines, compared to the baseline. To be economically attractive (i.e. offer a better rate of return than the baseline and the WACC of 7%), the combined acquisition costs of aircraft and engine need to be up to approximately 5% more expensive than the baseline engine. If maintenance costs also increase from the base level, then the acceptable acquisition costs reduces. The maintenance costs can increase to approximately 16-17% from the base level for the new technologies to be attractive, for no increase in acquisition costs. Comparing the two engines, the CUEJ-GT1-SR offers slightly increased margins due to the slightly better fuel burn for the short range mission.

If fuel costs increase, however, then the margins increase. Figure 6.56 shows the same maps using a fuel price of $140 per barrel, which is the all-time high for a barrel of jet fuel and approximately 100% higher than the average 2015 jet fuel price.

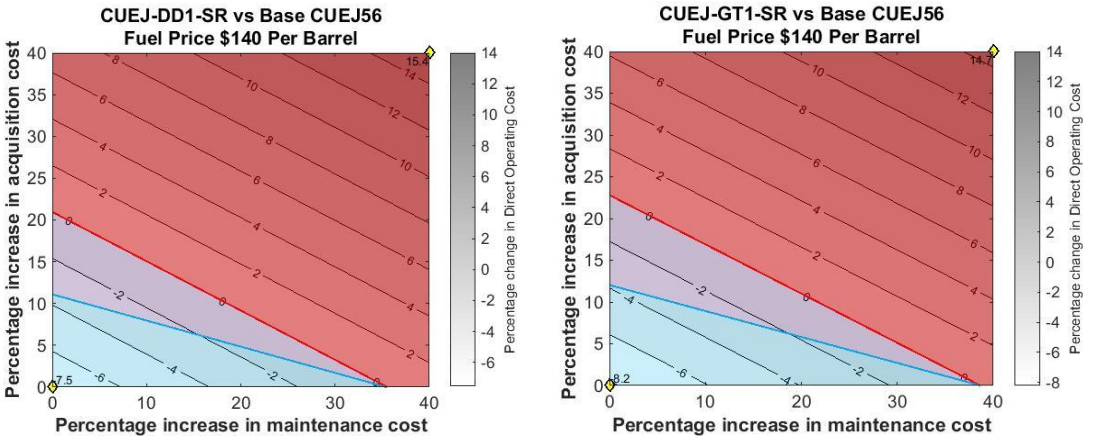

FIGURE 6.56: SENSITIVITY ANALYSIS FOR SHORT RANGE CEUJ-DD1 AND CUEJ-GT1 MODELS AT A FUEL PRICE OF $140 PER BARREL IN COMPARISON TO BASELINE

The maps show that an increase in fuel price means a significant increase in the profitable area for both engines. For the CUEJ-DD1-SR, it can accommodate an approximately 11% rise in aircraft and engine acquisition costs to remain economically attractive, while maintenance costs can increase to approximately 35%. Once again the CUEJ-GT1-SR shows a slightly better margin to 12% acquisition and 36% maintenance costs.

For the long range cases, shown in Figures 6.57 and 6.58, the same general trends are followed; larger acquisition and maintenance costs can be absorbed as the fuel price increases. This reinforces what was seen during the 1970's and 1980's during the fuel price shock, which saw increased demand and interest in developing more fuel efficient aero-engines. Once the price reduced, interest in these new technologies waned. As the charts show, an increase in the fuel price allows room for acquisition costs to increase (allowing manufacturers to invest in research and development) and maintenance costs to increase (to allow for the potential of more difficult or expensive to maintain technologies) and still provide an acceptable rate of return for the airline.

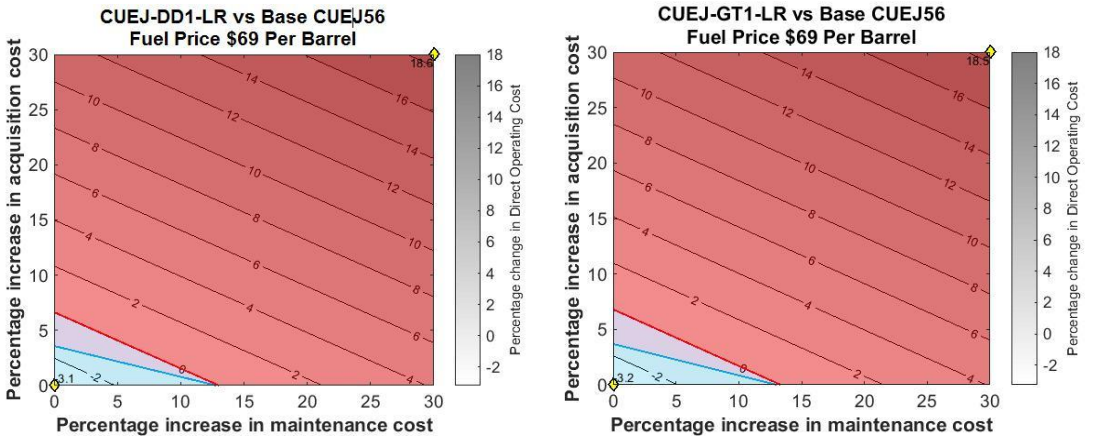

FIGURE 6.57: SENSITIVITY ANALYSIS FOR LONG RANGE CEUJ-DD1 AND CUEJ-GT1 MODELS AT A FUEL PRICE OF $69 PER BARREL IN COMPARISON TO BASELINE

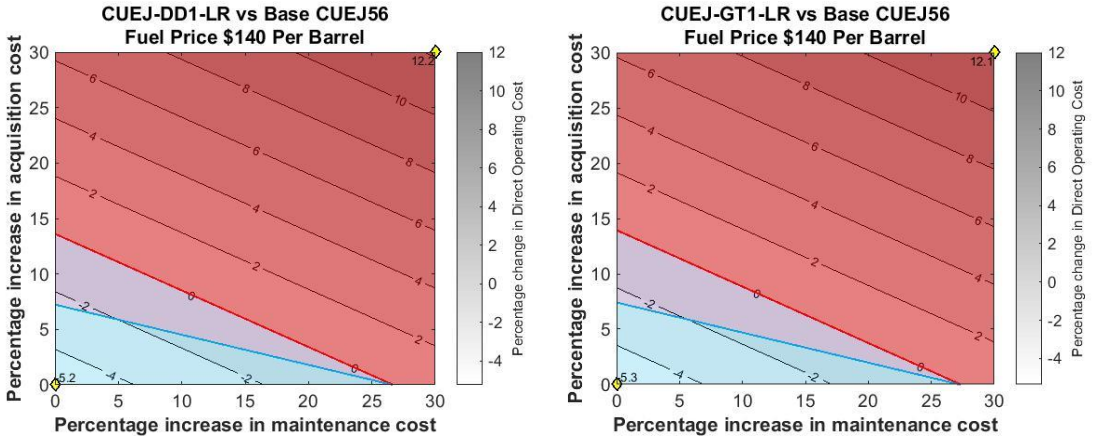

FIGURE 6.58: SENSITIVITY ANALYSIS FOR LONG RANGE CEUJ-DD1 AND CUEJ-GT1 MODELS AT A FUEL PRICE OF $140 PER BARREL IN COMPARISON TO BASELINE

Comparing the long range cases with the previous short range cases, the charts show that there is a slightly lower benefit to be gained from the longer range missions. The main reason is that the biggest proportion in efficiency for the new engines comes during the climb phase, meaning that as the mission length increases, climb becomes a progressively smaller portion of the mission.

Figures 6.59, 6.51, 6.52 and 6.53 provide a comparison of the DD1 and GT1 engines with the updated CUEJ-LEAP and CUEJ-PPGT engines for the short and long range missions. The charts show the same trends, but with reduced margins.

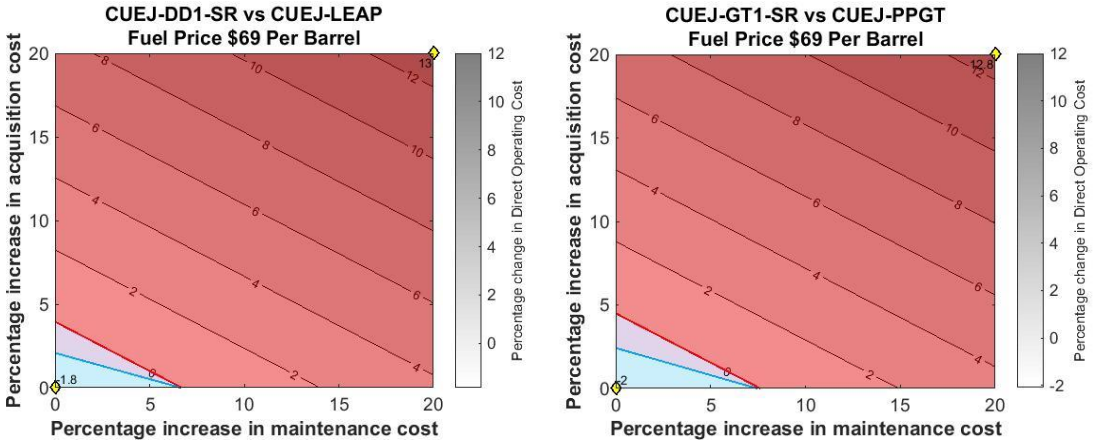

FIGURE 6.59: SENSITIVITY ANALYSIS FOR SHORT RANGE CEUJ-DD1 AND CUEJ-GT1 MODELS AT A FUEL PRICE OF $69 PER BARREL IN COMPARISON TO A320 NEO ENGINES

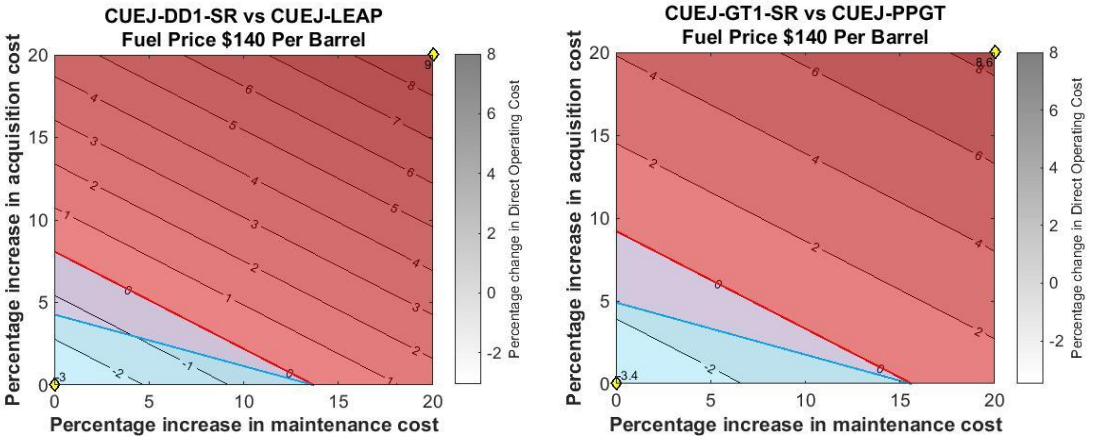

FIGURE 6.60: SENSITIVITY ANALYSIS FOR SHORT RANGE CEUJ-DD1 AND CUEJ-GT1 MODELS AT A FUEL PRICE OF $140 PER BARREL IN COMPARISON TO A320 NEO ENGINES

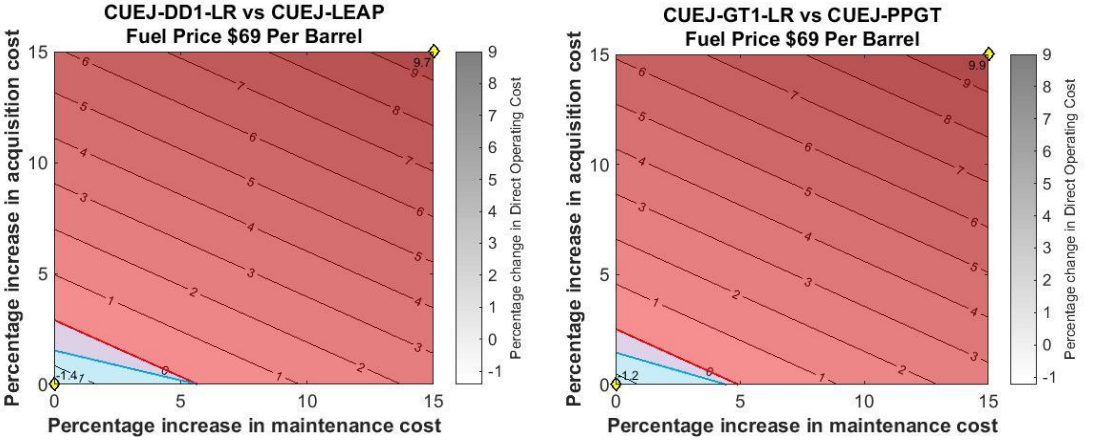

FIGURE 6.61: SENSITIVITY ANALYSIS FOR LONG RANGE CEUJ-DD1 AND CUEJ-GT1 MODELS AT A FUEL PRICE OF $69 PER BARREL IN COMPARISON TO A320 NEO ENGINES

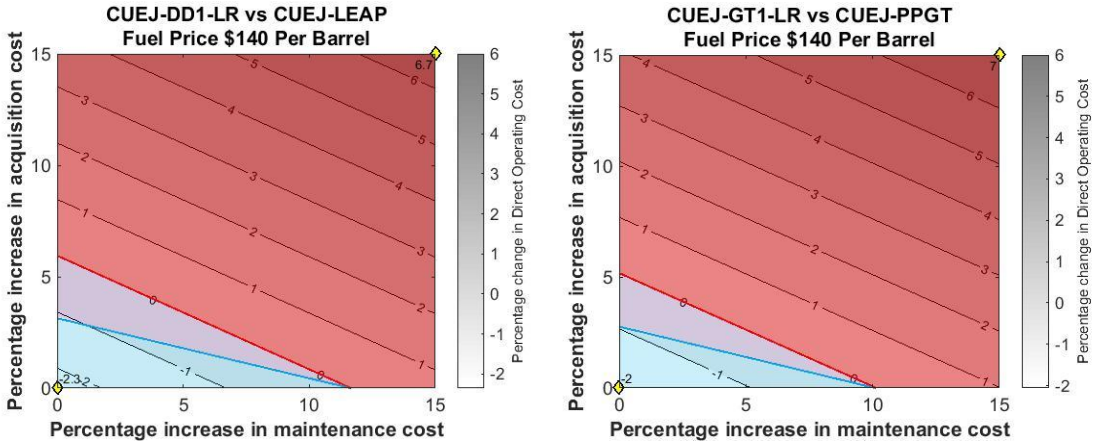

FIGURE 6.62: SENSITIVITY ANALYSIS FOR LONG RANGE CEUJ-DD1 AND CUEJ-GT1 MODELS AT A FUEL PRICE OF $140 PER BARREL IN COMPARISON TO A320 NEO ENGINES

6.1.8 Discussion

The main conclusion that can be drawn from the results is that an improvement in fuel burn reduction can still be achieved by conventional turbofan engines in a conventional configuration on an Airbus A320 type aircraft - somewhere between 5 and 10% depending on mission length. The key to achieving these gains depends mainly spatial considerations- the amount of space available around the airframe to accommodate a larger fan and how narrow the hub diameter of the HPC (and consequently HPC shaft) can be made. This is before other factors such as turbine and compressor blade materials are considered.

These two factors relate to the two efficiencies of a gas turbine engine - the propulsive and thermal efficiencies, and their relationship with each other. Propulsive efficiency in an engine is improved by accelerating a larger quantity of air more slowly while thermal efficiency is improved by increasing pressure ratios and turbine entry temperatures. There is a trade-off however, as improving thermal efficiency tends to reduce propulsive efficiency as higher jet velocities come from the core.

Propulsive efficiency is improved by increasing the bypass ratio of the engine - this is done by increasing the size of the fan relative to the core (i.e. making the fan bigger and keeping the core the same size, shrinking the core and keeping the fan the same size, or

combinations of the two). A thrust requirement exists for the airframe and engine combination in order for the aircraft to carry out its mission which means that the overall engine will have to be of a sufficient size to provide the required thrust. Ultimately the limit to the bypass ratio for an engine on a conventional airframe will be the amount of space available to accommodate a larger bypass ratio and fan. Current jet aircraft designs mount the engines under the wing, limiting the amount of space available for the engine - the Boeing 737 suffers from this with a modified nacelle design and a smaller bypass ratio for the 737 MAX engines compared to the A320 NEO. Increasing the fan diameter further will eventually require the engine being mounted elsewhere upon the airframe, necessitating a whole new aircraft design.

Thermal efficiency is improved by increasing the pressure ratio and/or the combustion temperature of the engine, although these will also be linked to the thrust required by the engine and bypass ratio of the engine. As pressure ratio increases, this has the effect of reducing the hub radius of the HPC in particular, due to the shrinking annulus area and the requirement to have acceptable blade hub-tip ratios for good component efficiency. There will also be a limit to how small the HPC hub radius can be, as multiple shafts, oil systems, bearings and cooling systems will have to fit into a smaller and smaller spaces. This can be offset to some degree, by designing turbomachinery blades having larger hub-tip ratios or altering the axial flow velocity profile within the core of the engine so that the annulus cross sectional area shrinks at a smaller rate. However there also limits to this and these changes would have an impact on efficiencies within the components.

Ultimately, there will be a limit for a conventional turbofan engine on how big the fan can be and how small the core can be, which then places limits on the propulsive and thermal efficiencies achievable by the engine.

Other considerations such as HPC blade and disc materials and turbine cooling flows determine whether extra gains can be made by conventional turbofans for short to medium range passenger aircraft. HPC delivery temperature would increase up to 970K for these engines. Although current nickel superalloys are capable of withstanding this

temperature, lighter titanium based alloys would be preferable for weight considerations, although not critical for delivering performance benefits. Turbine cooling technology, including cooling flows, materials and thermal barrier coatings would need to improve so that the same level of turbine cooling could be used, given higher HPC delivery temperatures.

The study has also shown the advantages that geared turbofans can bring, particularly as fan sizes and bypass ratios get larger. Although the gearbox itself results in an additional weight, both from itself and additional oil cooling, as well as its own set of inefficiencies, the significant reduction in number of LPT stages required and consequent reduction in overall weight and size mean that overall mission fuel burn is reduced.

The question then becomes, which technologies could conceivably be used to offer better fuel burn consumption than the advanced conventional turbofan engines considered. To start we can consider the use of heat exchangers used for intercooled and recuperated engines. Although these have the potential to offer significant benefits for larger, long range engines and aircraft through an increase in thermal efficiency, they would not be suitable for the short to medium range passenger aircraft of Airbus A320 size. Intercooling is useful because it offers the opportunity for much higher overall pressure ratios to be achieved by keeping HPC delivery temperatures at low enough temperatures for HPC material limits. However, as has been seen with the optimised engines in this study, increasing overall pressure ratio shrinks the size of the core for a given mass flow, meaning that HPC hub diameters in particular need to shrink. There is a limit to how narrow the hubs can be made, due to stress limits and the fact that multiple shafts, bearings and oil systems run inside this space. This constraint could not be overcome by intercooling, meaning it offers little benefit in this regard.

While recuperation offers the potential to recover some energy that would otherwise be lost in the exhaust, overall it probably would not be too useful for short to medium range aircraft. Boggia and Rud (2005) found that minimal benefit could be gained through intercooled and recuperated engines for short to medium range passenger

aircraft. This is because the main fuel benefit is offered in cruise, while for the climb phase, where shorter range aircraft spend proportionally more of their time than long range aircraft, the additional weight penalty of the heat exchangers could potentially result in a lower fuel burn.

Even if the use of heat exchangers offered some small fuel burn benefit compared to conventional engines, it is likely that the additional purchase and maintenance costs of these engines would mean that an economic advantage could not be gained, unless the fuel price were significantly higher. Overall, the use of intercooled and recuperated engines are unlikely to offer enough of a benefit to be appealing for short to medium range passenger aircraft.

Continuing with increasing thermal efficiency of the engine, we can next consider another technology - the wave rotor. Although the wave rotor topped turbofan was found by Noppel (2011) to be less efficient than a conventional turbofan with equivalent cycle parameters, he also saw potential in the arrangement where size was limited. As already discussed, it is difficult to increase overall pressure ratio through the use of axial flow compressors due hub diameter considerations. Although wave rotors are less efficient at compression than axial flow compressors, if an increase in pressure ratio is sought and conventional compressors cannot be used, then additional compression, albeit not quite as efficiently, may be of benefit. Wave rotors also offer a benefit by keeping turbine entry temperatures down, which would affect the life of the HPT and help lower maintenance costs, although the cost of purchase and maintenance of the wave rotor itself would need to be considered.

However, one major drawback of the wave rotor cycle is that the pressure of the flow entering the first row of turbine blades would be higher than that of the HPC outlet. This would cause a problem with turbine cooling, as the cooling flow would normally come from the HPC. With a higher pressure in the first set of turbine stages, no flow could come directly from the HPC without the use of additional compression for the cooling flow. This necessarily begs the question, if axial compression is more efficient than compression from a wave rotor, why not axially compress to achieve the higher

pressure ratios? Ultimately it would need to be studied how narrow the high pressure hub can be made, what acceptable hub-tip ratios could be achieved to deliver acceptable tip losses, and whether the benefits gained from wave rotor compression outweigh the additional work required and losses generated from the additional, but smaller mass flow compression if a separate compressor is used for the turbine cooling flow.

Despite turbine entry temperatures being kept lower with a wave rotor, NOx formation could still be an issue as higher temperature and pressures are reached inside the combustion chamber, therefore the design of the combustor chamber would be important.

Overall, the wave rotor has the potential to offer some benefit for short to medium range aircraft turbofans over the longer term, as it offers the potential for increased pressure ratios which may be otherwise difficult to achieve due to space constraints. However, whether the wave rotor sealing challenges can be overcome is an uncertainty. In addition, a potential better solution to increasing overall pressure ratio may exist by the use of pulse detonation.

Another way to increase the overall pressure ratio is through the use of a pulse detonation cycle within the turbofan in place of the combustor. Similar to the wave rotor, the pulse detonation engine allows for higher overall pressure ratios to be reached without increasing turbine entry temperatures, assisting with turbine life, however the pulse detonation engine achieves the pressure rise through a more efficient combustion at constant volume process, meaning the potential fuel burn benefits are better for the pulse detonation hybrid cycle. The pulse detonation engine also has the advantage of providing higher pressure ratios without the need to reduce hub diameters or alter hub tip ratios to less acceptable levels.

Similar to the wave rotor, the turbine cooling would become an issue, as the cooling flow would require additional compression to meet the turbine entry pressure. There would be more scope to do this with the pulse detonation cycle due to the inherently better compression achieved although a study would be required to quantify this.

NOx formation would perhaps be a greater issue with a hybrid pulse detonation cycle than with the wave rotor, as the wave rotor cycle would still have a conventional constant pressure combustor, of which research is continuing to provide lower NOx emission combustors. In the case of the pulse detonation cycle, which is essentially a cylinder, NOx formation would likely be more difficult to control, especially as current research is focussed on increasing the reliability of the detonations.

An issue with both wave rotors and pulse detonation engines is that they introduce unsteady flows into engines designed for steady flows. Accordingly, to accommodate the additional vibrations generated, extra strengthening would likely be required throughout the engine, adding extra weight, which could override any performance benefits gained. Weight would likely be more of an issue for the wave rotor compared to the pulse detonation engine, as the wave rotor would be added to an engine, while the pulse detonation cycle would replace the combustor in an engine.

Overall, the pulse detonation has the potential to offer a greater fuel benefit than the wave rotor through the more efficient compression process and likely lower overall weight. Both engines, however, are still in the very early stages of development and have many challenges to overcome. Therefore, it appears that significant near term gains in thermal efficiency for short to medium range aircraft will be difficult to achieve. Accordingly, could propulsive efficiency gains offer a better solution?

The two technologies considered earlier in the thesis that offer improvements in propulsive efficiency, open rotors and turbo-props, are very similar. They both produce thrust in the same way, with the use of a propeller, the difference being that an open rotor is designed for higher flight speeds, similar to that of current turbofan engines. Turboprops have been in service for several decades and are still used on small, regional aircraft. While turboprops offer better fuel burn benefits than current turbofan aircraft, they suffer from an image problem, being seen as unsafe and old fashioned (Brancatelli, 2009), largely due to the loud noise and lower flight speeds. The fact that despite the fuel benefits turboprops bring they haven’t seen service on larger passenger aircraft in

recent years, shows that unless there is no other option, turboprops are unlikely to be a serious consideration for future larger passenger aircraft, especially in Europe and America.

However, the open rotor may offer the solution. The open rotor is essentially a turboprop with a high speed propeller. By calling it an open rotor, or unducted fan, a differential exists to the turboprop from a marketing perspective. The higher flight speeds and cruise altitude offered by the open rotor also makes the flight experience more similar to a conventional turbofan aircraft.

Open rotors have the potential to offer significant fuel benefits from increased propulsive efficiency due to a much higher bypass ratio than turbofans - up to about 50. In terms of fuel burn advantages, Guynn et al (2012) undertook an a preliminary aircraft system level study of an Airbus A320/Boeing 737 size aircraft with two open rotor engines mounted on the rear of the aircraft. They estimated that block fuel burn savings of 18% could be achieved over a 500 nm mission compared to an advanced geared turbofan engine with a BPR of about 15 and OPR of 42, while savings of up to 12% could be achieved over a 3,250 nm mission.

These projected fuel burn savings appear better than for the optimised turbofan engines analysed in this study. These very mature conventional turbofan engines could offer fuel burn benefits of up to 9% for a short range mission and 5% for a longer range mission when compared to a geared turbofan of similar technology level as that examined by Guynn et al (2012) (BPR 12 and OPR 50). This demonstrates the superior propulsive efficiency of the open rotor due to the much higher bypass ratio.

Several issues need to be considered with open rotors, however. The first is noise, both in the cabin and around airports. Recent studies by SAFRAN and General Electric show that noise levels can be kept to acceptable levels through the use of effective rotor designs. In addition, mounting the engines to the rear of the fuselage can help mitigate cabin noise. This rear mounting of the engine also helps with another issue – rotor blade failure. With no duct to contain the failure of the main rotor blades, the potential for

aircraft damage increases. By mounting the engines further to the rear and away from the wings, the potential damage caused by a failure can be reduced. While mounting the engines elsewhere on the aircraft than under the wings would require a complete airframe redesign, as has been seen in the study, there is already limited space under the wings for future engines. It is likely that any future engine options for Airbus A320 size aircraft would require a new airframe. Other issues to be resolved are rotor gearbox and pitch control mechanisms, although much research is being carried out to solve these issues, and SAFRAN is confident in carrying out flight testing trials in the near future.

Overall, the open rotor seems the logical choice for engine options for short to medium range passenger aircraft, as they offer superior fuel efficiency due to a significantly higher overall pressure ratio and a similar flight experience to existing aircraft. In addition, the thermal efficiency of these engines could conceivably be increased over the longer term through the use of pressure rise combustion devices such as pulse detonation or wave rotors.

7.0 Conclusions

Uncertain economic climates, fluctuating fuel prices, increasing environmental awareness and greater competition mean that airlines are looking to lower their aircraft fuel burn, both to reduce their own costs and a desire to offer customers more environmentally responsible transport options. Since the beginning of manned flight, the jet engine has come to represent a defining feature of modern passenger air travel. In the 1940s and 50s, the jet engine was a disruptive technology that allowed for higher, faster flight. Since that time, the jet engine has evolved to become more powerful, quieter and more efficient through the use of higher bypass ratio fans, higher pressure ratios and higher turbine entry temperatures. However, the evolution of the conventional turbofan over the last 60 years appears to be approaching its limits and new technologies will likely be required to take aviation propulsion to the next stage.

This thesis uses a short to medium range passenger aircraft and mission and profile to try and explore what the limit of conventional turbofan technology might be and to assess what different technologies may offer an improvement in this specific case.

A TERA approach was used to investigate this limit. TERA is a flexible multi-disciplinary framework that allows for factors other than engine SFC to be investigated, such as fuel burn over different types of missions, as well as engine sizes and weights. The TERA framework in this study consisted of engine and aircraft performance models, and engine size and weight models. This allowed the fuel burn effects of potential mature turbofan engines to be investigated.

A baseline aircraft and engine configuration was modelled, based on the Airbus A320 aircraft with CFM56-5B/4 engines. Thrust and SFC was validated against publically available data. Two additional engines based on the Airbus A320 NEO re-engining were then modelled to estimate the potential fuel burn benefits these engines could give.

A design space exploration was then carried out using the TERA framework. Assuming another potential re-engining of the A320 aircraft, two different types of conventional

turbofan engine – direct drive and geared - were optimised over short and long range missions. The geared turbofan engine showed slightly better fuel burn characteristics compared to the direct drive engine, due to the fewer stages required to drive the larger fan resulting in a lower size and weight. Up to a 9% improvement in block fuel burn over the A320 NEO engines could be observed.

A qualitative discussion of some disruptive technologies that could be used to improve either the thermal or propulsive efficiency of the turbofan cycle was carried out. The main fuel burn benefits are summarised in Figure 7.63.

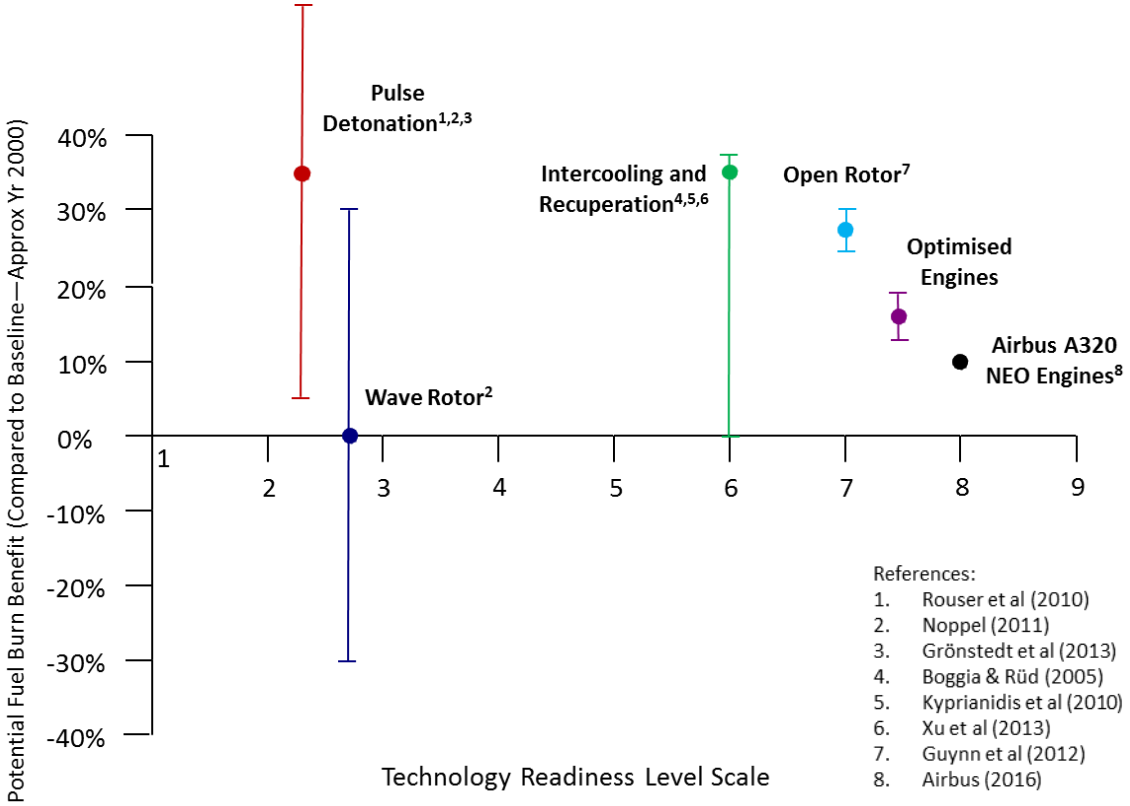

FIGURE 7.63: SUMMARY OF DIFFERENT TECHNOLOGIES – FUEL BURN VS TECHNOLOGY READINESS LEVEL COMPARED TO APPROXIMATELY YR 2000 BASELINE

Figure 7.63 shows a summary of potential fuel burn benefits that could be obtained from different cycle technologies compared to the baseline engine (approximately

technology that was available in the year 2000), against an opinion of technology readiness level (please see Appendix 3 for a description of technology readiness level).

The potential fuel burn benefit either comes from within this study, or within literature discussed in Chapter 2. The error bars represent the fuel burn benefit depending on mission length for the open rotor and advance very mature turbofan points. For the intercooled recuperated engines, the error bar represents that although they can offer the potential for significant fuel burn gains, this is mainly for larger, longer range aircraft which can accommodate the smaller core sizes for higher overall pressure ratios. For the short to medium range aircraft in this study, they may not offer much, if any, benefit, due to the extra weight and difficulty in physically achieving the higher overall pressure ratios.

For the wave rotor and pulse detonation engines, the error bars are function of the very early stages of development that these technologies are at, with some research work carried out in the laboratory. As such, it is difficult to assess the benefits of these technologies when applied to a short to medium range passenger jet aircraft.

This study shows that there is still potential for some fuel burn benefit to be gained from the evolution of the conventional turbofan, up to 9% improvement compared to the A320 NEO engines, or between 15-20% compared to year 2000 levels. This assumes that HPC material technology improves to help keep weight down and a narrow enough high pressure shaft diameter can be accommodated.

In terms of economics, the financial viability of the engines depends on fuel price. For a relatively low fuel price of $69 per barrel, the mature turbofans could accommodate between a 5-6% increase in purchase price for constant maintenance cost or 16-18% increase in maintenance cost for the same purchase cost, compared to the baseline engine. This rises significantly to 10-12% purchase price and up to 35% maintenance cost increase when the fuel prices rises to $140 per barrel. Compared to the A320 NEO engines, 1-2% increases in purchase price and 8-10% increases in maintenance costs for a fuel price of $69 per barrel, and 3-4% increases in purchase price and 15-20% in

maintenance costs for a fuel price of $140 per barrel could potentially be accommodated. What this means is that development and material costs of any potential new engine needs to be kept low enough by the manufacturer to offer a potential benefit or advantage to an operator compared to existing technology. As fuel price increases, or uncertainty about fuel prices increases, the scope to develop new engines increases, as was seen for the initial development and then abandonment of the UDF engine in the 1980s, when fuel prices lowered. Accordingly, a manufacturer would need to weigh up whether developing and offering an evolutionary turbofan could be carried out for an increase in purchase price of maybe one or two percent.

However, while a new technology such as the open rotor has the potential for a significant step change in fuel burn, it is likely that the airframe to accommodate it would require a complete redesign, needing far more development time and costs, as well as certification costs. If the fuel price lowers, it may be more attractive and indeed may even have scope for another re-engining of the airframe similar to the A320 NEO. If, however, fuel prices increase, or physical constraints mean that an open rotor becomes attractive to develop a new aircraft, then although there would be more scope for more space for a better conventional turbofan, any such engine would likely be outclassed by the open rotor due to the significantly higher bypass ratio and hence propulsive efficiency that it offers. Any thermal efficiency gains that could be developed for the turbofan would likely also be included in an open rotor. Development costs would therefore likely be better spent on developing the new technology.

Accordingly, while there is some scope for another evolution of the conventional turbofan engine along the lines of the Airbus A320 NEO program for short to medium range passenger aircraft, this would be limited by the narrowness of the high pressure shaft hub. If this could not be accommodated, or larger improvements in efficiency are sought, then a new aircraft development would be required. In this case, the most promising new technology would be the open rotor, as it appears to be sufficiently along its development path and offers enough of an improvement to be viable. Over a much longer timescale, improvements in thermal efficiency are likely to be sought. While intercooling and recuperation may not be suitable for a short to medium range aircraft,

increased pressure ratios through the use of pulse detonation could potentially be incorporated.

7.1 Recommendations for Future Work

Further work could include:

- Further development of the Tethys sizing code: The code could become more useful for additional engine types and configurations with the addition of gearbox, combustor and duct sizing methods, as well as introducing multi-stage fan and propeller sizing. Adding an option for a mixed flow nozzle would also be useful. Perhaps moving the sizing code to a more modular arrangement, such as that used in TURBOMATCH, could be investigated.

- Introducing a feedback mechanism between the Tethys and TURBOMATCH codes, so that the effect of hub-tip ratios on component efficiencies (and vice-versa) could be investigated.

- Investigation of the turbine cooling flow and secondary air system to see what effect on the potential fuel burn gains these flows have.

- Addition of bricks within the TURBOMATCH code that could be used to model pressure rise combustion, such as for pulse detonation, wave rotors and potentially internal combustion engines.

8.0 References

ACARE, 2011, *Flightpath 2050: Europe's Vision for Aviation*, European Union: Luxembourg

Airbus, 2010, *Airbus offers new fuel saving engine options for new A320 family*, Airbus.com 1 December 2010, http://www.airbus.com/presscentre/pressreleases/press-release-detail/detail/airbus-offers-new-fuel-saving-engine-options-for-a320-family/

Airbus, 2010a, *Airbus A320 Airplane Characteristics*, Airbus: Blagnac Cedex, France

Airbus, 2015, *Airbus Price List 2015*, http://www.airbus.com/presscentre/pressreleases/press-release-detail/detail/new-airbus-aircraft-list-prices-for-2015/

Airbus, 2015a, *AutoCAD 3-View Drawings of Airbus Aircraft*, http://www.airbus.com/support/maintenance-engineering/technical-data/autocad-3-view-drawings-of-airbus-aircraft/

Airbus, 2016, *A320 Family, Spotlight on… A320 NEO*, http://www.airbus.com/aircraftfamilies/passengeraircraft/a320family/spotlight-on-a320neo/

Aircraft Commerce, 2006, *Aircraft Owner's & Operator's Guide: A320 Family*, Aircraft Commerce Issue No. 44, February/March 2006

Akbari, P., Nalim, R., 2006, *Analysis of Flow Processes in Detonative Wave Rotors and Pulse Detonation Engines*, 44th AIAA Aerospace Sciences Meeting and Exhibit, 9-12 January 2006, Reno, Nevada, AIAA 2006-1236

Akbari, P., Nalim, R., Mueller, N., 2006, *A Review of Wave Rotor Technology and Its Applications*, Journal of Engineering for Gas Turbines and Power, October 2006, Vol. 128, p. 717-735

Alexiou, A, 2014, *Introduction to Gas Turbine Modelling with PROOSIS*, Empresarios Agrupados Internacional (EAI) S.A., Madrid, Spain

Anderson, N.E., Loewenthal, S.H., Black, J.D., 1984, *An Analytical Method to Predict Efficiency of Aircraft Gearboxes*

Apostolidis, A., Sampath, S., Laskaridis, P., Singh, R., 2013, *Webengine – A Web Based Gas Turbine Performance Simulation Tool*, Proceedings of the ASME TurboExpo 2013, June 3-7 2013, San Antonio, Texas, GT2013-95296

Barnard, R.H., Philpott, D.R., 2004, *Aircraft Flight: A Description of the Physical Principles of Aircraft Flight*, Pearson Education Ltd, Edinburgh

Bala, A., Sethi, V., Lo Gatto, E., Pachidis, V., Pilidis, P., 2007, *PROOSIS - A Collaborative Venture for Gas Turbine Performance Simulation using an Object Oriented Programming Schema*, 18th ISABE Conference, ISABE-2007-1357, Beijing, China

Bellocq, P., 2012, *Multi-Disciplinary Preliminary Design Assessments of Pusher Counter-Rotating Open Rotors for Civil Aviation*, Ph.D. thesis, Department of Power and Propulsion, School of Engineering, Cranfield University, Bedford, UK.

Bellocq, P., Sethi, V., Capodanno, S., Patin, A., Rodriguez Lucas, F., 2014, *Advanced 0-D Performance Modelling of Counter Rotating Propellers for Multi-Disciplinary Preliminary Design Assessments of Open Rotors*, ASME TurboExpo 2014, June 16-20th, Dusseldorf, Germany, GT2014-27141

Bellocq, P., Garmendia, I., Sethi, V., 2015, *Multidisciplinary Assessment of the Control of the Propellers of a Pusher Geared Open Rotor – Part I: Low Pressure System Design Choices, Engine Preliminary Design Phiosophyand Modelling Methodology*, ASME TurboExpo, June 15-19, Montreal, Canada, GT2015-43812

Bellocq, P., Garmendia, I., Sethi, V., Patin, A., Capodanno, S., Rodriguez Lucas, F., 2016, *Multidisciplinary Assessment of the Control of the Propellers of a Pusher Geared Open Rotor – Part II: Impact on Fuel Consumption, Engine Weight, Certification Noise and NOx Emissions*, Journal of Engineering for Gas Turbines and Power, July 2016, Vol. 138, 072603-1 - 8

Birch, N., 2000, *2020 Vision: The Prospects for Large Civil Aircraft Propulsion*, RAeS Aeronautical Journal, p.347-352

Boggia, S., Rüd, K., 2005, *Intercooled Recuperated Gas Turbine Concept*, 41st AIAA/ASME/SAE/ASEE Joint Propulsion Conference and Exhibit, 10-13 July 2005, Tucson, Arizona, AIAA 2005-4192

Brady C., 2012, *The Boeing 737 Technical Guide*, Tech Pilot Services Ltd: Cheshire

Brancatelli, J., 2009, *Commuter Hell, Turbo-prop planes, regional jets crucial, but road warriors hate flying them*, Business Travel on NBC News, 25 February 2009

BreakingTravelNews, 2012, *Airbus begins A320NEO production*, 10 July 2012, http://www.breakingtravelnews.com/news/article/airbus-begins-a320neo-production/

Camillieri, W., Anselmi, E., Sethi, V., Laskaridis, P., Rolt, A., Cobas, P., 2015, *Performance Characteristics and Optimisation of a Geared Intercooled Reversed Flow Core Engine*, Proceedings of the Institution of Mechanical Engineers, Part G: Journal of Aerospace Engineering, February 2015, Vol. 229, No. 2 p. 269-279

CAA, 2012, *Civil Aviation Authority Database Search* http://www.caa.co.uk/application.aspx?catid=60&pagetype=65&appid=1

CAEP7, 2007, *Environmental Design Space (EDS) Progress*, Committee on Environmental Protection (CAEP) Seventh Meeting, 5-16 February 2007, Montreal, Canada, CAEP/7-IP/23

Celis C., Moss B., Pilidis P., 2009, *Emissions Modelling for the Optimisation of Greener Aircraft Operations*, Proceedings of ASME Turbo Expo 2009, June 8-12 Orlando, Florida, GT2009-59211

CFM, 2013, *'LEAP – The Power of the Future'*, CFM LEAP Brochure 2013, CFM

Clean Sky, 2016, *Clean Sky, Innovation Takes Off*, http://www.cleansky.eu/

Clean Sky, 2012, *About Us*, http://www.cleansky.eu/content/homepage/about-us

Clean Sky, 2012a, *ITD Leaders and Associates*, http://www.cleansky.eu/content/page/itd-leaders-and-associates

Clean Sky, 2012b, *Mission and Objectives*, http://www.cleansky.eu/content/article/mission-objectives

Coleman, M.L., 2001, *Overview of Pulse Detonation Propulsion Technology*, Chemical Propulsion Information Agency, The John Hopkins University, Whiting School of Engineering, Columbia, Maryland, 20010517 003

Colmenares, F., Pascovici, D., Ogaji, S., Pilidis, P., 2007, *A Preliminary Parametric Study for Geared, Intercooled and/or Recuperated Turbofan for Short Range Civil Aircrafts*, ASME TurboExpo 2007, May 14-17, Montreal, Canada, GT2007-27234

Colmenares, F., 2009, *Techno-economic and Environmental Risk Assessment of Innovative Propulsion Systems for Short-Range Civil Aircraft*, PhD Thesis, Cranfield University, Cranfield

Cooper, M., Jackson, S., Austin, J., Wintenberger, E., Shepherd, J.E., 2002, *Direct Experimental Impulse Measurements for Detonations and Deflagrations*, Journal of Propulsion and Power, Vol. 18, No. 5, p 1033-1041

Costi, F., 2012, *Investigation on Boundary Layer Ingestion Effects on a Ducted Axial Fan for a Distributed Propulsion System,* MSc Thesis, Cranfield University, Cranfield

Cranfield University, 1999, *The TURBOMATCH Scheme*, Cranfield University

Cranfield University, 2009, *HERMES v5 and TURBOMATCH Calls: User Manual* Cranfield University

Croft, J., 2012, "Open Rotor Noise not a Barrier to Entry: GE", Flight Global 5, July 2012, https://www.flightglobal.com/news/articles/open-rotor-noise-not-a-barrier-to-entry-ge-373817/

Dickson, N., 2014, *Local Air Quality and ICAO Engine Emissions Standards*, Powerpoint Presentation, http://www.icao.int/SAM/Documents/2014-ENV/4.1LAQ%20TechnologyV2.pdf

DREAM, 2012, *Cranfield University and Dream*, http://www.dream-project.eu/cranfield-university.aspx

DREAM, 2012a, *DREAM Introduction*, http://www.dream-project.eu/

easyJet, 2007, *The "easyJet ecoJet": to cut CO_2 emissions by 50% by 2015*, http://corporate.easyjet.com/latest-news-archive/news-year-2007/14-06-07a-en.aspx?sc_lang=en

easyJet, 2014, *easyJet 2014 Annual Report*, http://corporate.easyjet.com/~/media/Files/E/ Easyjet-Plc-V2/pdf/investors/result-center-investor/annual-report-2014.pdf

EC, 2001, *European Aeronautics: A Vision for 2020*, http://ec.europa.eu/research/transport/publications/items/european_aeronautics__a_vision_for_2020_en.htm

EC, 2016, *validation of Radical Engine Architecture systeMs*, http://ec.europa.eu/research/transport/projects/items/dream_en.htm

el_Hossaini, M.K., 2014, *Review of the New Combustion Technologies in Modern Gas Turbines*, Progress in Gas Turbine Performance, Chapter 6, IntechOpen

Endara Mayorga, C., 2015, *Development of a Component Based Preliminary Weight Estimation Method for Mission Level Assessment of a Geared Turbofan*, MSc Thesis, Cranfield University, Cranfield

English, Cdr C.R., 2003, *The WR-21 Intercooled Recuperated Gas Turbine Engine – Integration into Future Warships*, Proceedings of the International Gas Turbine Congress, 2003, Tokyo, November 2-7, IGTC2003Tokyo OS-203

EC, 2001, *European Aeronautics: A Vision for Europe 2020*, European Commission: Luxembourg

EU, 2006, *'VITAL' Workshop Promotes Cleaner Air Transport*, http://ec.europa.eu/research/transport/news/items/_vital__workshop_promotes_cleaner_air_transport_en.htm

Farokhi, S., 2009, *Aircraft Propulsion*, John Wiley & Sons, Hoboken, N.J.

Flight Global, 2007, *Whatever happened to propfans?*, Flight Global, 12 June 2007

Follen, G.J., 2002, *An Object Oriented Extensible Architecture for Affordable Aerospace Propulsion Systems*, RTO AVT Symposium on Reduction of Military Vehicle Acquisition Time and Cost through Advanced Modelling and Virtual Simulation, 22-25 April 2002, Paris, France, RTO-MP-089

Gayraud, S., 1996, *Technical and Economic Assessments for Industrial Gas Turbines Selection*, MSc Thesis, Cranfield University: Cranfield

Goldberg, C., Nalianda, D., Singh, R., 2015, *Techno-economic and Environmental Risk Assessment of a Blended Wing Body with Distributed Propulsion*, AIAA/SAE/ASEE Joint Propulsion Conference, 27-29 July 2015, Orlando, Fl, AIAA 2015-4024

Goldberg, D., 1989, *Genetic Algorithms in Search, Optimization and Machine Learning*, Addison-Wesley Longman Publishing Co., Boston, MA

Goold, I, 2012, *Airbus A320NEO Design Frozen, First Flight in 2014*, AINOnline 9 July 2012, http://www.ainonline.com/aviation-news/2012-07-08/airbus-a320neo-design-frozen-first-flight-2014

Grönstedt, T., Irannezhad, M., Lei, X., Thulin, O., Lundblah, A., 2013, *First and Second Law Analysis of Future Aircraft Engines*, Proceedings of ASME Turbo Expo 2013, June 3-7, San Antonio, Texas, GT2013-95516

Grieb, H., Eckardt, D., 1986, *Turbofan and Propfan as Basis for Future Economic Propulsion Concepts*, 22nd Joint Propulsion Conference, Huntsville, Alabama, AIAA 1986-1474

Gubisch, M., 2014, *Snecma plans 2019 open-rotor flights*, Flight International, 14-20 January 2014

Guynn, M.D., Berton, J.J., Hendricks, E.S., Tong, M.T., Haller, W.J., Thurman, D.R., 2011, *Initial Assessment of Open Rotor Propulsion Applied to an Advanced Single-Aisle Aircraft*, 11th AIAA Aviation Technology, Integration, and Operations (ATIO) Conference, including the AIAA 20-22 September 2011, Virginia Beach, VA, AIAA 2011-7058

Guynn, M.D., Berton, J.J., Haller, W.J., Hendricks, E.S., Tong, M.T., 2012, *Performance and Environmental Assessment of an Advanced Aircraft with Open Rotor Propulsion*, NASA Report TM-2012-217772

Horlock, J., Watson, D. & Jones, T., 2001, *Limitations on Gas Turbine Performance Imposed by Large Turbine Cooling Flows*, ASME Journal of Engineering for Gas Turbines and Power 123(3): 487–494

House of Commons, 2011, *Science and Technology Committee – Second Report: Technology and Innovation Centres*, The Stationary Office, 9 February 2011

Hudson, M., 1999, *The Foundation of Propulsion Products*, Proceedings of the 14th ISABE Conference, Florence, Italy, September 1999

IATA, 2015, *Jet Fuel Price Analysis*, http://www.iata.org/publications/economics/fuel-monitor/Pages/price-analysis.aspx

ICAO, 2012, *Aircraft Engine Emissions: Definition of the Problem*, http://www.icao.int/environmental-protection/Pages/aircraft-engine-emissions.aspx

IPCC, 1999, *Aviation and the Global Atmosphere: A Summary for Policy Makers*, http://www.ipcc.ch/pdf/special-reports/spm/av-en.pdf

Jackson, A.J.B, 2009, *Optimisation of Aero and Industrial Gas Turbine Design for the Environment*, PhD Thesis, Cranfield University, Cranfield

Janes, 2011, *Janes Aero Engines Issue 29*, Daly M. Ed. & Gunson B. Assoc Ed., IHS Janes: Surrey

Jenkinson, L.R., Simpkin, P., Rhodes, D., 1999, *Civil Jet Aircraft Design*, Arnold, London

Jensen, D.T., Leonard, J.M., 2002, *The Forgotten Allison Engines*, 38th AIAA/ASME/SAE/ASEE Joint Propulsion Conference and Exhibit, 7-10 July 2002, Indianapolis, Indiana, AIAA 2002-3566

Joyce, I., 2011, *Flightglobal Engine Directory: CFM*, http://www.flightglobal.com/directory/searchresults.aspx?manufacturerType=Engine&searchMode=Manufacturer&keyword=&manufacturer=3279&navigationItemId=382

Kailasanath, L., 2009, *Research on Pulse Detonation Combustion Systems – A Status Report*, 47th AIAA Aerospace Sciences Meeting Including The New Horizons Forum and Aerospace Exposition, 5-8 January 2009, Orlando, Florida, AIAA 2009-631

Kim, H.J., Felder, J.L., Tong, M., T., Berton, J.J., Haller, W.J., 2014, *Turboelectric Distributed Propulsion Benefits on the N3-X Vehicle*, Aircraft Engineering and Aerospace Technology: An International Journal, Vol 86, Issue 6, p. 558-561

Khalid, S.A., Lurie, D., Breeze-Stringfellow, A., Wood, T., Ramakrishnan, K., Pliath, U., Wojno, J., Janardan, B., Goering, T., Opalski, A., Barrett, J., 2013, *FAA CLEEN Program Open Rotor Aeroacoustic Technology Non-Proprietary Report*, GE Aviation, Evandale, Ohio, DOT/FAA/AEE/2014-03

Koch, P.N., Evans, J.P., Powell, D., 2002, *Interdigitation for Effective Design Space Exploration using iSIGHT*, Journal of Structural and Multidisciplinary Optimization, Vol 23, Issue 2, p. 111-126

Korsia, J.J., 2009, *VITAL – European R&D Programme for Greener Aero-Engines*, ISABE 2009 Proceedings, ISABE-2009-1114 , Montreal, Canada.

Korsia, J.J. & Guy, S, 2007, *VITAL – European R&D Programme for Greener Aero-Engines*, ISABE 2007 Proceedings, ISABE-2007-1118 , Beijing, China.

Kurzke, J., 2015, *GasTurb 12- Design and Off Design Performance of Gas Turbine Engines*, GasTurb GmbH, Germany

Kyprianidis K.G., Colmenares Quintero R.F., Pascovici D.S., Ogaji S.O.T., Pilidis P., 2008, *EVA - A Tool for Environmental Assessment of Novel Propulsion Cycles*, ASME Turbo Expo 2008, June 9-13 2008 Berlin, Germany, GT2008-50602

Kyprianidis, K.G., Grönstedt, T., Ogaji, S.O.T., Pilidis, P., Singh, R., 2010, *Assessment of Future Aero Engine Designs with Intercooled and Intercooled Recuperated Cores*, Journal of Engineering for Gas Turbines and Power, 133(1), 011701

Kyprianidis, K.G., 2010, *Multi-disciplinary Conceptual Design of Future Jet Engine Systems*, PhD Thesis, Cranfield University, Cranfield

Kyprianidis, K.G., 2011, Future Aero Engine Designs: An Evolving Vision, *Advances in Gas Turbine Technology* ISBN: 978-953-307-611-9

Larsson, L., Lundbladh, A., Grönstedt, T., 2014, *A Conceptual Design Study of an Open Rotor Powered Regional Aircraft*, ASME TurboExpo 2014, June 16-20, Dusseldorf, Germany, GT2014-26091

Laskaridis, P., 2004, *Performance Investigations and Systems Architectures for More Electric Aircraft*, PhD Thesis, Cranfield University, Cranfield

Laskaridis, P., Pilidis, P., Kotsiopoulos, P., 2005, *An Integrated Engine – Aircraft Performance Platform for Assessing New Technologies in Aeronautics*, ISABE2005-1165, Proceedings of 17th International Symposium on Air Breathing Engines, Munich, 2005

Lee, S.Y., Watts, J., Saretto, S., Pal, S., Conrad, C., Woodward, R., Santoro, R.J., 2004, *Deflagration to Detonation Transition Processes by Turbulence-Generating Obstacles in Pulse Detonation Engines*, Journal of Propulsion and Power, Vol. 20, No. 6, p.1026-1036

Lefebvre, A., 2010, *Gas Turbine Combustion, 3rd Ed*., Taylor & Francis, PA, USA

Leyens, C., 2004, *Advanced Materials and Coatings for Future Gas Turbine Applications*, 24th Congress of the International Council of the Aeronautical Sciences, 29 August – 3 September 2004, Yokohama, Japan, ICASE 2004-5.5.1

Li, X., Sun Bo., You, H., Wang, L., 2014, *Evolution of Rolls-Royce Air-Cooled Turbine Blades and Feature Analysis*, APOSAT2014, Aisa-Pacific International Symposium on Aerospace Technology,

Lolis, P., Giannakis, P., Sethi, V., Jackson, A.J.B., Pilidis, P., 2014, *Evaluation of Aero Gas Turbine Preliminary Weight Estimation Methods*, Aeronautical Journal, Vol. 118, No. 1204, p.625-641

Lolis, P., 2014a, *Development of a Preliminary Weight Estimation Method for Advanced Turbofan Engines*, PhD Thesis, Cranfield University, Cranfield

Macalister, T., 2011, *Background: What Caused the 1970's Oil Price Shock*, Guardian, 3 March 2011

Mankins, J.C., 1995, *Technology Readiness Levels – A White Paper*, Office of Space and Technology, Advance Concepts Office, NASA, 1995

M'Bengue, L, 2010, *Towards Acare 2020: Innovative Engine Architectures to Achieve Environmental Goals?* ICAS 2010: 27th International Congress of the Aeronautical Sciences

McKenzie, A.B., 1997, *Axial Flow Fans and Compressors: Aerodynamic Design and Performance*, Ashgate, Aldershot

Mellor, A.M., 1990, *Design of Modern Turbine Combustors*, Academic Press: San Diego

Michalewicz, Z., 1996, *Genetic Algorithms + Data Structures = Evolution Programs (3rd ed.)*, Springer-Verlag, London

Mikkelson, D.C., Mitchell, G.A., and Bober, L.J., 1984, *Summary of Recent NASA Propeller Research*, NASA Lewis Research Center, Cleveland, Ohio, NASA-TM-83733.

Mohammad, B.S., Jeng, S.M., 2009, *Design Procedures and a Developed Computer Code for Preliminary Single Annular Combustor Design*, 45th AIAA/ASME/SAE/ASEE Join Propulsion Conference and Exhibit, 2-5 August 2009, Denver, Colorado, AIAA 2009-5208

Morrell, P., & Dray, L., 2009, *Environmental Aspects of Fleet Turnover, Retirement and Lifecycle*, Final Report for the Omega Consortium 2009

Musielak, D.E., ND, *Fundamentals of Pulse Detonation (PDE) and Related Propulsion Technology*, PowerPoint Presentation, Aerospace Engineering Consulting, Arlinton, Texas

MacMillan, W.L., 1974, *Development of a Modular Type Computer Program for the Calculation of Gas Turbin Off-Design Performance*, PhD Thesis, Cranfield University, Cranfield

Nalianda D., 2012, *Impact of Environmental Taxation Policies on Civil Aviation - A Technoeconomic and Environmental Risk Assessment*, PhD Thesis, Cranfield University

NEWAC, 2016, *Project Home Page*, http://www.newac.eu/12.0.html

Noppel, F.G., 2011, *Comparison of Unconventional Aero Engine Architectures*, PhD Thesis, Cranfield University, Cranfield

Ogaji S., Pilidis P., Hales R., 2007, *TERA - A Tool for Aero-Engine Modelling and Management*, 2nd World Congress on Engineering Asset Management and the Fourth International Conference on Condition Monitoring, 11-14 June 2007, Harrogate, UK

Pachidis V., No Date, *Gas Turbine Performance Simulation* MSc Thermal Power Lecture Notes, Cranfield University

Pascovici D.S., Colmenares F., Ogaji S.O.T., Pilidis P., 2007, *An Economic and Risk Analysis Model for Aircrafts and Engines*, Proceedings of ASME TurboExpo 2007: Power for Land, Sea and Air, May 14-17 2007, Montreal, Canada, GT2007-27236

Pera R.J., Onat, E., Klees, G.W., Tjonneland, E., 1977, *A Method to Estimate Weight and Dimensions of Aircraft Gas Turbine Engines*, NASA Report, NASA-CR-135170, Vol. 1

Pervier, H., Nalianda, D., Espi, R., Sethi, V., Pilidis, P., Zammit-Mangion, D., Rogero, J-M., Entz, R., 2011, *Application of Genetic Algorithm for Preliminary Trajectory Optimization*, SAE Int. J. Aerosp. 4(2):973-987

Pilidis P., Palmer J.R., Gullia A., Jackson A.J.B., Janikovic J., *Gas Turbine Theory and Performance*, MSc Lecture Notes, Cranfield University

Pratt & Whitney, 2012, *PurePower PW1000G Engine*, http://www.purepowerengine.com/technology.html

Pratt & Whitney, 2012a, *PurePower Family of Engines Brochure*, http://www.purepowerengine.com/pdf/purepower_brochure_2012.pdf

Pratt & Whitney, 2013, *PurePower Engine Family Specs Chart*, https://www.pw.utc.com/Content/PurePowerPW1000G_Engine/pdf/B-1-1_PurePowerEngineFamily_SpecsChart.pdf

Ramsden, K.W., MacManus, D., Zachos, P., 2013, *Aerodynamic Design of Axial Compressors and Turbines*, Cranfield University Course Notes

Raymer, D.P., 2006, *Aircraft Design: A Conceptual Approach*, AIAA 2006

Rizk N.K., Mongia H.C., 1994, *Emissions predictions of different gas turbine combustors*, AIAA 94-0118, 1994

Rolls-Royce, 1966, *The Jet Engine*, Rolls-Royce Ltd: Derby

Rolt, A.M., Baker, N.J., 2009, *Intercooled Turbofan Engine Design and Technology Research in the EU Framework 6 NEWAC Programme*, ISABE 2009-1278

Rolt, A. & Kyprianidis, K., 2010, *Assessment of New Aero Engine Core Concepts and Technologies in the EU Framework 6 NEWAC Programme*, ICAS 2010 Congress Proceedings, Paper No. 408, Nice, France

Rouser, K.P., King, P.I., Schauer, F.R., Sondergaard, R., Hoke, J.L., 2010, *Unsteady Performance of a Turbine Driven by a Pulse Detonation Engine*, 48th AIAA Aerospace Sciences Meeting Including The New Horizons Forum and Aerospace Exposition, 4-7 January 2010, Orlando, Florida, AIAA 2010-1116

Roy, G.D., Frolov, S.M., Borisov, A.A., Netzer, D.W., 2004, *Pulse Detonation Propulsion Challenges, Current Status and Future Perspective*, Progress in Energy and Combustion Science, Vol. 30, No. 6 p.545-672

Saravanamuttoo, H.I.H., 2002, The Daniel and Florence Guggenheim Memorial Lecture - Civil Propulsion; The Last 50 Years, *ICAS 2002 Congress Proceedings*, Toronto, Canada

Saravanamuttoo, H.I.H., (ed.) 2008, *Gas Turbine Theory*, 6th ed. Pearson Prentice Hall, Upper Saddle River, N.J.

Sargerser D.A., Lieblein, S., Krebs, R.P., 1971, *Empirical Expressions for Estimating Length and Weight of Axial Flow Components of VTOL Powerplants*, NASA Technical Report TM X-2406

Schumann, U. 1997, *The Impact of Nitrogen Oxides Emissions from Aircraft upon the Atmosphere at Flight Altitudes – Results from the AERONOX Poject*, Atmospheric Environment, Vol. 31, No.12, p.1723-1733

Seitz, A., Gologan, C., 2015, *Parametric Design Studies for Propulsive Fuselage Aircraft Concepts*, CEAS Aeronautical Journal, Vol 6, Issue 1, p.69-82

Singh R., 2011, *Gas Turbine Combustors Volume 1*, MSc Thermal Power Lecture Notes, Cranfield University: Cranfield

Spindler P.M., 2007, *Environmental Design Space Model Assessment*, MSc Thesis, Massachusetts Institute of Technology, Massachusetts

Sweetman, B., 2005, *The Short, Happy Life of the Prop-Fan*, Air & Space Magazine, September 2005

Tacina, K.M., Chang, C.T., Zhuohui J.E., Lee, P., Dam, B., Mongia, H., 2014, *A Second Generation Swirl-Venturi Lean Direct Injection Combustion Concept*, 50th AIAA/ASME/SAE/ASEE Joint Propulsion Conference, AIAA 2014-3434

Tacina, R.R., 1990, *Combustor Technology for Future Aircraft*, 26th Joint Propulsion Conference cosponsored by the AIAA, SAE, ASME and ASEE, Orlando, Florida, July16-18, AIAA-90-2400

United Nations, 1998, *Kyoto Protocol to the United Nations Framework Convention on Climate Change*, http://unfccc.int/resource/docs/convkp/kpeng.pdf

Van Zante, D.E., 2013, *The NASA Environmentally Responsible Aviation Project/General Electric Open Rotor Test Campaign*, 5st AIAA Aerospace Sciences Meeting, 7-10 January, Grapevine (Dallas Ft Worth Region), Texas, AIAA 2013-0415

Walker, A.D., Carrotte, J.F., Rolt, A.M., 2009, *Duct Aerodynamics for Intercooled Aero Gas Turbines: Constraints ,Concepts and Design Methodology*, ASME TurboExpo 2009, June 8-12, Orlando, Florida, GT2009-59612

Walsh, P.P., Fletcher, P., 2004, *Gas Turbine Performance*, 2nd ed., Blackwell Science, Oxford

Watts, R., 1978, *European air transport up to the year 2000*, RAeS Aeronautical Journal pp. 300–312

Welch, G.E., Jones, S.M., Paxson, D.E., 1995, *Wave Rotor Enhanced Engine*, NASA Technical Memorandum, 106998, AIAA-95-2799

Wilcock, R., Young, J. & Horlock, J., 2005, *The Effect of Turbine Blade Cooling on the Cycle Efficiency of Gas Turbine Power Cycles*, ASME Journal of Engineering for Gas Turbines and Power 127(1): 109–120.

Wilfert, G., Sieber, J., Rolt, A., Baker, N., Touyeras, A. & Colantuoni, S., 2007, *New Environmental Friendly Aero Engine Core Concepts*, ISABE 2007 Proceedings, ISABE-2007-1120, Beijing, China

Williams, D., 2014, *Propulsion Systems, Performance and Integration*, Cranfield University Course Notes

Willis R.J. Jr, 1963, *New Equations and Charts Pick Off Lightest Weight Gears*, Product Engineering, January 21 1963

van der Mark K., 2012, *Register Review* Aviation News May 2012, KeyPublishing: Stamford, Lincs.

Vicente, E., 1994, *Effect of Bypass Ratio on Long Range Subsonic Engines*, MSc Thesis, Cranfield University: Cranfield

Whellens M.W., 2002, *Multidisciplinary Optimisation of Aero-Engines using Genetic Algorithms and Preliminary Design Tools*, PhD Thesis, Cranfield University: Cranfield

Whellens M.W., Singh R., Pilidis P., Taguchi, H., 2003, *Genetic Algorithm Based Optimisation of Intercooled Recuperated Turbofan Design*, 41st Aerospace Sciences Meeting and Exhibit 6-9 January 2003, Reno, Nevada, AIAA 2003-1210

Xu, L., Kyprianidis, K.G., Grönstedt, T.U.J., 2013, *Optimization Study of an Intercooled Recuperated Aero-Engine*, Journal of Propulsion and Power, March-April 2013, Vol. 29, No. 2

Appendix 1 - HERMES Input File

```
                        GeomMissionEngineSpecMasterCUEJ56MR
!Input file for the geometric, mission and engine specifications for an Airbus
A320-200 type aircraft, with CFM56-5B/4 type engines
ENGINE_SPEC:CUEJ56-30-4-12.dat !prepared by Alex Nind
!GEOMETRIC DETAILS
! Wing Geometry
122.6           ! AcWingAInit - Wing area
9.5             ! AcWingAspr - Aspect ratio
0.105           ! AcWingCThir - Thickness chord ratio
25              ! AcWingSwpa - Sweep angle (in degrees)
0.239           ! AcWingTpr - Taper ratio
0.130           ! AcWingRtThir - Root thinkness ratio
0.1             ! AcWingOtThir - Outer thikness ratio
! Tailplane Geometry =horizontal plane
28.0            ! AcTailAInit - Tailplane area
5               ! AcTailAspr - Aspect ratio
0.1             ! AcTailCThir - Thickness chord ratio
34              ! AcTailSwpa - Sweep angle (in degrees)
0.313           ! AcTailTpr - Taper ratio
0.095           ! AcTailRtThir - Root thinkness ratio
0.095           ! AcTailOtThir - Outer thikness ratio
! Fin Geometry= vertical tail
18              ! AcFinA - Fin area
5.9             ! AcFinSpan - Span
0.115           ! AcFinCThir - Thickness chord ratio
48              ! AcFinSwpa - Sweep angle (in degrees)
0.235           ! AcFinTpr - Taper ratio
0.095           ! AcFinRtThir - Root thinkness ratio
0.135            ! AcFinOtThir - Outer thikness ratio
! Fuselage Geometry
4.044           ! AcFusDia - Diameter
37.57           ! AcFusLen - Length
! Landing Gear Characteristics
2               ! AcLGTyp1 - Landing gear type ***0=default, 1=Bogie, 2=Small twin
wheel***
1               ! AcLgTyp2= 0,1,2
1               ! AcLgTyp3= 0,1,2
-1              ! AcLgTyp4= 0,1,2,-1 *** -1=if the aircraft only has 3 LG -1 has to
be declared
-1              ! AcLgTyp5= 0,1,2,-1 *** for the last 2 values
2               ! AcLGDepl - Number of segments with LG down for descent
! High lift systems
1               ! AcFlapSegTo -Number of Segments with flaps deployed during TO
3               ! AcFlapSegApp - Number of Segments with flaps deployed for
approach
2               ! ACFlapSegLand - Number of Segments with flaps deployed during
Landing
1.10            ! AcExtSrTo - Wing area extension ratio TO
1.15            ! AcExtSrApp - Wing area extension ratio approach
1.20            ! AcExtSrLand - Wing area extension ratio Landing
10              ! AcFlapAngleTo - Flap Angle TO IN DEGREES
20              ! AcFlapAngleApp - Flap Angle Approach
35              ! AcFlapAngleLand - Flap Angle Land
1               ! AcFlapSlots - Number of Flap Slots (1-3)
! Engine Geometry
2.15            ! EngNacDiaInit - Diameter
4.5             ! EngNacLenInit - Length
!XXXXXXXXXXXXXXXXXXXXXXXXXXXXXXXXXXXXXXXXXXXXXXXXXXXXXXXXXXX
!MISSION/WEIGHT SPECIFICATION DATA
36937           ! AcAfrWtInit - Airframe weight
2               ! AcEngNb - Number of Engines
2932            ! EngWtInit - Engine weight,  (kg/engine) (dry weight - 5250lbs -
source CFM)
0               ! AcPldWt - Payload weight, (kg)
0               ! AcFuelWtInit - Fuel weight,  (kg)
18729           ! AcPldWtmax  - Maximum payload weight, kg (Airbus)
25000           ! AcFuelWtmax - Maximum fuel weight,  kg (Airbus) (Is actually
18729kg - has been set much higher so HERMES still gives a result)
64500           ! AcLandWtmax - Maximum landing weight, kg (Airbus)
                                    Page 1
```

```
                    GeomMissionEngineSpecMasterCUEJ56MR
73500          ! AcToWtmax - Maximum take-off weight, kg (Airbus)
0.0            ! DVFuelRatio - Diversion fuel weight to total fuel weight (%)
0.0            ! AcFuelContpc - Relative contigency fuel to remain after landing
(%)
6660           ! AcRng - Range to be flown (km)       ! Mission (2)
370            ! AcRngdv - Diversion Range to be flown (km)
2              ! AcMisType - Mission to be flown (1-fixed fuel get range) or
(2-fixed range for given Pload get fuel)
1              ! DvMission - specify if diversion mission is to be run (1- NO
diversion mission) or (2- YES to diversion mission)
!XXXXXXXXXXXXXXXXXXXXXXXXXXXXXXXXXXXXXXXXXXXXXXXXXXXXXXXXXXXXXXXX
!CRUISE MAIN/DIVERSION AND HOLDING DATA
2              ! number of cruise altitudes and Mach numbers
1              ! number of cruise Temperature Deviations from ISA day (the trip
is splitted equally into this number of parts. Every part has the respective
DTisa)
1              ! number of diversion cruise altitudes
5.             ! Cruise small segment time Interval in (min). This value affects
the accuracy of the calculations, so keep it small.
10668.,11887. ! Cruise altitudes in [m] (WARNING: THE ALTITUDES CANNOT BE THE
SAME!!!!!!!!!!)
0.76,0.76      ! Cruise Mach numbers, the same number with cruise altitudes
10.            ! Cruise ambient temperature deviation from ISA, in [K]
6096.          ! Diversion cruise altitudes (m)
0.65           ! Diversion cruise Mach numbers,
10.            ! Diversion cruise ambient temperature deviation from ISA, in [K]
457.0          ! Holding altitude (m)
30.            ! Hold Time in (min)
!XXXXXXXXXXXXXXXXXXXXXXXXXXXXXXXXXXXXXXXXXXXXXXXXXXXXXXXXXXXXXXXX
!CLIMB DATA
22               ! Climb segments Number
! Altitudes(m)  | DTisa(K) | EAS(knots) | Power(0.-1.)
557.20 10. 250. 1.
900.00 10. 250. 1.
1500.00 10. 250. 1.
1981.20 10. 250. 1.
2438.40 10. 250. 1.
2743.20 10. 250. 1.
3048.00 10. 250. 1.
3048.10 10. 320. 1.
3657.60 10. 320. 1.
4267.20 10. 320. 1.
4876.80 10. 320. 1.
5486.40 10. 320. 1.
6096.00 10. 320. 1.
7620.00 10. 320. 1.
8077.20 10. 320. 1.
9144.00 10. 320. 1.
10058.00 10. 320. 1.
10668.00 10. 320. 1.
11227.00 10. 320. 1.
11887.00 10. 320. 1.
12000.00 10. 320. 1.
12496.8 10. 320. 1.
!XXXXXXXXXXXXXXXXXXXXXXXXXXXXXXXXXXXXXXXXXXXXXXXXXXXXXXXXXXXXXXXX
!DESCENT DATA
10               ! Descent segments Number
! The altitudes are dependant on the final cruise altitude. So they are
calculated inside the code.
! DTisa(K)      | TAS(knots) | Power(0.-1.) ****Note: the last 3 power settings
use the Approach rating
10. 233.1 1.                              ! Flight Idle Rating
10. 221.5 1.                              ! Flight Idle Rating
10. 202.9 1.                              ! Flight Idle Rating
10. 195.0 1.                              ! Flight Idle Rating
10. 183.1 1.                              ! Flight Idle Rating
10. 164.7 1.                              ! Flight Idle Rating
10. 150.9 1.                              ! Flight Idle Rating
                                  Page 2
```

```
10. 140.0 1.                              ! Approach Rating
10. 135.0 1.                              ! Approach Rating
10. 135.0 1.                              ! Approach Rating
!XXXXXXXXXXXXXXXXXXXXXXXXXXXXXXXXXXXXXXXXXXXXXXXXXXXXXXXXXXX
!LANDING DATA
0.01      ! Note: Do not put final landing altitude = 0.0, use a very small
value instead.
135.00    ! Approach speed (TAS), in [m/s]
10        ! Deviation from standard atmosphere for Landing in [K]
6.00      ! Duration of Landing phase in [min]
!XXXXXXXXXXXXXXXXXXXXXXXXXXXXXXXXXXXXXXXXXXXXXXXXXXXXXXXXXXX
!TAXI and TAKE-OFF DATA
0.02      ! AcTaxiCf1 - Runway Friction Coefficient
0.3       ! AcTaxiCf2 - Runway Friction Coefficient,BREAKES-OFF
0         ! AcTaxiTime - Taxi time in [min] (12mins for LR, 9mins for SR)
0.7       ! AcToTime - Take-off time in [min]
0.00      ! AcToALT - Take-off altitude in [m]
10        ! Take-off temperature deviation from ISA in [K]
0.0             ! TakeOff Derate (Real Values from 0 to 1, 0.0->100% of
Maximum Thrust, 1.0->0% of Maximum Thrust)
!XXXXXXXXXXXXXXXXXXXXXXXXXXXXXXXXXXXXXXXXXXXXXXXXXXXXXXXXXXX
!NUMERICAL TOLERANCES AND INITIAL GUESSES
1.D-11                          ! Climb and Descent internal loops relative
accuracy
1.D-09                          ! Main mission range relative accuracy
1.D-09                          ! Diversion mission range relative accuracy
1.D-07                          ! Fuel weight outer iteration loop relative
accuracy
480.D00                         ! Main mission duration guess 1 (for secant
method, modify it only if there is a convergence problem)
260.D00                         ! Main mission duration guess 2 (for secant
method, modify it only if there is a convergence problem)
!XXXXXXXXXXXXXXXXXXXXXXXXXXXXXXXXXXXXXXXXXXXXXXXXXXXXXXXXXXX
!TMATCHCALLS SPECIFICATIONS (*****HERMES DOES NOT READ THIS PART*****)
!-------------------------------------------------------------------------
!Number of points in the Engine Design Point input file to be skipped
!before the mission profile starts (including the design point)
0
!-------------------------------------------------------------------------
!Burner exit station number
10
!-------------------------------------------------------------------------
!ENGINE TET RANGE FOR EACH PHASE
10                              ! TET number for Take Off
6                               ! TET number for Climb
24                              ! TET number for Main and Diversion Cruise
4                               ! TET number for Flight Idle(Descent) and Ground
Idle
5                               ! TET number for Approach
5.                              ! TET step change in [K] for Take Off
5.                              ! TET step change in [K] for Climb
5.                              ! TET step change in [K] for Main and Diversion
Cruise
5.                              ! TET step change in [K] for Flight
Idle(Descent) and Ground Idle
5.                              ! TET step change in [K] for Approach
1605.                   ! Max TET in [K] for Take Off
1470.                   ! Max TET in [K] for Climb
1411.                   ! Max TET in [K] for Main Mission Cruise
1100.                   ! Max TET in [K] for Flight Idle(Descent) and Ground
Idle
1150.                   ! Max TET in [K] for Approach
!-------------------------------------------------------------------------
!ADDITIONAL ENGINE PERFORMANCE STATION VECTOR DATA (STATION, ITEM)
29                              ! Number of additional engine performance
station vector data
!Station | Item
2 4
```

```
3 4
2 6
3 6
2 2
4 2
4 4
5 4
4 6
5 6
6 4
7 4
7 6
9 2
9 6
9 4
11 1
11 2
11 6
12 6
11 4
12 4
12 6
13 6
12 4
13 4
32 8
14 8
32 7
!------------------------------------------------------------------------
!ADDITIONAL ENGINE PERFORMANCE BRICK DATA (DESCRIPTION, BRICK NO, ITEM)
1                               ! Number of additional engine performance brick
data
!Description | BrickNo | Item   (WARNING: The BrickNo is defined according to
the tabular output file of turbomatch )
Null 1 1
!------------------------------------------------------------------------
!ADDITIONAL OFF DESIGN ENGINE CONFIGURATIONS (LIKE BLEEDS etc.)
!Specify additional off design specification for each flight phase (e.g. for
brick data 26 "26 0.95")
1                               ! Number of additional off design specifications
for each flight phase
!You have to specify the same number of additional specs for all the phases,
i.e. if you specify something you have to do it for every flight phase
!------------------------------------------------------------------------
!TAKE OFF SPECIFICATIONS
!------------------------------------------------------------------------
225 1200. 0. 0. ! BDnum TET ValueBelowTET ValueAboveTET
!------------------------------------------------------------------------
!CLIMB SPECIFICATIONS
!------------------------------------------------------------------------
225 1200. 0. 0. ! BDnum TET ValueBelowTET ValueAboveTET
!------------------------------------------------------------------------
!CRUISE SPECIFICATIONS
!------------------------------------------------------------------------
225 1200. 0. 0. ! BDnum TET ValueBelowTET ValueAboveTET
!------------------------------------------------------------------------
!FLIGHT/GROUND IDLE SPECIFICATIONS
!------------------------------------------------------------------------
225 1200. 0. 0. ! BDnum TET ValueBelowTET ValueAboveTET
!------------------------------------------------------------------------
!APPROACH SPECIFICATIONS
!------------------------------------------------------------------------
225 1200. 0. 0. ! BDnum TET ValueBelowTET ValueAboveTET
!------------------------------------------------------------------------
!INPUT AND OUTPUT FILE PATHS
!Engine Design Point Specification file (input to Hermes)
CUEJ56-v2.dat
```

Appendix 2 – Tethys Input File – CUEJ56

```
                                TethysInputMasterCUEJ56
********************************************************************************
Tethys v1.0 - Gas turbine sizing and general arrangement program
Currently only works with 2 spool aero gas turbine engines with single stage fan
********************************************************************************
Section 1 - Number of Stages in each section
--------------------------------------------------------------------------------
1                           !No. of fan stages - at the moment use only 1, this
needs to be updated in the future
-1                          !No. of low pressure compressor stages (use -1 if you
want the code to calculate this for you)
0.5                         !LPC max stage loading per stage (only used if -1
selected in the previous input)
 0.583                      !LPC Inlet total pressure (atm)
 1.644                      !LPC Outlet total pressure (atm)
-1                          !No. of high pressure compressor stages (use -1 if
you want the code to calculate this for you)
0.26                        !HPC max stage loading per stage (only used if -1
selected in the previous input)
 1.644                      !HPC inlet total pressure from turbomatch (atm)
11.511                      !HPC outlet total pressure from turbomatch (atm)
-1                          !Number of high pressure turbine stages (use -1 if
you want the code to calculate this for you)
2                           !Max stage loading coefficient allowed per stage of
HPT (if -1 was selected previously - Code calculates based on a value of U at
entrance to stage - rough and ready calcuation)
-1                          !Number of low pressure turbine stages (use -1 if you
want the code to calculate this for you)
3                           !Max stage loading coefficient allowed per stage of
LPT (if -1 was selected previously - Code calculates based on a value of U at
entrance to stage - rough and ready calcuation)
********************************************************************************
Section 2 - Fan input details
--------------------------------------------------------------------------------
 0.353000                   !Fan inlet total pressure (atm)
 0.583000                   !Fan outlet total pressure (atm)
246.670                     !Fan inlet total temperature (K)
289.630                     !Fan outlet total temperature (K)
169.000                     !Fan inlet mass flow (kg/s)
25.857                      !Fan outlet mass flow to core (kg/s)
0.99, 0.95                  !Fan blockage factors (number of values need to be
number of stages +1)
1735                        !Fan diameter (mm)
0.94                        !Fan reduction factor (about 0.94)
5300                        !Fan rotational speed (RPM)
195, 180                    !Fan mean axial velovity (first is inlet & number of
values need to be number of stages +1)
4                           !Fan blade mean aspect ratio
3.5                         !Bypass stator mean aspect ratio
2                           !Core stator mean aspect ratio
18.86                       !Scaling factor from drawing (drawing to real life
distance) - if unkown use 18.86
22, 10                      !Distance of spinner from fan from drawing (2 values
required - tip and intermediate - if unknown use 22 and 10)
********************************************************************************
Section 3 - Compressor input details
--------------------------------------------------------------------------------
1                           !LPC line type selector (1 for mean line, 2 for
rising line, 3 for falling line)
3                           !HPC line type selector (1 for mean line, 2 for
rising line, 3 for falling line)
289.630                     !LPC Inlet total temperature (K)
403.550                     !LPC Outlet total temperature (K)
5300                        !LPC Rotational speed (rpm)
2                           !LPC blade aspect ratio
2.5                         !LPC stator aspect ratio
3                           !LPC blade & stator length selection (1 - initial
uses AR, followed by reduction factor 2 - all use AR, 3 - manually input initial
length follwed by reduction factor
                                    Page 1
```

```
0.043236375, 0.032526769   !Blade and stator inital chord lengths (m)
0.8922, 0.8922             !Blade and stator reduction factors (in conjunction
with 1 and 3 above
0.2                        !LPC - Gap between rotor and stator as % of rotor
blade chord (0.2 to 1 normally 0.2)
0.5                        !LPC - Gap between stator and rotor as % of stator
blade chord (0.2 to 1 normally 0.5)
0.15                       !Duct lambda
0.88                       !Intermediate duct blockage factor (about 0.88)
20                         !Length of intermediate compressor duct from drawing
(if unknown use 20)
-1                         !Intermediate duct mass flow (kg/s) (use -1 to use
LPC mass flow)
-1                         !HPC inlet mass flow (kg/s) (use -1 to use
intermediate duct mass flow)
-1                         !HPC inlet total temperature (use -1 to use LPC
outlet temperature) (K)
 731.480                   !HPC outlet total temperature (K)
15183                      !HPC Rotational speed
2.5                        !HPC Blade aspect ratio
3                          !HPC Stator aspect ratio
3                          !HPC blade & stator length selection (1 - initial
uses AR, followed by reduction factor 2 - all use AR, 3 - manually input initial
length follwed by reduction factor
0.038025893, 0.029296756   !Blade and stator inital lengths (m)
0.8717, 0.873              !Blade and stator reduction factors (in conjunction
with 1 and 3 above
0.2                        !HPC - Gap between rotor and stator as % of rotor
blade chord (0.2 to 1 normally 0.2)
0.5                        !HPC - Gap between stator and rotor as % of stator
blade chord (0.2 to 1 normally 0.5)
143                        !HPC inlet axial velocity (m/s)
0.67                       !HPC initial Hub/tip ratio
*******************************************************************************
Section 4 - Combustor input details
-------------------------------------------------------------------------------
17.5                       !Length of combustor from drawing (if unknown use 20)
*******************************************************************************
Section 5 - Turbine input details
-------------------------------------------------------------------------------
1                          !HPT line type selector (1 for mean line, 2 for
rising line, 3 for falling line)
2                          !LPT line type selector (1 for mean line, 2 for
rising line, 3 for falling line)
0.018                      !Fuel to air ratio at inlet to turbine (inlcude
cooling flow)
 24.037                    !HPT Mass flow (kg/s)
1374.200                   !HPT inlet total temperature (K)
1067.400                   !HPT outlet total temperature (K)
10.935                     !HPT inlet total pressure (Atm)
 3.460                     !HPT outlet total pressure (atm)
15183                      !HPT rotational speed (rpm)
120, 170                   !HPT axial velocities inlet + outlet (m/s) - must
have 2 values separated by comma (i.e. 120, 170)
0.8993585                  !HPT Initial hub-tip ratio
0                          !HPT initial flow angle relative to blade at exit of
combustor (usually 0)
0.98                       !HPT work done factor (usually 0.98)
3                          !HPT blade & ngv length selection (1 - initial uses
AR, followed by reduction factor 2 - all use AR, 3 - manually input initial
length follwed by reduction factor
0.025149096, 0.038951565   !Blade and ngv inital lengths (m)
1.135, 1.1                 !Blade and ngv increase factors (in conjunction with
1 and 3 above
0.2                        !HPT - Gap between NGV and blade as % of blade chord
(between 0.2 and 1, normally about 0.2)
-1                         !LPT Mass flow (kg/s) (use -1 to use HPT outlet mass
flow)
```

```
1067.400                    !LPT inlet total temperature (K)
 691.280                    !LPT outlet total temperature (K)
 3.460                      !LPT inlet total pressure (atm)
 0.527                      !LPT outlet total pressure (atm)
5300                        !LPT rotational speed (RPM)
150, 250                    !LPT axial velocities inlet + outlet (m/s) - must
have 2 values separated by comma (i.e. 150, 250)
0.98                        !LPT work done factor (usually 0.98)
3                           !LPT blade & ngv length selection (1 - initial uses
AR, followed by reduction factor 2 - all use AR, 3 - manually input initial
length follwed by reduction factor
0.019845057, 0.036381036    !Blade and ngv inital lengths (m)
1.1275, 1.085               !Blade and ngv increase factors (in conjunction with
1 and 3 above
0.2                         !HPT - Gap between NGV and blade as % of blade chord
(between 0.2 and 1, normally about 0.2)
0.83                        !LPT Initial hub-tip ratio
-1                          !LPT inlet flow angle (use -1 if you want to use HPT
exit flow angle)
2.5                         !Turbine intermediate duct length from drawing (if
unknown use 2.5)
*****************************************************************************
Section 6 - Nacelle input details
-----------------------------------------------------------------------------
0.8                         !Top of climb mach no
1.35                        !Ratio
0.99                        !Intake pressure recovery - from turbomatch
0.05                        !Nacelle forebody drag rise Mach no (about 0.05)
11                          !Nacelle bypass afterbody final boattail angle in
degrees (about 11)
 1.036                      !Nacelle bypass afterbody nozzle area (sq m) - from
turbomatch
16                          !Nacelle core afterbody boattail angle in degrees
(about 15)
5.33333                     !Nacelle core afterbody nozzle outer to hub ratio
(about 5.3333 for CFM56)
 0.293                      !nacelle core afterbody nozzle area (sq m) - from
turbomatch
0.002                       !nacelle drag factor - (about 0.002 to 0.003)
1.2                         !Nacelle cowl interference factor - (about 1.2)
 313.470                    !Nacelle core afterbody velocity (m/s) - from
turbomatch bypass nozzle exit velocity
0.65                        !Fan diameter to nacelle front ratio (about 0.65)
0.05                        !Nacelle throat Mach No. difference from top of climb
(about M0.05)
0.63                        !Fan face Mach No. (from turbomatch)
```

Appendix 3 – Technology Readiness Level

The Technology Readiness Level (TRL) is a classification system that aims to provide a logical measure of the maturity of a particular technology, which then allows for the consistent comparison of the maturity of different types of technology (Mankins, 1995). TRLs were used by NASA during their space programs (ibid.) and have since been widely used in research programs across the world. TRLs use a scale from 1 to 9, with 1 being the earliest stages of development, with basic principles observed to 9, which is a fully mature technology that has been proven over several operations. Different organisations can have different definitions for each of the levels. The UK Parliament uses the following scale (House of Commons, 2011, Annexe 1):

*"**TRL 1:** Basic principles observed and reported*
***TRL 2:** Technology concept and/or application formulated*
***TRL 3:** Analytical and experimental critical function and/or characteristic proof-of-concept*
***TRL 4:** Technology basic validation in a laboratory environment*
***TRL 5:** Technology basic validation in a relevant environment*
***TRL 6:** Technology model or prototype demonstration in a relevant environment*
***TRL 7:** Technology prototype demonstration in an operational environment*
***TRL 8:** Actual technology completed and qualified through test and demonstration*
***TRL 9:** Actual technology qualified through successful mission operations"*